VOLUME 84 NUMBER 2

THE ASTROPHYSICAL JOURNAL

AN INTERNATIONAL REVIEW OF SPECTROSCOPY AND ASTRONOMICAL PHYSICS

Founded in 1895 by GEORGE E. HALE *and* JAMES E. KEELER

Edited by

HENRY G. GALE
Ryerson Physical Laboratory of the University of Chicago

FREDERICK H. SEARES
Mount Wilson Observatory of the Carnegie Institution of Washington

OTTO STRUVE
Yerkes Observatory of the University of Chicago

SEPTEMBER 1936

THE UNIVERSITY OF CHICAGO PRESS
CHICAGO, ILLINOIS, U.S.A.

September 1936 Vol. 84, No. 2

THE ASTROPHYSICAL JOURNAL

AN INTERNATIONAL REVIEW OF SPECTROSCOPY AND ASTRONOMICAL PHYSICS

The Astrophysical Journal is published by the University of Chicago at the University of Chicago Press, 5750 Ellis Avenue, Chicago, Illinois, during each month except February and August. ¶The subscription price is $6.00 a year; the price of single copies is 75 cents. Orders for service of less than a half-year will be charged at the single-copy rate. ¶Postage is prepaid by the publishers on all orders from the United States, Mexico, Cuba, Porto Rico, Panama Canal Zone, Republic of Panama, Dominican Republic, Canary Islands, El Salvador, Argentina, Bolivia, Brazil, Colombia, Chile, Costa Rica, Ecuador, Guatemala, Honduras, Nicaragua, Peru, Hayti, Uruguay, Paraguay, Hawaiian Islands, Philippine Islands, Guam, Samoan Islands, Balearic Islands, Spain, and Venezuela. ¶Postage is charged extra as follows: for Canada and Newfoundland, 30 cents on annual subscriptions (total $6.30); on single copies, 3 cents (total 78 cents); for all other countries in the Postal Union, 80 cents on annual subscriptions (total $6.80), on single copies, 8 cents (total 83 cents). ¶Patrons are requested to make all remittances payable to The University of Chicago Press, in postal or express money orders or bank drafts.

The following are authorized agents:

For the British Empire, except North America, India, and Australasia: The Cambridge University Press, Fetter Lane, London, E.C. 4. Prices of yearly subscriptions and of single copies may be had on application.

For Japan: The Maruzen Company, Ltd., Tokyo.

For China: The Commercial Press, Ltd., 211 Honan Road, Shanghai. Yearly subscriptions, $6.00; single copies, 75 cents, or their equivalents in Chinese money. Postage extra, on yearly subscriptions 80 cents, on single copies 8 cents.

Claims for missing numbers should be made within the month following the regular month of publication. The publishers expect to supply missing numbers free only when losses have been sustained in transit, and when the reserve stock will permit.

Business correspondence should be addressed to The University of Chicago Press, Chicago, Illinois.

Communications for the editors and manuscripts should be addressed to: Otto Struve, Editor of THE ASTROPHYSICAL JOURNAL, Yerkes Observatory, Williams Bay, Wisconsin.

The cable address is "Observatory, Williamsbay, Wisconsin."

The articles in this journal are indexed in the *International Index to Periodicals*, New York, N.Y.

Applications for permission to quote from this journal should be addressed to The University of Chicago Press, and will be freely granted.

Entered as second-class matter, January 17, 1895, at the Post-Office, Chicago, Ill., under the act of March 3, 1879.
Acceptance for mailing at special rate of postage provided for in Section 1103, Act of October 3, 1917, authorized on July 15, 1918.

PRINTED IN THE U.S.A.

THE ASTROPHYSICAL JOURNAL

AN INTERNATIONAL REVIEW OF SPECTROSCOPY AND ASTRONOMICAL PHYSICS

VOLUME 84 SEPTEMBER 1936 NUMBER 2

THE AGE OF THE MILKY WAY

HENRI MINEUR

ABSTRACT

The dynamical consequences of a variation in the masses of the stars, treated in accordance with the theory of relativity, are discussed: the motion of such a mass in a given gravitational field is the same as that of a constant mass. As a first approximation, Newton's law holds. The diminution in the masses of the stars causes our Milky Way system to expand in inverse proportion to its mass, and the velocities increase in proportion to the mass.

As a result of the variation in the masses of the stars, the equipartition of energy for various groups of stars is upset, and the effect of the passages is insufficient to reestablish the equipartition.

A study of the mean energy of various groups of stars permits us to determine the age of the Milky Way (or at least an upper limit for this age) if we assume that equipartition of energy existed at the time when the stars were formed. A numerical evaluation of the equipartition of energy leads to the conclusion that the interval of time since the formation of the stars cannot be greater than approximately 10^{10} years.

We are led to consider the possibility that the stars have, since their formation, retained very nearly the same masses and have not undergone a process of evolution such as has been generally accepted.

This result is in agreement with the hypothesis of the origin of the Milky Way proposed by G. Lemaitre as a result of his theory of the expanding universe.

1. The purpose of this paper is to investigate the problem of the age of the Milky Way by comparing the observed equipartition of energy of the translational motions of the stars with the theory of this phenomenon. The new element introduced by me into the theory is the secular variation of the masses of the stars.

MECHANICS OF VARIABLE MASSES

2. For some twenty years it has been generally accepted that the radiation of the stars results from the destruction of their masses by

some unknown physical process. This phenomenon was predicted by the theory of Einstein and was suggested as an explanation of the radiation of the stars by J. Perrin.[1] This opinion has been recently confirmed by laboratory experiments[2] in which positive electrons have actually been observed to disappear, following which there occurred emissions of photons.

According to this hypothesis, the mass of a star, M, varies as a function of the time t. This variation is approximately represented by the equation

$$\frac{dM}{dt} = -2\alpha M^3 , \tag{1}$$

where $\alpha = 5 \cdot 10^{-14}$, if the year is taken as the unit of time and the solar mass as the unit of mass. This value of α is the one which represents best the mass-luminosity relation in the interval we are to consider later: $-0,3 < \log M < 1,2$. This assumed variation of stellar mass makes it necessary to re-examine the dynamical equations of stellar motions.

3. The first problem which we shall consider is the following: Adopting the Newtonian dynamics in order to simplify the notations, what will be the equation of motion of a mass m having the co-ordinates $x, \ldots$, which varies with the time t, and is in a field of forces $mX, \ldots$?

Astronomers are divided into two groups with respect to this question. Some adopt the equation

$$m\frac{d^2x}{dt^2} = m \cdot X \qquad \text{or} \qquad \frac{d^2x}{dt^2} = X , \tag{2}$$

while the others prefer the expression

$$\frac{d}{dt}\left(m\frac{dx}{dt}\right) = mX , \tag{2'}$$

without, however, justifying this choice by physical reasoning.

[1] *Ann. de Phys.*, **2**, 89, 1919. See also A. S. Eddington, *British Assoc. Rept.*, 1920, p. 45.

[2] Jean Thibaud, *Ann. de la Soc. Sc. de Bruxelles*, Vol. **54**, seconde partie, "Mémoires," p. 36, 1934.

I have shown[3] that if the principle of relativity is accepted we are led to equation (2), while if the existence of a fixed ether is postulated we are led to equation (2′), which holds with respect to co-ordinates in the ether.

Since the theory of relativity is now universally accepted, we shall adopt equation (2). I shall show briefly how this expression is obtained.

In all points of space time we choose four axes: $\vec{e}_0, \vec{e}_1, \vec{e}_2, \vec{e}_3$, the first being the time axis and the others the space axes. A displacement $\vec{dM}$ of an event M has the expression

$$\vec{dM} = \sum_{i=0}^{3} \omega^i \vec{e}_i ,$$

where $\omega^i (i = 0, 1, 2, 3)$ are linear forms of the differentials of the co-ordinates of M. The structure of space is defined by six forms ω_i^k, such that

$$(\omega^k)' = \sum_{i=0}^{3} \omega_i^k \omega^i ,$$

and the parallel displacement of the vector $\vec{e}_i$ is defined by

$$\vec{de}_i = \sum_{k=0}^{3} \omega_i^k \vec{e}_k .$$

The interval between two events has the expression

$$ds^2 = (\omega^0)^2 - (\omega^1)^2 - (\omega^2)^2 - (\omega^3)^2 .$$

Let us consider a particle, and let m_0 be its mass at rest. $\vec{V} = \vec{dM}/ds$ is the vector velocity of the particle in space and time. $\vec{I} = m_0 \cdot \vec{V}$ is the vector whose space components are the momenta and whose time component is cm, m being the relative mass. We call this the "world-momentum."

The equations of mechanics for the particle are $\vec{dI} = 0$. When m_0

[3] Henri Mineur, *Ann. de l'Ecole Normale Supérieure*, Ser. 3, **5**, 1, 1933.

is a constant, this equation is equivalent to $d\vec{V}=0$. Let us assume m_0 to be variable. Stated more precisely, let us assume that during the interval of time t, $t+dt$, a portion, $-dm_0$, of the mass m_0 has been destroyed and spherically radiated by the particle. We shall determine the motion of the particle by equating its world-momentum at the time t, $\vec{I}=m_0\vec{V}$, to the sum of two terms: the world-momentum of the particle at the time $t+dt$,

$$\vec{I}+d\vec{I}=m_0\vec{V}+dm_0\vec{V}+m_0d\vec{V}\,,$$

and the world-momentum $\vec{I'}$ of the emitted radiation. Hence

$$dm_0\vec{V}+m_0d\vec{V}+\vec{I'}=0\,. \tag{3}$$

$\vec{I'}$ is to be estimated. This quantity constitutes a vector, and particular axes can be chosen in order to facilitate the computation. Let us consider axes moving with the particle.

The world-momentum of a photon of mass μ, emitted in the direction whose direction cosines are α, β, γ, is the four-dimensional vector

$$\mu,\ \mu\alpha c,\ \mu\beta c,\ \mu\gamma c\,,$$

c being the velocity of light.

We shall say that $-dm_0$ is spherically radiated when, with respect to axes moving with the particle, the sum along each space axis of the momenta of the photons emitted after the destruction of dm_0 is equal to zero.

The components of the vector $\vec{I'}$ relative to the total radiation emitted in the interval of time dt, when referred to the chosen axes, are then

$$-dm_0,\ 0,\ 0,\ 0\,.$$

Now the components of $\vec{V}$ with regard to the sames axes are

$$1,\ 0,\ 0,\ 0\,.$$

Therefore

$$\vec{I'} = -dm_0 \cdot \vec{V} .$$

Both sides of this equation being vectors, the equality holds in any system of reference whatever, and equation (3) reduces to $d\vec{V} = 0$. Hence the motion of a variable mass emitting spherical radiation in a given gravitational field is the same as that of a constant mass.

This result justifies the choice of equation (2), at least to the approximation of the Newtonian dynamics.

4. We must now give the expression of the gravitational field set up in its neighborhood by a variable mass, that is to say, the ds^2 of a variable mass.

I have discussed this problem in the above-mentioned paper, starting from Einstein's gravitational equations. I shall review briefly the results:

Let $M(t)$ be the variable mass. Its ds^2 is

$$ds^2 = c^2\left[1 - \frac{2K}{c^2 r} M(x)\right] dx^2 + 2c\, dx\, dr - r^2[d\theta^2 + \cos^2\theta\, d\varphi^2] ,$$

where x and r are functions of the time t and of the radial vector r_1, defined by

$$x = t - \frac{r}{c} , \qquad \frac{2}{c}\frac{\partial r}{\partial x} = 1 - \frac{2K}{c^2 r} M(x) .$$

I also studied the force which acts upon a particle in such a ds^2: this force may be considered as the sum of three forces F_1, F_2, F_3. F_1 is the force which would act upon a particle if its mass were constant. Its components along and perpendicular to the radius vector are well known:

$$R_1 = -\frac{K \cdot M}{r^2}\left[1 - \frac{2 \cdot K \cdot M}{c^2 \cdot r}\right]\psi^{-2} + \frac{3 \cdot K \cdot M}{c^2 \cdot r} \cdot \left(\frac{dr}{dt}\right)^2 \cdot \frac{1}{1 - \dfrac{2 \cdot K \cdot M}{c^2 \cdot r}} - \frac{2 \cdot K \cdot M}{c^2}\left(\frac{d\theta}{dt}\right)^2$$

$$T_1 = \frac{2 \cdot K \cdot M}{c^2 \cdot r}\frac{dr}{dt} \cdot \frac{d\theta}{dt} \cdot \frac{1}{1 - \dfrac{2 \cdot K \cdot M}{c^2 \cdot r}} \cdot$$

ψ is a function of r and t very nearly equal to 1. The expression of F_2 is approximately

$$R_2=\frac{K}{c}\frac{dM}{dt}\cdot\frac{1}{r}\cdot\left(1-\frac{2}{c}\cdot\frac{dr}{dt}\right),$$

$$T_2=\frac{K}{c}\frac{dM}{dt}\cdot\frac{d\theta}{dt}.$$

F_3 may be neglected. Let us notice that the main term in F_1 is $-KM/r^2$. The force F_2 varies as $1/r$, but the computations show that for distances of the order of those of the stars in the Milky Way, F_2 may be overlooked when compared with F_1. As a first approximation, therefore, the force set up by a variable mass has the same expression as Newton's classical force of attraction.

I have shown, for instance, that the motion of a particle in the ds^2 of a variable mass is a Keplerian motion whose major semi-axis increases proportionally to a factor very nearly equal to $1/M$ and whose eccentricity increases very slowly. This result is practically the one which is obtained through the application of Newton's law, at any rate when an interval of time of the order of the age of the stars is considered.

5. We shall now investigate the evolution of the Milky Way due to the variation of the masses of which it is composed:

Let us consider a space time (s), x, y, z, t. Let δ be the material density at a given point. The potential u is

$$u(x, y, z)=-K\int\frac{\delta d\tau}{r}.$$

Let (S), X, Y, Z, T, be another space time, Δ its material density, and U its potential:

$$U=-K\int\frac{\Delta d\theta}{R}.$$

Let us establish between the two space times a correspondence defined by the formulas

$$\left.\begin{aligned} X &= ax \\ Y &= ay \\ Z &= az \\ \Delta &= \frac{m\delta}{a^3} \\ \frac{dT}{dt} &= \lambda \end{aligned}\right\} \tag{4}$$

where a, m, and λ are either constants or functions of T. We have

$$d\theta = a^3 . d\tau$$

and

$$U(X, Y, Z) = \frac{m}{a} \cdot u\left(\frac{X}{a}, \frac{Y}{a}, \frac{Z}{a}\right)$$

$$\frac{d^2X}{dT^2} = \frac{a}{\lambda^2}\frac{d^2x}{dt^2} + \frac{I}{a} \cdot \frac{d}{dT}\left(\frac{a^2}{\lambda}\right)\frac{dx}{dt} + \frac{d^2a}{dT^2}x$$

$$\frac{\partial U}{\partial X} = \frac{m}{a^2}\frac{\partial u}{\partial x} .$$

6. Let us apply the preceding considerations to the case of the Milky Way, supposed to be the system S.

We will assume that in all points of the Milky Way the law of probability of the stellar masses is the same. This is an assumption which can be made at least as a first approximation.

Let μ be the mass of a region of the Milky Way and $\varphi(M)dM$ the law of probability of the stellar masses, that is to say, the probability for the mass of a star to be $M \mp \frac{1}{2}dM$. Let N be the total number of stars situated in this region. We have

$$\mu = \int_0^{+\infty} NM\varphi(M)dM .$$

When the time dt has elapsed, each mass M has undergone a variation of $-2aM^3dt$, and the variation of μ is

$$d\mu = -2 \cdot N \cdot a dt \int_0^{+\infty} [4M^3\varphi(M) + M^4\varphi(M)]dM .$$

It is to be noticed that $1/\mu \cdot d\mu/dt$ does not depend on N, and therefore is independent of the region considered, since we have assumed that $\varphi(M)$ is the same in all points of the Milky Way. Therefore the mass of any region of the Milky Way varies proportionally to a factor, $m(T)$, which is a function of the time only and does not depend upon the region considered. This factor is also proportional to the total mass of the Milky Way.

The order of magnitude of dm/dt is readily obtained on the assumption that the Milky Way is composed of n masses M equal to one another and not very different from that of the sun: $m = n \cdot M$. Hence

$$\frac{dm}{dt} = -\frac{2a}{n^2} m^3 .$$

Let us take $m(T)$ as the factor m in section 5, the factors a and λ still remaining arbitrary.

Formulas (4) establish a correspondence, event for event, between the actual Milky Way and a fictitious Milky Way which is an image of the first one.

To the motions of the points of S which are defined by

$$\frac{d^2X}{dT^2} = -\frac{\partial U}{\partial X} \tag{5}$$

correspond, for the points of s, motions defined by

$$\frac{d^2x}{dt^2} = -\frac{m\lambda^2}{a^3}\frac{\partial u}{\partial x} - \frac{\lambda^2}{a^2}\frac{d}{dT}\left(\frac{a^2}{\lambda}\right) \cdot \frac{dx}{dt} - \frac{\lambda^2}{a}\frac{d^2a}{dT^2} \cdot x . \tag{6}$$

Let us determine a and λ so that the motions defined by (6) obey the laws of dynamics, that is to say, so that (6) be equivalent to

$$\frac{d^2x}{dt^2} = -\frac{\partial u}{\partial x} . \tag{7}$$

Setting the conditions

$$\frac{m\lambda^2}{a^3}=1 \qquad \text{and} \qquad \frac{a^2}{\lambda}=1\,,$$

we obtain $a=1/m$ and $\lambda=1/m^2$. We notice that the motion defined by (6) may be considered as occurring according to the laws of dynamics, provided a disturbing force is introduced whose first component is

$$-\frac{\lambda^2}{a}\cdot\frac{d^2}{dT^2}\left(\frac{1}{m}\right)\mu\cdot x\,.$$

This force may be neglected. If the Milky Way were composed of stars of equal mass, it would be equal to $-4a^2$. This is not the case; but the disturbing force is nevertheless of the aforesaid order of magnitude, and it is easily shown that its influence may be ignored.

Thus, setting

$$\left.\begin{aligned}\lambda&=\frac{1}{m^2}\\ a&=\frac{1}{m}\end{aligned}\right\}\,, \tag{8}$$

the motions in s and S which obey the laws of dynamics correspond to one another.

Let us suppose, at the time O, the Milky Way to be in statistical equilibrium, and let us take it as system s. The motions in the Milky Way decrease proportionally to a factor $m(T)$. We set $m(1)=1$. The evolution of the Milky Way at the time O is defined by equation (7).

As a consequence of the radiation emitted by the stars, the mass of the Milky Way is defined by equations (5), and we have just shown that the integral $X(T)$ of (5) is given by

$$\left.\begin{aligned}&X=\frac{1}{m}x\,;\qquad Y=\frac{1}{m}y\,;\qquad Z=\frac{1}{m}z\,;\\ &t=\int_0^T m\,dT\,,\end{aligned}\right\} \tag{9}$$

$x(T)$ . . . . being an integral of (6).

Equations (9) are readily interpreted as follows:

The Milky Way at the time T is identical to the Milky Way at the time O where all dimensions are multiplied by $1/m$ and in which the time is multiplied by $1/m^2 \cdot 1/m$ is greater than unity for $T > 0$.

It follows that should the masses cease varying at the time t, the Milky Way would be in statistic equilibrium.

7. The velocities in the Milky Way at the time T are equal to the velocities at the time O multiplied by m.

Let us notice that at the end of $2 \cdot 10^{11}$ years, for instance, the factor m, as to order of magnitude, remains equal to $1 - 10^{-3}$, that is to say, very nearly equal to 1.

Let us notice further that, if we consider a group of stars, the mean velocity of the group and the residual velocities of the stars are all multiplied by m.

We conclude that the result of the variation of the mass of the Milky Way and of the masses of the stars of which it is composed is that every stellar velocity is multiplied by a factor m which remains equal to 1, within a hundredth, for $2 \cdot 10^{11}$ years.

THE EFFECT OF VARIATION OF THE MASSES UPON THE KINETIC ENERGY OF A GROUP OF STARS

8. Let us recall briefly the result obtained by Jeans concerning the action of passages upon the stellar velocities.

We take the following units: for the time, the year; for the velocity, 1 km/sec; for the mass, the solar mass. The cumulative effect of the passages upon a star during the time t is to communicate to the star a transverse velocity v whose magnitude is approximately given by $v^2 = 10^{-11} \cdot t$. It is to be noted that v is independent of the mass of the disturbed star.

From this expression the time of relaxation of the Milky Way was deduced, that is to say, the time τ necessary for the passages to impart to the stars velocities v of the same order of magnitude as they were originally. This time τ is approximately $\tau = 3 \cdot 10^{13}$ years.

It is known that the effect of the passages is to establish the equipartition of energy between the various categories of stars; and as it is observed that the equipartition is approximately established,

the conclusion was derived some years ago that τ gives the order of magnitude of the age of the Milky Way.

It appears from the results obtained in sections 3 and 4 that the discussion concerning the effect of a passage upon the velocities of two stars whose masses are supposed to be constant remains valid when the masses are supposed to be variable, for the passage of two stars in the vicinity of one another does not last long, compared with the age of the Milky Way, and the variation in the masses of the stars is too insignificant to modify the circumstances of the passages.

9. Let us study the effect of the variation of the mass and of the passages upon the mean kinetic energy of a group of stars.

Let us consider, at the time $t=0$, a group of stars, G, all having the same mass μ_0. Let V_0 stand for the mean residual quadratic velocity of these stars. We have for the mean kinetic energy of G

$$\theta_0=\tfrac{1}{2}\mu_0 V_0^2 .$$

Let μ_t and V_t stand for the same quantities at the time t, and let us first consider the variation with t of θ_t which is due to the variation of the masses. We shall then examine to what extent the passages can modify this quantity.

As has been shown in section 7, when the time t has elapsed, the mean quadratic velocity of the stars of G is V_0, to within a hundredth, provided t be less than $2\cdot10^{11}$ years. In what follows we consider only intervals of time less than this, and we may write $V_t=V_0$. In the case of t being small enough, we have:

$$\mu_t=\mu_0-2\cdot a\mu_0^3\cdot t .$$

Hence

$$\theta_t=\theta_0-a\mu_0^3V_0^2\cdot t .$$

Whatever the value of t, we have exactly

$$\mu_t=\frac{\mu_0}{\sqrt{I+2\cdot at\cdot\mu_0^2}} .$$

Hence

$$\frac{\theta_t}{\theta_0}=\frac{I}{\sqrt{I-2\cdot at\cdot\mu_0^2}}=\frac{\mu_t}{\mu_0},$$

or

$$\frac{\theta_t}{\theta_0}=\sqrt{I-2\cdot a\cdot t\cdot\mu_t^2}\,.$$

10. Let us classify the stars of the Milky Way according to their masses in groups such as G, and let us suppose that at the time $t=0$ equipartition of energy exists between the various groups. Is the equipartition preserved at the time t? Let us consider two groups of stars G and G'. We have $\theta_0=\theta_0'$. Then

$$\frac{\theta_t'-\theta_t}{\theta_0}=-2\cdot a(\mu_0'^2-\mu_0^2)t\,. \tag{10}$$

Thus, equipartition of energy does not exist any more, and the relative difference between the energies of two groups of stars increases in proportion to the time t.

11. It is well known that if the effect of the variation of the masses is to upset the equipartition of energy, that of the passages is to reestablish this equipartition. We must now examine to what extent the passages may modify θ.

Let $\Delta\theta$ be the variation introduced by the passages in the mean kinetic energy of the stars of group G. The effect of the passages being to impart to the stars a transverse velocity v defined by $v^2=10^{-11}\cdot t$, we have:

$$\frac{\Delta\theta}{\theta_0}=\frac{v^2}{V_0^2}\,.$$

Or, setting $V_0=17$ km/sec,

$$\frac{\Delta\theta}{\theta_0}=3\cdot10^{-14}\cdot t\,.$$

Thus the effect of the passages, $\Delta\theta/\theta$, is greater than the effect of the variation of mass, $(\theta_t'-\theta_t)/\theta_0$, if

$$\mu_0'^2-\mu_0^2<\tfrac{1}{3}\,.$$

12. The mean kinetic energy of the various groups G at the time t is then readily found.

Let $\Theta_0=\overline{\theta_0(\mu)}$ be the mean kinetic energy common to all the groups at the time 0.

At the time t, the kinetic energy $\theta_t(\mu)$ of each group has decreased, owing to the variation of mass, the diminution being $a\mu_0^2\theta_0 t$, a quantity which differs from one G to another.

Let Θ_t be the mean kinetic energy of all groups and $\bar{\mu}$ the mass of the stars for the group where the kinetic energy is precisely Θ_t. For the groups G where the mass μ_t is such that

$$\bar{\mu}^2-\frac{I}{3}<\mu_t^2<\bar{\mu}^2+\tfrac{1}{3}\,, \tag{11}$$

which is to say

$$\bar{\mu}-\frac{1}{6\bar{\mu}}<\mu_t<\bar{\mu}+\frac{1}{6\bar{\mu}}\,,$$

the passages are nearly sufficient to keep the kinetic energies equal. The effect of the passages is indeed to impart to all groups the energy Θ_t, and we have just seen that for masses which satisfy the preceding inequalities the effect of the passages prevails over that of the variation of mass. It may be seen that for $\bar{\mu}=1$, for instance, the interval of variation for μ_t is small.

On the contrary, for masses such that

$$\mu_t<\bar{\mu}-\frac{1}{6\bar{\mu}}\,,$$

or

$$\mu_t>\bar{\mu}+\frac{1}{6\bar{\mu}}\,,$$

the effect of the passages is insufficient to re-establish the equipartition of energy, since this effect $\Delta\theta/\theta$ is less than $(\theta_t-\Theta_t)/\Theta_t$. With $\bar{\mu}=1$, for instance, and $\mu_t=10$, we have

$$\frac{\theta_t-\Theta_t}{\Theta_t}=300\,\frac{\Delta\theta}{\theta}\,.$$

The curve which represents, at the time t, the relation between μ_t and θ_t is then readily found. It is given by Figure 1.

The equation of this curve could be computed with precision, but the computations are long and difficult and are not necessary for the application we are considering.

AN ESTIMATE OF THE AGE OF THE MILKY WAY

13. If the masses and velocities of the stars were known with sufficient accuracy, one might compare the observed curve (μ_t, θ_t)

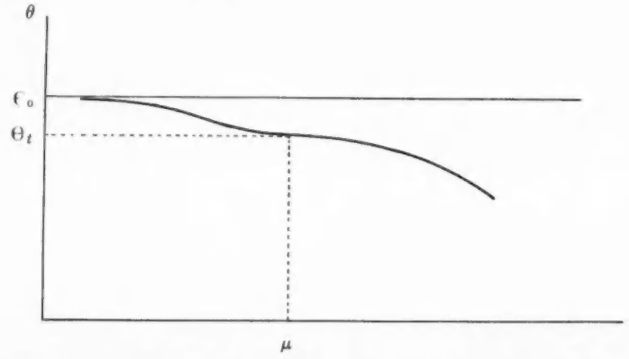

FIG. 1.—Abscissae: μ_t, masses of the stars at the time t; ordinates: θ_t, mean kinetic energies of stars of mass μ_t. The curve is represented according to the theory. If there were no passages, the curve which gives θ_t as a function of μ_t would be a segment of the ellipse $(\theta^2/\theta_0^2)+2a\mu^2=1$. The effect of the passages is to make the curve horizontal for $\overline{\mu_t}$, the mass corresponding to the mean kinetic energy.

with the curve calculated according to the foregoing theory; and if observation and theory were in agreement, one could estimate the time t elapsed since the instant when equipartition of energy existed in the Milky Way.

Our knowledge of the masses and velocities is insufficient. However, if it is observed that equipartition of energy does exist between groups of stars having masses μ and μ', an upper limit may be inferred for the age of the Milky Way.

Indeed, the inequality

$$\left|\frac{\theta'_t-\theta_t}{\theta}\right|<\epsilon$$

gives

$$t < \frac{10^{13}\epsilon}{|\mu'^2 - \mu^2|}. \qquad (13)$$

14. In order to obtain a numerical result from the preceding considerations, we are led to compare the kinetic energies of stars of various masses. Such an investigation is difficult because we know little of the exact values of the stellar masses and because the computations are very long. I shall use only a few investigations concerning stellar motions which have been made in recent years:

a) F. H. Seares[4] estimated the masses of the stars of the dwarf sequence by means of data concerning binary stars, and computed the mean kinetic energy of 12 groups of dwarf stars of types B_3 to Ma.

b) W. S. Adams, G. Strömberg, and A. H. Joy[5] estimated the mean radial velocity ρ of dwarf and giant stars of types F, G, K, and M. As they also give the mean absolute magnitudes of the stars in each group, the average mass can be computed by means of the mass-luminosity relation. In order to do this, I have determined the bolometric absolute magnitudes, adopting for the bolometric index of a star of a given type the values given in Table I. From this, I derived the corresponding average mass by means of the mass-luminosity relation expressed in Table II. The mean quadratic velocity v is the mean value of $v = 2.17\rho$ and $v = 1.25\bar{v}$.

c) Strömberg[6] has calculated the axes of the ellipsoidal distribution of the velocities for groups of stars classified according to spectral type and to $H = m + 5 \log \mu + 5$. The average mass of the stars in each group was estimated by means of the mass-luminosity relation in Table II. For giants and for B stars the value adopted for M_{bol} was taken from a paper by Strömberg[7] upon the distribution of the absolute magnitudes of stars brighter than magnitude 6. For the dwarf stars I computed the visual absolute magnitude by means of the formula established by Gorakh Prasad,[8] which gives M_v as a function of H, then the bolometric magnitude, by adopting the

[4] *Mt. W. Contr.*, No. 226, p. 26, 1922.

[5] *Ibid.*, No. 210, p. 12, 1921.

[6] *Ibid.*, No. 293, p. 7, 1925.

[7] *Ibid.*, No. 442, p. 11, 1932.

[8] *M.N.*, **85**, 157, 1924.

bolometric index given in Table I. The mean quadratic velocity was given by $v^2=a^2+b^2+c^2$.

d) Gerasimovič[9] estimated the stellar masses, assuming the reversing layers to be in radiative equilibrium and assuming each spectral line to originate at the same optical depth for all stars of a given type. He thus computed the average kinetic energy of the stars of types F, G, and K.

TABLE I

		Spectral Type								
		A0	A5	F0	F5	G0	G5	K0	K5	M
M_v-M_{bol}	g....	0.4	0.1	0	0	0.1	0.2	0.5	1.0	1.5
	d....	0.4	0.1	0	0	0	0.1	0.2	0.4	0.8

TABLE II

M_{bol}	−6	−4	−2	0	2	4	6	8	10	11
log μ.....	1.76	1.50	1.88	0.55	0.29	0.05	9.87	9.68	9.50	9.3

Table III gives the values thus obtained for log μv^2. Figure 2 represents log μv^2 as a function of log μ. The dots obtained present a noticeable dispersion around the mean value 3.58. But it is to be noted that log μv^2 does not vary systematically with μ. This may be seen by forming mean values of this quantity for stellar groups taken from Table III and arranged according to μ.

15. Before we draw any conclusions from the results of the observations, it is to be noted that the methods adopted to determine stellar masses in Table III do not give the masses accurately, especially for giants. This is particularly the case for masses determined from H, M_v, M_{bol}, and the mass-luminosity relation. Hence it follows that we must expect some uncertainty in our conclusions.

Let us assume that all the stars of the Milky Way originated at one instant when equipartition of energy existed, and let us consider the numbers in Table IV as expressing the relation between log μ and log μv^2.

[9] *A.N.*, **227**, 145, 1926.

According to this table, $\overline{\mu v^2}$ does not decrease with increasing μ. Only an upper limit for the age of the Milky Way can therefore be deduced from it. It can be considered that $\overline{\mu v^2}$ remains constant, with a relative error $\epsilon = 0.05$, for stars whose masses vary from

TABLE III

Stars	M_v	No.	Mbol	log $\bar{\mu}$	log $\overline{\mu v^2}$	Reference
Ma	9.8	.....	.....	9.77	3.55	Seares
K5	7.1	.....	.....	9.79	3.53	Seares
Ko	5.9	.....	.....	9.83	3.63	Seares
dK	6.2	148	+5.8	9.88	3.49	Adams, etc.
G5	5.2	.....	.....	9.88	3.66	Seares
G	4.8	184	+4.7	9.99	3.60	Adams, etc.
Go	4.4	191	.....	9.99	3.61	Seares
K4–M9	$H>$ 3.1	79	+4.4	0	3.61	Strömberg
F	3.5	191	+3.5	0.10	3.43	Adams, etc.
Fo–F9	$5.1<H<14.0$	38	+3.3	0.12	3.49	Strömberg
Go–G8	$5.1<H<10.0$	111	+3.1	0.15	3.77	Strömberg
F5	3.3	.....	.....	0.19	3.55	Seares
Fo–F9	$-1.9<H<5.0$	398	+1.6	0.32	3.53	Strömberg
Fo	2.4	.....	.....	0.40	3.51	Seares
Go–G8	$H<5$	429	+0.3	0.50	3.57	Strömberg
B6–A9	$-1.9<H<2.7$	254	+0.3	0.50	3.21	Strömberg
K	0.8	320	+0.2	0.53	3.72	Adams, etc.
G	0.3	216	+0.1	0.54	3.69	Adams, etc.
F	0.1	152	+0.1	0.54	3.52	Adams, etc.
G9–K3	$H<12$	.....	0	0.55	3.71	Strömberg
A5	1.5	.....	.....	0.60	3.55	Seares
M	0.1	114	−0.9	0.69	3.76	Adams, etc.
A2	1.0	.....	.....	0.70	3.57	Seares
K4–K9	$H<3$	167	−1.2	0.72	3.86	Strömberg
Ao	0.7	.....	.....	0.78	3.56	Seares
B8–B5	0.4	.....	.....	0.81	3.21	Seares
Mo–M9	.....	172	−2.1	0.90	4.05	Strömberg
B3	−0.6	.....	.....	0.95	3.29	Seares
Bo–B5	$-3.9<H<0.1$	.....	−2.5	0.97	3.34	Strömberg
Fo–F9	$H<-2.0$	86	−3.0	1.10	3.94	Strömberg
B6–A9	$H<-2$	326	−3.7	1.23	3.77	Strömberg
Bo–B5	$H<-4$	123	−4.5	1.40	3.72	Strömberg
F	.....	.....	.....	.....	3.47	Gerasimovič
G	.....	.....	.....	.....	3.45	Gerasimovič
K	.....	.....	.....	.....	3.60	Gerasimovič

$\mu' = 10$ to $\mu = 0.7$. According to section 13, the age of the Milky Way is then less than $5 \cdot 10^9$ years. This result gives the order of magnitude only, even if our hypotheses are accepted.

Adopting, for instance, the exaggerated limits $\epsilon = 0$, 1 $\mu' = 7$, we find $t < 20 \cdot 10^9$ years.

We may conclude that since the formation of the stars of the Milky Way not more than a few tens of thousands of millions of

years have elapsed. This conclusion would not hold if the masses of the stars did not vary. But with such a hypothesis it is known that it is impossible to account for the radiation of the stars for more than a few thousand million years, and the age of the Milky Way would still be less than the preceding limit.

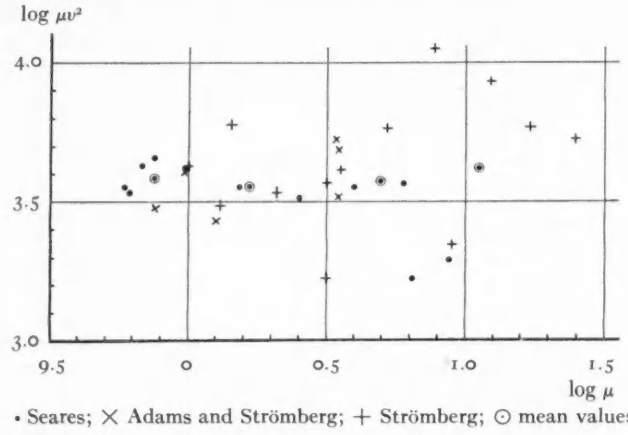

• Seares; × Adams and Strömberg; + Strömberg; ⊙ mean values

FIG. 2.—Equipartition of energy in the Milky Way. Abscissae: log μ; ordinates: log μv^2. The data of Tables III and IV are shown on the diagram.

TABLE IV

Limits for log μ	$\overline{\log \mu}$	$\overline{\log \mu v^2}$
$\leqslant 9.99$	9.88	3.58
$0 \leqslant \leqslant 0.50$	0.22	3.55
$0.50 \leqslant \leqslant 0.99$	0.70	3.57
$0.80 \leqslant$	1.05	3.62

If the stars have been formed simultaneously, it is difficult to admit that equipartition of energy did not exist at that time, but that μv^2 was then a function of μ such that, as a consequence of the variation in the masses of the stars, the equipartition has now become established accidentally.

According to Table IV, the mean value of log μv^2 seems to be independent of μ; but it is to be noted that this quantity seems to depend on spectral type, as may be seen from Table V. If this result is not attributed to systematical errors in the masses depending

on the spectral type, we must admit that the B stars and the K and M giants were not formed simultaneously from cosmic matter in which equipartition existed, since their masses are nearly the same and their energies are different.

On the contrary, it may be admitted that the dwarf sequence, including the B stars, were formed at the same time. For these stars μv^2 decreases with increasing μ, according to formula (10), which then gives: $t = 40 \cdot 10^9$ years, that is to say a value of the order of a few tens of thousands of millions of years for the age of the Milky Way.

TABLE V

Class	$\overline{\log \mu}$	$\overline{\log \mu v^2}$
Dwarfs	0.1	3.58
B stars	1.0	3.42
K and M giants	0.7	3.82

16. The upper limit we have found for the age of the stars is so small that, in so brief a time, the great majority of the stars cannot have lost more than a hundredth part of their mass. We must therefore believe that the stars were formed with nearly the same masses as they have now, and that the differences in temperature and spectral type actually observed are due to the fact that the stellar masses were already different at the time of their formation.

An evolution of the stars such as has generally been accepted is, then, impossible. Our result is, however, in perfect agreement with the theory of the expansion of the universe. G. Lemaitre[10] has suggested a hypothesis for the formation of the extragalactic nebulae based upon his theory of the expansion of the universe, according to which the age of the Milky Way would not exceed ten thousand million years.

I shall conclude by directing the attention of astronomers to the exceptional interest presented by the equipartition of energy in the Milky Way. It is to be hoped that researches based on more recent data concerning stellar motions and masses will be undertaken.

OBSERVATOIRE DE PARIS
October 1935

[10] See, e.g., *Bull. Soc. Astr. de France*, **49**, 159, 1935, and *Lecture faite à la Séance publique de l'Académie royale de Belgique*, December 15, 1934.

ABSORPTION AND SPACE REDDENING IN THE GALAXY FROM THE COLORS OF GLOBULAR CLUSTERS*

JOEL STEBBINS[1] AND A. E. WHITFORD[2]

ABSTRACT

Measures of the colors of 68 globular clusters have been secured with a photoelectric cell attached to the 100-inch reflector. The effective wave-lengths of the cell and filters used for color index were 4340 and 4670 A, giving the difference $A_0 - K_0 = 0^M.44$ for giant stars. For comparison with B stars the color excesses are reduced to the scale used for those stars, $A_0 - K_0 = 0^M.74$.

There is a close relation between the color excess and the space absorption, as shown by the number of extra-galactic nebulae in the field of a globular cluster. In the fields tested, nebulae are present when the color excess $E < 0^M.19$; they are absent when $E > 0^M.20$.

The clusters in high latitudes are of uniform color, corresponding to spectrum about F6; they grow redder toward the galactic equator, with maximum redness equal to that of an M star near the narrow zone of avoidance (Fig. 2). The absorption is not uniform but is spotted in its effect. The greatest observed color excess of a cluster is $+0^M.82$, corresponding to a photographic space absorption of not less than three magnitudes.

The differential absorption on our scale from pole to pole is $0^M.08$, from which would be inferred a total photographic absorption of about $0^M.25$. Comparison of this latter value with $0^M.50$ found by Hubble, or $0^M.80$ by van de Kamp, from counts of nebulae, shows that only part of the space absorption is due to Rayleigh scattering.

The visible system of globular clusters is incomplete; the clusters in the direction of the center of the galaxy are probably on the near side of the center. When the dimensions of the system are corrected for space absorption, the overall diameter of the galaxy is not much greater than 30,000 parsecs, which is of the same order as that of the Andromeda Nebula.

The transparency of space in our galactic system may be tested by measures of the light and color of globular clusters, which can be observed at much greater distances than individual stars. The photoelectric cell, when applied to the photometry of the clusters, has the advantage of integrating the light effect from a luminous surface; and thus the total light or color of a cluster may be compared with that of a standard star. In 1932[3] a preliminary report was made on observations obtained at Mount Wilson with a photoelectric cell at-

* *Contributions from the Mount Wilson Observatory, Carnegie Institution of Washington*, No. 547.

[1] Research Associate of the Mount Wilson Observatory, Carnegie Institution of Washington.

[2] National Research Fellow, 1933–35.

[3] Stebbins, *Mt. Wilson Comm.*, No. 111; *Proc. Nat. Acad.*, **19**, 222, 1933.

tached to the 100-inch reflector. It was shown that there was a distinct reddening of the globular clusters in low latitudes, which indicated in some cases a photographic absorption of as much as two or even three magnitudes. For clusters whose light has been diminished to one-sixteenth of normal by space absorption, the distances inferred from the apparent magnitudes of their bright stars, or from the total light of the clusters, should be divided by four. On the assumption of a thin uniform layer of absorbing material near the plane of the galaxy which reduces the light of objects according to the cosecant law, a rough attempt was made to improve the dimensions in Shapley's general system of globular clusters. The solution gave 10,000 parsecs instead of 16,000 for the distance from the sun to the center of the system, a value which will probably turn out to be nearer the truth than would be expected from the simple assumptions on which it was based.

The installation.—The first results on 47 globular clusters were derived from observations with the combination of a photoelectric cell and Lindemann electrometer which had been developed and used at Madison and later transferred to Mount Wilson. In 1933, however, the use of the thermionic amplifier in place of the electrometer was perfected by Mr. Whitford[4] at Madison; and since 1933 the improved "photoelectric amplifier," as we call it, has been used on the 100-inch telescope.

The details of the installation on the large reflector will be given in another paper. All the measures of the present work were made at the Newtonian focus, where the cell and amplifying tube are mounted in a brass tank attached to the regular plateholder base of the Newtonian cage. A metal-covered cable about one hundred feet long carries the circuit wires to the control box and galvanometer at the base of the north column. The batteries are mounted below, in a room inclosed in the great cement pier where the temperature changes are small.

The optical parts for guiding have been the same for both the electrometer and the amplifier arrangements. At the focus of the large mirror is a circular diaphragm of several millimeters diameter, behind which is a sliding prism which reflects the light of a star

[4] *Ap. J.*, **76**, 213, 1932.

through a suitable lens to a pair of cross-wires in the guiding eyepiece. The observer can thus see exactly what object or objects are to be measured. When the prism is withdrawn, the light passes through to the cell. At 5 cm outside the main focus is a double-convex quartz lens which makes the beam parallel, and the star image on the photocell is thus about 1 cm in diameter; but when a cluster, nebula, or patch of sky is measured with a diaphragm of 1 cm, the extra-focal image is 2 cm across. As the aperture of the quartz lens and the clear opening of the photocell are each 2.5 cm, there is plenty of clearance in the optical system. By measuring the sky in twilight or moonlight with different focal diaphragms, and by measuring stars in different positions off the axis, the cell was found to be uniformly sensitive over the surface. Areas of 1–2 cm diameter are large enough to smooth out any local irregularities.

For faint extended objects the allowance for the sky background (in all strictness, the foreground) becomes important. In the rate-of-drift method with the electrometer it was necessary always to measure the blank sky and to subtract the proper correction from the measured light of cluster plus sky. In the constant-deflection method with the amplifier it is simpler to use the slide motion of the large plate base. The object can be placed in or out of the field by giving the screw a definite number of turns; the zero reading is on the sky. In this manner satisfactory measures of the light and the color of clusters or nebulae can be made when the sky effect is as much as five or six times that of the object.

Cell and filters.—The same potassium photoelectric cell has been used on the 100-inch in all the measures of globular clusters. This cell, our number QK 31-2, was constructed for us by Dr. Jacob Kunz in 1931 and has remained of uniformly excellent quality for five years. For measures of the colors of globular clusters a pair of blue and yellow filters was selected which give equal deflections at about spectral class G. The color-curves of the filters were determined in the physics laboratory at Madison with the setup that was used for the heavier filters for B stars. The photocell was too precious to transport from California to Madison just for calibration, but from comparative measures on stars it is known that cell QK 31-2 has a color sensitivity nearly the same as cell QK 302, the one cali-

brated at Madison. Table I gives the color sensitivities of cell QK 302, also of the filters used on the globular clusters. The reflecting power of silver mirrors is taken from the *Smithsonian Physical Tables* and presumably refers to fresh surfaces. The data in Table I are shown graphically in Figure 1.

TABLE I

COLOR SENSITIVITIES OF CELL WITH FILTERS

WAVE-LENGTH	CELL QK 302	REFLECTIONS TWO MIRRORS	TRANSMISSION		ON REFLECTOR		
			77*a*	GG5*b*	Clear	77*a*	GG5*b*
3300	12	.10	.00	.....	1.2	0.0	.....
3400	15	.35	.28	.....	5.2	1.5	.....
3500	18	.50	.50	.....	9.0	4.5	.....
3600	22	.58	.65	.....	13	8.4	.....
3700	28	.62	.75	.....	17	13	.....
3800	36	.65	.80	.....	23	18	.....
3900	50	.68	.83	.....	34	28	.....
4000	71	.71	.83	.00	50	42	0.0
4100	112	.74	.81	.05	83	67	4.2
4200	168	.76	.77	.14	128	99	18
4300	222	.78	.72	.27	173	125	47
4400	277	.80	.64	.45	222	142	100
4500	298	.82	.55	.62	244	134	151
4600	238	.82	.45	.74	195	88	144
4700	160	.82	.35	.82	131	46	107
4800	105	.83	.25	.86	87	22	75
4900	70	.83	.16	.88	58	9.3	51
5000	51	.83	.11	.89	42	4.6	37
5100	35	.84	.07	.90	29	2.0	26
5200	25	.84	.04	.90	21	0.8	19
5300	18	.85	.02	.91	15	0.3	14
5400	14	.85	.01	.91	12	0.1	11
5500	11	.86	.00	.91	9.5	0.0	8.6
5600	7	.86	.....	.92	6.0	.....	5.5
5700	4	.86	.....	.92	3.4	.....	3.1
5800	2	.86	.....	.92	1.7	.....	1.6
5900	0	.86	.....	.92	0.0	.....	0.0
Effective wave-length	.....	.....	.....	.....	4480	4340	4670

The combination of cell and filters with the large reflectors did not show much more sensitivity to the violet than did the same combination with the 15-inch glass objective, presumably because the sensitivity of the cell drops off rapidly to the violet of 4500 A. The absorption of the small quartz lens in the system has been neglected in

Table I; also that of a thin glass window in the vacuum tank for the amplifier. Neither of these is as important as the condition of the silvered mirrors of the telescope. Most of the observations in the present paper were taken before the 100-inch mirror was aluminized.

The effective wave-lengths at the bottom of Table I are given by the centroids of the areas under the corresponding curves. A check on the color system is furnished by the calculated and observed colors of Ao and Ko stars, assumed to be black-body radiators of

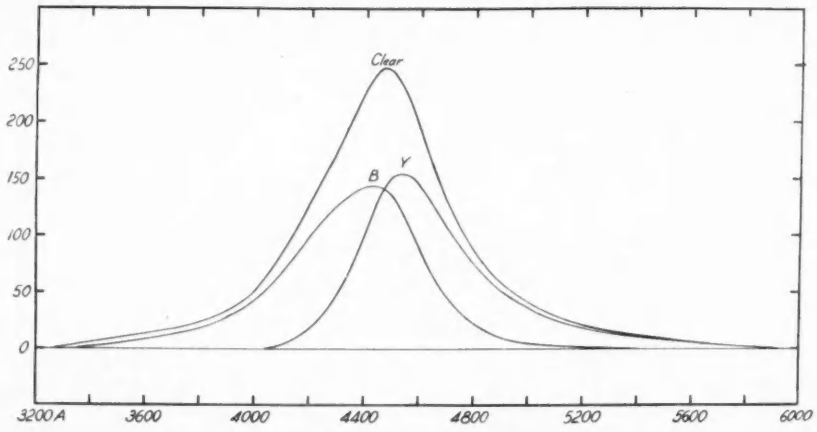

FIG. 1.—Color-curves of cell and filters

11,000° and 4000°. The value of the relative energy at each wave-length was computed from Planck's law and multiplied in turn by the respective sensitivities in the last two columns of the table. The sums of these two sets of products were then converted into the corresponding color indices. The discrepancies between the calculated and observed values may easily be due to the difference between the two photocells, but more probably to errors in the assumed temperatures, and to the deviations of the stars from true black-body radiators.

	Ao	Ko	Difference
Temperature	11,000°	4000°	.....
Calculated color index	$-0^{M}20$	$+0^{M}19$	$0^{M}39$
Observed color index	$-0^{M}27$	$+0^{M}17$	$0^{M}44$

The small separation between the effective wave-lengths of the two filters on the cell means that the observations must be precise to get color measures that are of value. Nevertheless, the combination of the potassium cell and these filters is the best that we have found for the purpose. Sodium oxide or cesium cells would furnish a much greater range of wave-lengths, but for faint objects the utmost sensitivity and freedom from dark current in a cell are required. The color of a diffuse cluster of magnitude 13 is more difficult to measure than the total light of a star of magnitude 14 with the 100-inch, corresponding to magnitude 10 with a 15-inch telescope. This limit is three or four magnitudes fainter than the published measures made with red-sensitive photocells. The faintest object we have ever attempted was a cluster in the Andromeda nebula which gave a photoelectric magnitude of 16.1 ± 0.1, but such a measure is an extreme case.

Atmospheric extinction.—The well-known quality of the sky at Mount Wilson is such that most of the results of the present paper would follow just the same if we should simply ignore the earth's atmosphere. At Madison there is a constant attempt to measure or guess at the absorption factor for a night, but at Mount Wilson any such efforts to distinguish between different nights would be futile. For photoelectric magnitudes we have adopted the uniform correction,

$$\text{Total extinction} = 0^{M}.30 \sec z .$$

For colors observed with the light filters the adopted correction is

$$\text{Differential extinction} = 0^{M}.06 \sec z.$$

Measures on various nights and a comparison with other filters indicate that the coefficient of differential extinction is sometimes nearer $0^{M}.05$ than $0^{M}.06$, but for uniformity we have continued to use the value first adopted. In any event, the effect of differential extinction is small compared with the apparent dispersion in color of the globular clusters themselves.

Color scale.—In the course of the work on globular clusters many measures were made on standard stars both for magnitude and

color. These stars were also often measured with the heavier filters used for the B stars. The adopted scale for the spectral classes is given in Table II.

These values, which are for giant stars, were taken for each class, with proper reduction in scale, as the average of the previous value used for B stars[5] and Seares's value for giant stars.[6]

Standard magnitudes.—As the diaphragms at the focus of the 100-inch were not large enough to take in all of any but the smallest clusters, the measured photoelectric magnitude refers usually to only a central region of a cluster. This limitation of the method is un-

TABLE II

NORMAL COLORS

Spectrum	Color Index	Spectrum	Color Index
B5	$-0^{M}.32$	G0	$-0^{M}.01$
A0	.27	G5	+ .08
A5	.20	K0	+ .17
F0	.16	K5	+0.30
F5	−0.09		

avoidable, unless the optical system is reconstructed to admit the light from much larger areas of the sky. Either in this manner or by transferring the amplifier to a smaller telescope the integrated magnitudes of the larger and brighter clusters could be measured; but because of the increased sky effect and the interference of more field stars, the colors could not be determined satisfactorily with openings much larger than were actually used. Such tests as were made with different diaphragms on the same cluster have failed to indicate measurable differences in color at different apparent distances from the center. The photoelectric magnitudes of the measured portions of the clusters were determined and referred to the same system of standard stars as was used for the nebulae. The procedure will be described in a later communication on magnitudes and colors of nebulae.

The observations.—Sample observations of two globular clusters are given in Table III, which shows the method of measurement and

[5] *Pub. Washburn Obs.*, **15**, 221, 1934.

[6] *Mt. Wilson Contr.*, No. 226, p. 34; *Ap. J.*, **55**, 198, 1922.

reduction. These two clusters were very difficult when measured with the electrometer, and the results of 1932 have been rejected. The new measures with the amplifier are quite satisfactory; the sky

TABLE III

OBSERVATIONS OF GLOBULAR CLUSTERS

	NGC 6426 AUGUST 16, 1933			NGC 6517 SEPTEMBER 16, 1933		
	Pointing	Reading	Deflection	Pointing	Reading	Deflection
		mm	mm		mm	mm
	Dark	38.5	.....	Dark	17.0	.....
	Sc	92.5	54.0	Sc	85.0	68.0
	Clc	127.0	32.8	Clc	132.0	45.0
	Sc	96.0	.....	Sc	89.0	.....
	Sy	72.5	.....	Sy	60.0	.....
	Cly	92.0	18.0	Cly	91.0	30.0
	Sy	75.5	.....	Sy	62.0	.....
	Sb	74.0	.....	Sb	60.0	.....
	Clb	89.5	14.5	Clb	80.0	19.5
	Sb	76.0	.....	Sb	61.0	.....
	Clb	93.0	15.5	Clb	83.5	21.5
	Sb	79.0	.....	Sb	63.0	.....
	Sy	82.0	.....	Sy	64.5	.....
	Cly	99.5	16.5	Cly	95.0	29.2
	Sy	84.0	.....	Sy	67.0	.....
	Sc	109.5	.....	Sc	97.0	.....
	Clc	141.0	29.8	Clc	143.0	44.5
	Sc	113.0	56.0	Sc	100.0	67.0
	Dark	57.0	.....	Dark	33.0	.....
	Clear	Yellow	Blue	Clear	Yellow	Blue
Deflection	31.3	17.2	15.0	44.8	29.6	20.5
log	1.496	1.236	1.176	1.651	1.471	1.312
Δ log	.....	0.260	0.320	.....	0.180	0.339
Δ mag	.....	0.65	0.80	.....	0.45	0.85
B−Y	.....	+ 0.15	.....	.....	+ 0.40	.....
Extinction	.....	− 0.11	.....	.....	− 0.10	.....
Color index C_2	.....	+ 0.04	.....	.....	+ 0.30	.....
Magnitude	.....	13.08	.....	.....	12.70	.....

R = 2.4×10^{11} ohm, shunt 1/3, diaphragm 64″
S = sky, Cl = cluster, c = no filter, y = yellow, b = blue

effect, which is nearly double the effect from the cluster, was readily eliminated by the new procedure of moving the cluster in and out of the field. The readings were taken every 45 seconds, making 13.5 minutes for a set. The drift of the galvanometer was between 1 and 2

mm per minute. The galvanometer was shunted to one-third sensitivity; at full sensitivity the deflections would have been larger but without any effective gain. The reductions are given in the table. Other observations of the colors of these clusters in the same year differ by only $0^{M}01$ in each case. The inferred magnitudes are based on several comparison stars.

From the constants of the circuit on the two nights, it was found that under the conditions of measurement 1 mm deflection corresponded to 1.2×10^{-16} amperes, and to stellar magnitude 16.8. A deflection of 5 mm for magnitude 15 could be measured with a probable error of less than say 0.5 mm, or 10 per cent. The useful limit for colors would have been about magnitude 14. Brighter clusters, say of magnitudes 10 and 11, were of course much easier than the faint ones, and with a lower resistance in the circuit the readings could be taken at intervals of 20 seconds instead of 45 seconds.

The observed magnitudes and colors of 69 globular clusters which have been derived in the past four years are given in Table IV. The second column gives the year of observation. Measures in 1932 were made with the electrometer; those in 1933 and later, with the amplifier. In one of the next three columns is the photoelectric magnitude for the corresponding diaphragm; in some cases the measures were repeated with a different diaphragm. In the next two columns are the average deviation and number of observations; all measures of one night were grouped into one observation. As noted before, the magnitudes are for limited central areas of the clusters, and they serve principally as indicators of the relative difficulty of the measures of color.

The eighth column gives the color class, which follows from the measured color index in the next column and the scale in Table II. The ninth column gives the color index C_2 measured with the filters described in Table I. The average deviation and the number of observations are counted in the same fashion as for the magnitudes. The values of C_2 have been corrected for small seasonal errors which depend upon the state of the mirrors of the telescope and probably also upon a progressive change in color sensitivity of the photocell. The following corrections to the measured values of C_2 were deter-

TABLE IV

COLOR OF GLOBULAR CLUSTERS

NGC	YEAR	Pe MAGNITUDE			A.D.	No.	COLOR CLASS	COLOR INDEX C_2	A.D.	No.	l	b	E
		42″	64″	128″									
(1)	(2)	(3)	(4)	(5)	(6)	(7)	(8)	(9)	(10)	(11)	(12)	(13)	(14)
	1900+												
288	35	.....	.....	10.56	±0M02	2	f6	−0M08	±0M03	2	203°.3	−89°.2	0M00
2419	32	.....	12.10	.....	.....	1	a9	− .17	.....	1	147.1	+25.2	− .15
4147	32, 34	.....	11.25	.....	.02	2	f6	− .07	.00	2	218.6	+78.1	+ .02
5024	32, 33	.....	9.66	.....	.02	2	f6	− .08	.01	2	304.9	+80.2	.00
5053	32	.....	.....	12.50	.....	1	.....	.....	.....	.....	307.4	+79.3	.....
5272	33	.....	8.48	.....	.00	2	f8	− .05	.02	2	13.2	+78.2	+ .05
5466	32	.....	.....	11.27	.01	2	f8	− .05	.03	2	11.9	+73.0	+ .05
5634	32, 34	.....	10.60	.....	.04	2	f6	− .07	.04	2	310.5	+49.6	+ .02
5694	35	.....	11.06	.....	.02	2	f6	− .07	.02	2	298.7	+30.9	+ .02
5824	33, 34	.....	9.85	.....	.06	2	f8	− .05	.02	2	300.1	+22.6	+ .05
5897	33	.....	.....	10.71	.....	1	f8	− .05	.....	1	310.7	+30.7	+ .05
5904	32, 34	.....	8.33	.....	.04	2	f8	− .05	.01	2	332.1	+46.8	+ .05
5986	33, 34	.....	9.53	.....	.....	1	f9	− .02	.01	2	304.4	+13.8	+ .10
6093	33, 34	.....	8.76	.....	.05	2	f9	− .02	.01	2	320.2	+19.7	+ .10
6121	32, 33	.....	9.89	8.69	.01	2	g3	+ .05	.02	2	318.4	+16.1	+ .22
6139	33, 34	11.62	10.98	.....	.04	2, 1	g9	+ .15	.06	3	309.6	+ 7.4	+ .39
6144	32, 34	.....	.....	10.97	.07	2	g1	+ .01	.01	2	319.3	+15.9	+ .15
6171	33, 34	.....	11.31	.....	.14	2	k0	+ .18	.02	2	331.0	+23.0	+ .44
6205	33, 34	.....	.....	7.59	.15	2	f9	− .03	.01	2	26.8	+40.0	+ .08
6218	32, 34	.....	10.18	9.26	.....	1, 1	g1	.00	.01	2	343.4	+26.1	+ .13
6229	33, 34	10.74	10.29	.....	.....	1, 1	f8	− .04	.00	2	41.1	+39.4	+ .07
6235	33, 34	.....	11.79	.....	.02	2	g1	.00	.05	2	326.3	+13.6	+ .13
6254	32, 33	.....	9.59	.....	.02	2	g2	+ .03	.00	2	342.7	+23.0	+ .19
6266	33, 34	.....	8.75	.....	.02	3	g5	+ .08	.02	3	320.9	+ 7.5	+ .27
6273	33, 34	.....	9.29	.....	.02	2	g3	+ .04	.00	2	324.2	+ 9.5	+ .20
6284	33, 34	.....	10.63	.....	.01	2	g1	.00	.02	2	325.2	+10.1	+ .13
6287	33, 34	.....	11.39	.....	.06	2	g7	+ .12	.02	2	327.5	+11.1	+ .34
6293	32, 34	.....	10.08	.....	.18	3	g0	− .01	.03	3	325.0	+ 7.9	+ .12
6304	32, 33	.....	10.39	.....	.06	2	k0	+ .18	.03	2	323.1	+ 5.5	+ .44
6316	32, 34	.....	11.12	.....	.06	3	g9	+ .15	.04	3	324.4	+ 5.9	+ .39
6325	32, 33	.....	12.86	.....	.09	5	g9	+ .16	.05	3	328.3	+ 8.1	+ .40
6333	32, 34	.....	9.75	.....	.06	2	g4	+ .06	.02	2	332.9	+10.7	+ .24
6341	33, 34	.....	8.22	7.55	.....	1, 1	f5	− .09	.01	2	35.8	+33.9	− .02
6342	32, 34	.....	11.92	.....	.06	2	k0	+ .18	.00	2	332.2	+ 9.7	+ .44
6356	32, 34	.....	10.17	.....	.10	2	g7	+ .11	.00	2	334.1	+10.2	+ .32
6366	32, 3, 4	.....	.....	12.42	.13	3	k3	+ .25	.07	3	345.9	+15.8	+ .55
6402	32	.....	10.82	.....	.12	2	g7	+ .11	.02	2	348.8	+14.5	+ .32
6426	32, 3, 4	14.04	13.05	.....	.02	1, 3	g6	+ .04	.00	2	355.6	+15.8	+ .20
6440	32, 34	12.13	11.77	.....	.03	3, 2	m	+ .37	.08	4	335.0	+ 3.7	+ .76
6441	32, 34	.....	8.96	.....	.08	3	g8	+ .14	.03	3	320.6	− 4.8	+ .37
6453	32, 34	11.90	.....	.....	.14	4	g6	+ .10	.05	4	322.8	− 3.8	+ .30
6517	32, 33	13.29	12.80	.....	.09	2, 2	k5	+ .30	.00	2	346.5	+ 6.5	+ .64
6522	32, 34	.....	10.49	.....	.18	2	g8	+ .14	.02	2	328.2	− 3.9	+ .37
6528	32, 34	.....	11.51	.....	.20	2	k2	+ .22	.02	2	328.3	− 4.1	+ .50
6535	32	.....	12.46	.....	.00	2	g1	.00	.06	2	354.5	+10.0	+ .13
6539	32, 3, 4	14.19	13.21	.....	.06	1, 4	m	+ .41	.09	3	348.1	+ 6.5	+ .82
6553	32, 34	.....	11.07	.....	.10	3	m	+ .36	.03	3	332.4	− 3.1	+ .74
6569	32, 34	.....	10.89	.....	.03	2	g9	+ .15	.02	2	327.6	− 6.6	+ .39
6624	33, 34	.....	9.66	.....	.03	2	g4	+ .07	.02	2	329.9	− 7.9	+ .25
6626	32	.....	9.09	.....	.08	2	g6	+ .09	.01	2	334.9	− 5.6	+ .29
6637	32, 34	.....	9.53	.....	.12	3	g7	+ .12	.03	3	328.7	−10.2	+ .34
6638	32	.....	10.43	.....	±0.08	2	g4	+ .06	.02	2	335.0	− 7.2	+ .24
6652	33, 34	10.80	10.19	.....	.....	1, 1	g3	+0.05	±0.04	2	328.6	−11.4	+0.22

TABLE IV—*Continued*

NGC	Year	Pe Magnitude			A.D.	No.	Color Class	Color Index C_2	A.D.	No.	l	b	E
		42″	64″	128″									
(1)	(2)	(3)	(4)	(5)	(6)	(7)	(8)	(9)	(10)	(11)	(12)	(13)	(14)
	1900+												
6656	32, 34	.....	9.37	7.93	±0M08	1, 2	*g2*	+0M03	±0M01	2	336°9	− 7°6	+0M19
6681	33, 34	.....	9.48	.....	.05	2	*f8*	− .04	.02	2	329.9	−12.5	+ .07
6712	33, 34	.....	10.83	.....	.04	3	*g7*	+ .11	.03	3	352.5	− 4.7	+ .32
6715	33, 34	.....	8.73	.....	.02	2	*g1*	+ .01	.00	2	332.6	−14.1	+ .15
6723	33, 34	.....	9.46	8.67	.....	1, 1	*f7*	− .06	.02	2	326.9	−17.2	+ .03
6760	32, 3, 4	.....	11.95	.....	.02	3	*k5*	+ .30	.08	4	3.5	− 4.4	+ .64
6779	32	.....	10.36	.....	.06	2	*f8*	− .04	.02	2	29.8	+ 7.5	+ .07
6809	32, 34	.....	?	.....	.....	2	*f5*	− .09	.00	2	335.6	−23.3	− .02
6864	32	.....	9.54	.....	.13	3	*g1*	+ .01	.01	3	347.0	−26.0	+ .15
6934	32	10.55	10.17	.....	.06	2, 1	*f8*	− .04	.02	3	19.1	−19.6	+ .07
6981	32, 33	.....	11.10	.....	.....	1	*f8*	− .04	.00	2	1.8	−33.1	+ .07
7006	32	.....	11.61	.....	.14	4	*f6*	− .07	.04	4	30.8	−20.3	+ .02
7078	32	8.63	8.03	7.38	.04	2, 3, 1	*f6*	− .08	.01	3	32.0	−28.2	.00
7089	32	8.84	8.28	7.61	.03	1, 1, 3	*f7*	− .06	.02	3	19.9	−36.6	+ .03
7099	32	9.48	9.02	.....	.05	1, 2	*f4*	− .11	.01	2	353.3	−47.2	− .05
7492	32, 35	.....	.....	12.40	±0.04	3	*a5*	−0.20	±0.03	3	19.2	−64.2	−0.20

NOTES ON TABLE IV

NGC 2419 Only one observation, but apparently good.
5053 Too faint and diffuse for measurement of color.
6809 Magnitudes 8.7 and 9.6. Probably a mistake in record of diaphragm or shunt.
7492 The outstanding blue color of this cluster is apparently real.

mined from observations of the same standard stars and clusters in different years:

1932....0M00, 1933....−0M01, 1934....−0M05, 1935....+0M05.

The jump between 1934 and 1935 was due to the aluminizing of the mirrors of the 100-inch telescope.

In the twelfth and thirteenth columns are the galactic co-ordinates, l and b, taken from the Vatican tables, which are based on Newcomb's pole, R.A. = 12h44m4, Decl. = +26°8 (1900).

The last column gives the color excess E, which has been reduced to the color system C_1 of the heavier filters used for the B stars. The ratio of the two color scales is $C_1/C_2 = 0.74/0.44 = 1.682$. The average color of a cluster near the pole of the galaxy is taken as $C_2 = -0^M08$. The value of E is then given by the relation

$$E = 1.682(C_2 + 0^M08) . \qquad (1)$$

The normal colors for B stars were likewise found from the average colors in high latitudes, but a bright B star in high latitude may be immersed in the hypothetical thin layer of absorbing material within a hundred parsecs or so of the plane of the galaxy, whereas a globular cluster in the same direction will probably be quite outside such a layer. Neverthless, since the maximum selective absorption toward the galactic pole probably does not exceed $0^{M}.03$[7] on the scale of C_2, it is convenient to adopt the foregoing expression for E and treat the clusters as very distant B stars.

The precision of the results is indicated by the following probable errors:

Limits of magnitude	7–10	10–12	12–13
Probable error of one observation for magnitude	$\pm 0^{M}.064$	$\pm 0^{M}.088$	$\pm 0^{M}.069$
Probable error of one observation for color	$\pm 0^{M}.017$	$\pm 0^{M}.035$	$\pm 0^{M}.059$

The errors of the magnitudes are nearly independent of brightness, but the colors are increasingly discordant for fainter clusters. As there are two or three observations for each cluster, the probable error of a mean color index ranges from about $\pm 0^{M}.01$ to $\pm 0^{M}.04$.

Relation of colors to character of fields.—Perhaps the first and easiest test to apply to the colors of the globular clusters is to see how the colors are correlated with the number of nebulae or the richness of the star fields in the region of the clusters. Dr. Baade has kindly examined his available plates, taken with the large reflectors, and has noted for each cluster the character of the field both for nebulae and for stars. In a general way he has taken into account the latitude effect; the nebulae decrease and the stars increase from the pole toward the galactic equator. In Table V the clusters are arranged in the order of color excess, and the fields are divided into three classes for both nebulae and stars. For the nebulae, "normal" means that Baade estimates that the number of nebulae is about as expected with a rough allowance for absorption according to the cosecant law. "Less than normal" means that there is local obscuration. Similarly for the stars, the rich star fields of the Milky Way are marked as "nor-

[7] *Mt. Wilson Comm.*, No. 111, p. 2; *Proc. Nat. Acad.*, **19**, 223, 1933.

TABLE V

RELATION OF COLORS TO CHARACTER OF FIELDS

NGC	E	Number of Nebulae			Star Field		
		Normal	Less than Normal	None	Normal	Partially Obscured	Heavily Obscured
7492	$-0^{M}20$	×					
2419	− .15	×					
7099	− .05	×					
6341	− .02	×					
5024	.00	×					
7078	.00	×					
4147	+ .02	×					
5634	+ .02	×					
5694	+ .02	×					
7006	+ .02	×					
7089	+ .03	×					
5272	+ .05	×					
5466	+ .05	×					
5897	+ .05	×					
5904	+ .05	×					
6229	+ .07	×					
6779	+ .07	×			×		
6934	+ .07	×					
6981	+ .07	×					
6205	+ .08	×					
6093	+ .10		×		×		
6218	+ .13	×					
6235	+ .13		×		×		
6535	+ .13	×			×		
6864	+ .15	×					
6254	+ .19			×		×	
6656	+ .19			×	×		
6273	+ .20			×		×	
6426	+ .20		×		×		
6121	+ .22			×	×		
6333	+ .24			×		×	
6266	+ .27			×	×		
6356	+ .32			×	×		
6402	+ .32			×		×	
6712	+ .32			×	×		
6287	+ .34			×			×
6325	+ .40			×			×
6171	+ .44			×		×	
6366	+ .55			×		×	
6517	+ .64			×			×
6760	+ .64			×		×	
6440	+ .76			×			×
6539	+0.82			×			×

mal"; "partially obscured" and "heavily obscured" represent degrees of scarcity of stars in fields in low latitude.

The close correlation of the colors with the numbers of nebulae is striking. For all values of E less than $+0^{M}10$ the nebulae are marked as normal, but when E is greater than $+0^{M}20$ there are no nebulae on

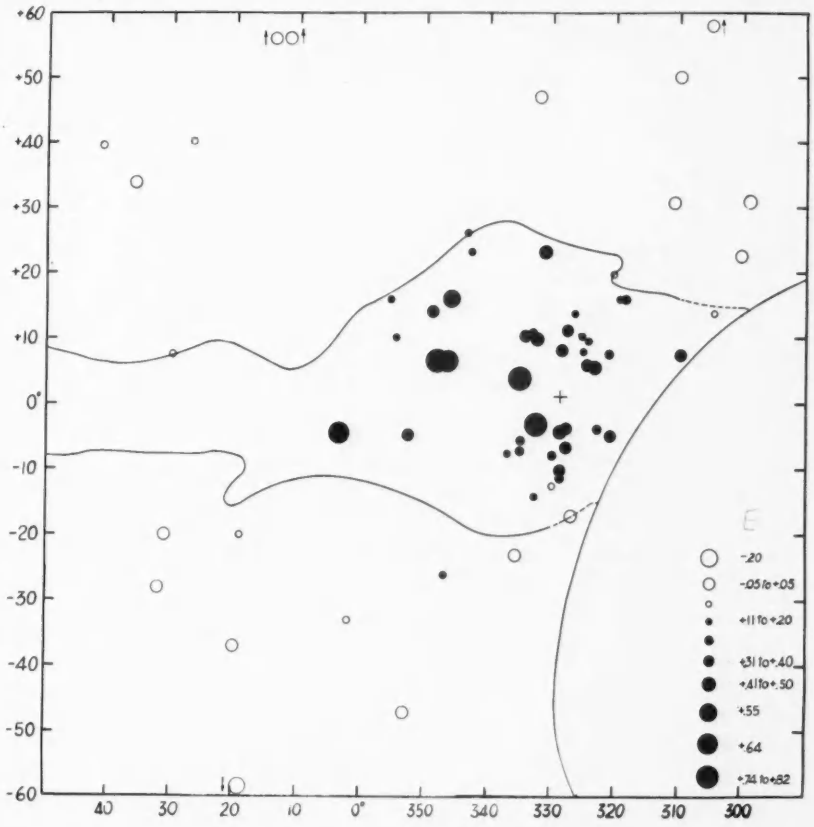

FIG. 2.—Colors of globular clusters

the plates. The break is more sudden if we count simply the presence or absence of nebulae. When E is less than $+0^{M}19$, there are nebulae on the plates; when E is greater than $+0^{M}20$, no nebulae are found. Perhaps longer exposures and a careful search in the regions where E is near $+0^{M}20$ would bring out some faint nebulae, since we should scarcely expect complete extinction where the selective absorption

is so small, unless indeed the cluster is immersed in the dark material and there is further absorption beyond.

The relation of the colored clusters to the star fields is not so definite. There may be rich star clouds in the foreground which conceal the presence of more distant absorbing regions; but whenever there is heavy nearby obscuration, as evidenced by scarcity of stars in low latitude, the globular clusters are strongly colored.

The quick transition in Table V from presence to absence of nebulae indicates that there are probably no large errors in the observations, and also that the dispersion in color of the clusters themselves is small. The only obvious cases of anomalous color are the two clusters at the top of the table, NGC 7492 and 2419; there may be others down the list which are hidden in the sequence.

TABLE VI

NGC	l	b	E
288	203°	−89°	−0^{M}00
1904	195	−29	.....
2298	213	−15	.....
2419	147	+25	− .15
4147	219	+78	+0.02
4590	267	+37	.....

The general system of globular clusters.—The globular clusters are charted in galactic co-ordinates in Figure 2. There are six other recognized globular clusters north of declination −40° which are not in the figure; they are given in Table VI. All are in latitude 15° or higher; three were observed and found to have little or no color excess, the others are probably likewise normal in color.

The concentration of the clusters near longitude 330° and near the zone of avoidance along the line of the galactic equator is well known; the strongly reddened clusters emphasize this apparent distribution. As in the case of the B stars, the irregular outlines of Hubble's zone of avoidance of the nebulae also mark roughly the limits of the reddened clusters, particularly within the bulge of Hubble's zone about the center of the galaxy. The limits are not sharp and definite; there are a few nebulae here and there within the zone. The slightly reddened cluster at $l = 347°$, $b = -26°$, is NGC 6864, for which the ob-

PLATE IV

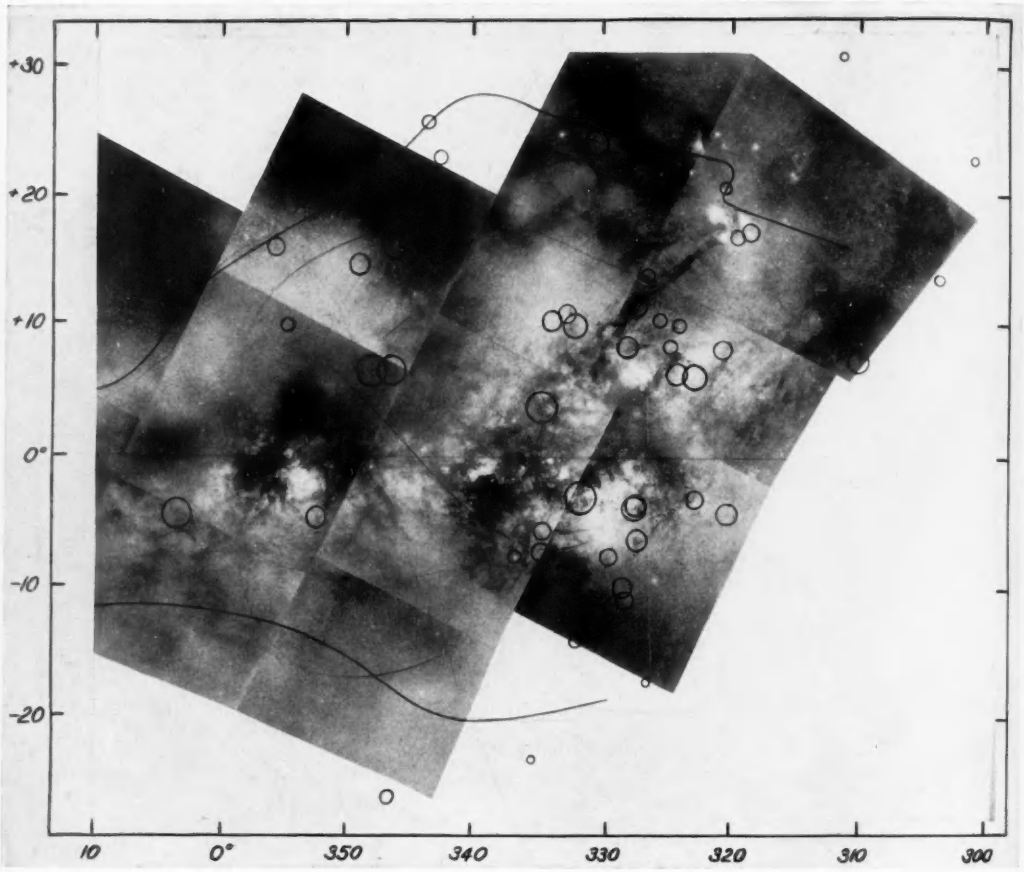

GLOBULAR CLUSTERS AND THE MILKY WAY

servations are accordant. There are other slight anomalies, but no matter what the physical interpretation, it is possible to arrange the clusters in a self-consistent diagram. The outer clusters are of uniform color, corresponding to spectrum about F6; they grow redder toward the galactic equator, with colors equal to that of an M star near the narrow zone of avoidance.

The relation of the globular clusters to the star clouds and obscured areas of the Milky Way is shown in Plate IV. The mosaic of photographs by Ross gives a general picture of the system which can be had in no other way. To avoid blotting out the stars, the clusters are represented by open circles, the larger the circle the redder the cluster. Each cluster has been identified first on a chart in Ross's *Atlas*, then on the mosaic, where it is the exact center of the corresponding circle. As was shown in Table V, the reddest clusters may or may not be located in heavily obscured areas; there may be rich star clouds in front of absorbing regions, which are in turn on this side of the clusters. The fundamental zone of avoidance along the plane of the galaxy is marked by many dark patches, but there are still many stars in the foreground.

If the cluster NGC 6440 at $l = 335^\circ.0, b = +3^\circ.7$, marks the northern edge, then the zone of avoidance is $6^\circ.8$ wide. We think it more probable that this cluster is actually a foreground object, between us and the main absorbing region, in which case the zone becomes $8^\circ.5$ wide between the limiting clusters, NGC 6304 and 6553. Incidentally, the median line would then be $1^\circ.2$ north of the galactic equator fixed by Newcomb's pole, which we have used, and $0^\circ.25$ south of the equator of the Harvard system with its pole at 12^h40^m, $+28^\circ.0$ (1900). We can scarcely fix the fundamental plane of the galaxy by the positions of two globular clusters, but we can come close to it until some new cluster is found.

It is fair to assume that the nucleus about the center of the system is marked by the group of some 26 clusters near longitude 330°, 13 on each side of the equator. By simply taking the centroid of the l's and b's of this group we find

	l	b
Newcomb's pole.....	$328^\circ.6$	$+1^\circ.0$
Harvard pole.....	329.2	−0.5

This position of the center is probably as good as can be derived from the entire visible system of globular clusters, for there are no doubt dozens, if not scores, of hidden or undiscovered clusters, and the inclusion of only a few additional objects would make a marked change in the calculated center. Edmondson,[8] from a study of the radial velocities of the globular clusters, concludes that the clusters which we see do not constitute half of the total number of the system.

There is now no doubt that Shapley's first distances of clusters must be corrected for absorption. In making the corrections the natural sequence of assumptions is (*a*) transparent space, (*b*) uniform absorption according to the cosecant law, (*c*) irregular absorption measured by individual colors of clusters. On the assumption that the absorption varies according to the cosecant law, we have for the optical thickness of the layer, or total photographic absorption from pole to pole, Hubble's[9] value of $0^{m}.50$, determined from the counts of nebulae. The formula for the correction factor f to be applied to Shapley's distances becomes

$$\log f = -0.05 \operatorname{cosec} |b|. \qquad (2)$$

Corrections on this basis have been made by Baade,[10] and the resulting form and dimensions of the general system are shown in his paper.

As a test of the plausibility of this improved system we have divided the clusters into two groups, according to their distances from the galactic plane, and have computed the distance to the centroid of each group:

For $|Z| > 3.0$ kpc, 46 clusters give $\overline{X} = +8.2$ kpc,

For $|Z| \leqq 3.0$ kpc, 46 clusters give $\overline{X} = +7.6$ kpc.

The agreement between the two centers is close enough; a couple of undiscovered clusters at 10 or 15 kpc beyond the nucleus would move the center of either group by a whole kiloparsec farther from the sun.

[8] *A.J.*, **45**, 1, 1935.

[9] *Mt. Wilson Contr.*, No. 485, p. 44; *Ap. J.*, **79**, 51, 1934.

[10] *Mt. Wilson Contr.*, No. 529; *Ap. J.*, **82**, 396, 1935.

In Shapley's original system the division into groups at $|Z| = 4.8$ kpc gives $\overline{X} = 18.5$ and 14.3 kpc, respectively.

We are far enough from the center of the galaxy to see for ourselves the central condensation of clusters, as shown in Figure 2. The clusters in that direction comprise about a fourth of the total visible number, and surely it is more probable that they are grouped together than that they are strung out radially from the sun. Therefore, a chart of this group in space will give a test of the plausibility of their inferred distribution. Baade used approximately Hubble's value of the optical thickness of $0^{M}.50$ for the absorbing layer, which is an average for all longitudes; but for this test of the group toward the center we have used van de Kamp's value of $0^{M}.80$ for the optical thickness, which gives

$$\left.\begin{aligned} \log f &= -0.08 \operatorname{cosec} |b| \\ R_1 &= fR \end{aligned}\right\}, \tag{3}$$

where R is the original and R_1 the corrected distance. We also used his revision of Shapley's distances, which omits the estimates based on apparent diameters. In effect, we have simply taken van de Kamp's co-ordinates for the clusters near the center and have charted them in Figure 3*a*.

The co-ordinates as corrected by means of equation (3) are in Table VII. In the second column the galactic latitude b is on the Harvard system, used by van de Kamp. The third and fourth columns give the uncorrected R and the corrected R_1, respectively; all distances are in kiloparsecs. Cases which seem to be relatively uncertain are marked with colons (:). In the next three columns X_1, Y_1, and Z_1 have been taken from Shapley's[11] X, Y, Z, each reduced in the ratio of R_1 to Shapley's R. The co-ordinates in the last four columns are the values derived subsequently from equation (10).

Other considerations, especially the distribution of colored B stars, have convinced us that the simple assumption of a uniform layer of absorbing material near the plane of the galaxy will not suffice. It may be convenient to conceive of a model of the galaxy with

[11] *Star Clusters*, pp. 173 and 225.

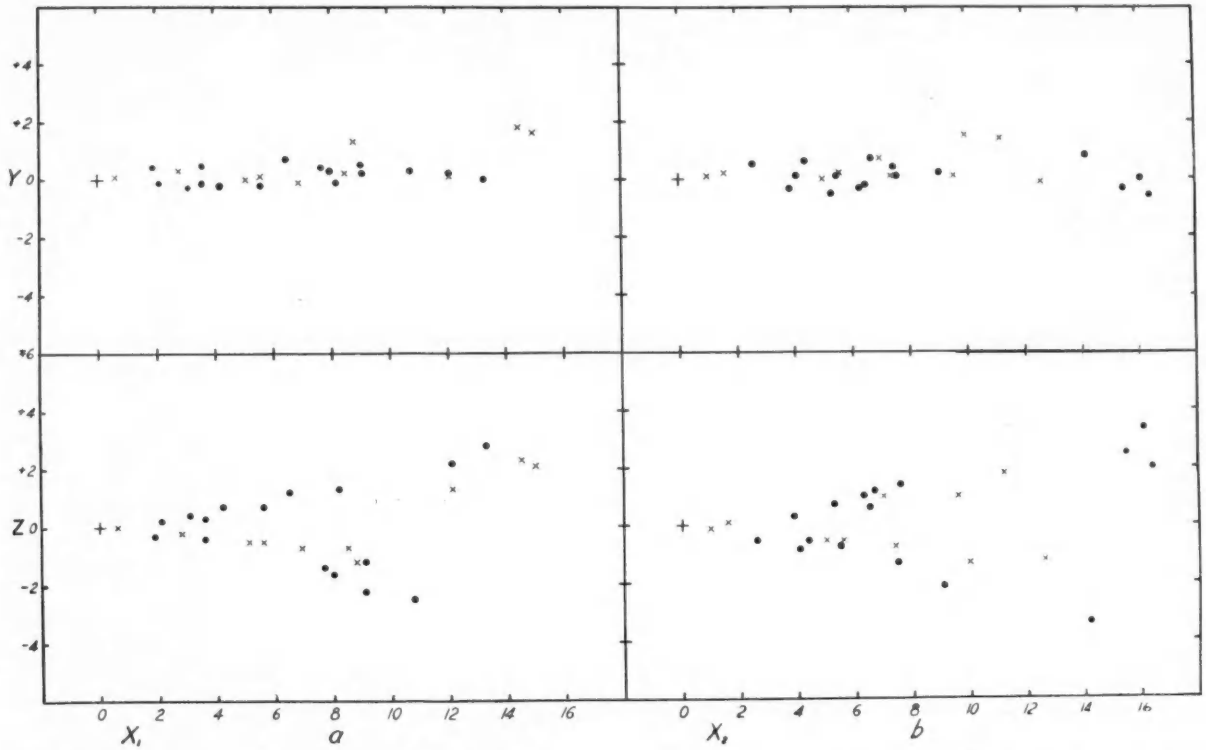

FIG. 3.—Globular clusters near the center of the galaxy: (*a*) distances corrected by $\log f = \log (R_1/R) = -0.08 \csc |b|$; (*b*) distances corrected by $\log f = \log (R_2/R) = -2.0E$.

such a distribution of dark material; but at least there should be a dependence upon the longitude, presumably with the greatest absorption toward the center. We have attempted to take the spotted nature of the effect into account by using the color of each cluster instead of the cosecant law as a guide to the amount of absorption in

TABLE VII

CO-ORDINATES OF CLUSTERS NEAR THE CENTER OF THE GALAXY

NGC (1)	b (2)	R (3)	R_1 (4)	X_1 (5)	Y_1 (6)	Z_1 (7)	R_2 (8)	X_2 (9)	Y_2 (10)	Z_2 (11)
6235	+12°.1	29.9	13.6	+13.3	0.0	+2.8	16.4	+16.1	0.0	+3.4
6266	+ 6.0	18.7	3.2	3.1	−0.3	+0.4	5.4	5.3	−0.5	+0.7
6273	+ 8.0	16.1	4.3	4.2	−0.2	+0.7	6.4	6.3	−0.3	+1.0
6284	+ 8.6	28.6	8.3	8.2	−0.1	+1.3	15.7	15.5	−0.3	+2.5
6287	+ 9.6	37.2	12.3	12.1	+0.2	+2.2	7.8	7.6	+0.1	+1.4
6293	+ 6.5	28.8	5.7	5.6	−0.2	+0.7	16.6	16.4	−0.6	+2.0
6304	+ 4.0	29.4	2.1	2.1	−0.1	+0.2	3.9	3.9	−0.3	+0.3
6316	+ 4.4	39.6	3.6	3.6	−0.1	+0.3	6.6	6.5	−0.2	+0.6
6325	+ 6.6	60.3:	12.1	12.1	+0.1	+1.3	9.6	9.6	+0.1	+1.0
6333	+ 9.3	20.8	6.7	6.5	+0.7	+1.2	6.9	6.7	+0.7	+1.2
6342	+ 8.3	55.0:	15.3	15.0	+1.6	+2.1	7.2	7.0	+0.7	+1.0
6356	+ 8.8	50.−:	15.0	14.5	+1.8	+2.3	11.5	11.2	+1.4	+1.8
6440	+ 2.3	53.0:	0.6	0.6	+0.1	0.0	1.6	1.6	+0.2	+0.1
6441	− 6.3	27.4:	5.1	5.1	0.0	−0.5	5.0	5.0	0.0	−0.5
6453	− 5.3	50.1:	6.9	6.9	−0.1	−0.7	12.6	12.6	−0.1	−1.2
6522	− 5.3	40.6:	5.6	5.6	+0.1	−0.5	7.4	7.4	+0.1	−0.7
6528	− 5.6	55.5:	8.5	8.5	+0.2	−0.7	5.6	5.6	+0.2	−0.5
6553	− 4.5	29.0:	2.8	2.8	+0.3	−0.2	1.0	1.0	+0.1	−0.1
6569	− 8.1	34.0	9.2	9.1	+0.2	−1.2	5.6	5.5	+0.1	−0.7
6624	− 9.4	24.4	7.9	7.7	+0.4	−1.4	7.7	7.5	+0.4	−1.3
6626	− 7.0	17.0	3.7	3.6	+0.5	−0.4	4.5	4.4	+0.6	−0.5
6637	−11.7	20.1	8.1	8.0	+0.3	−1.6	4.2	4.1	+0.1	−0.8
6638	− 8.6	30.9:	9.0	8.8	+1.3	−1.2	10.2	10.0	+1.5	−1.3
6652	−12.8	25.6	11.1	10.8	+0.3	−2.5	9.3	9.1	+0.2	−2.1
6656	− 9.0	6.7	2.1	1.9	+0.4	−0.3	2.8	2.6	+0.5	−0.5
6681	−13.9	20.1	9.3	+ 9.1	+0.5	−2.2	14.6	+14.2	+0.8	−3.4

any direction. This procedure involves the assumption that the ratio of the selective to the general absorption is constant, that the relative proportion of the light-scattering particles and the light-obstructing particles is the same throughout the space considered.

The first solution for the dependence of the colors upon the latitudes of the globular clusters gave the relation[7]

$$C_2 = -0^{M}.081 + 0^{M}.0237 \operatorname{cosec} |b| . \qquad (4)$$

This formula indicates a selective absorption from pole to pole of $2 \times 0^{M}.0237 = 0^{M}.0474$, which, multiplied by 1.682, gives the round figure $0^{M}.08$ on the scale of E. This last value could be improved by the inclusion of data from additional clusters; but the cosecant law is only a rough approximation. If the cosecant law represented the absorption closely, we should have at once the ratio of our selective absorption, $0^{M}.08$ pole to pole, to Hubble's $0^{M}.50$ total photographic absorption, or to van de Kamp's[12] $0^{M}.8$, both from counts of nebulae. The difficulty with such a comparison is that the computed selective absorption is fixed largely by the clusters in low latitudes where there are no nebulae visible, while the counts of nebulae are made in moderate to high latitudes. Moreover, Hubble's value is a mean for all longitudes; and we may expect a larger value, possibly as much as $0^{M}.8$, for the photographic optical thickness of the absorbing layer in the region between the sun and the galactic center. We have, then, 0.08/0.8, or roughly 1:10, for the ratio of our selective absorption on the scale of E to the total photographic absorption.

We have found in a comparison with the North Polar Sequence that the factor 1.6 is required to reduce our color scale of E to that of C, international photographic *minus* photovisual. If we assume, following the old rule for extinction in the earth's atmosphere, that the photographic absorption is twice the visual, then the color excess or differential absorption on the scale of C is just half of the total photographic absorption. We have, therefore, $2 \times 1.6\ E = 3.2\ E$ as the plausible photographic absorption due to selective scattering for a cluster of measured color excess E.

Or we may proceed in a different way: As shown in Table I, the effective wave-lengths of the two filters combined with the cell are 4670 and 4340 A. The effective wave-length of Eastman 40 plates, computed in the same way from data given by Mees,[13] allowing for two reflections from silver, is 4250 A. These computations are for an equal-energy spectrum. The slight variations in effective wave-length for stars of different color temperature, with radiation-curves modified more or less by space reddening, are neglected in this dis-

[12] *A.J.*, **42**, 97, 1932; 161, 1933. Van de Kamp derived $0^{M}.8$ from the Harvard survey, $1^{M}.4$ from Mount Wilson selected areas; he adopts $0^{M}.8$ as more probable.

[13] *J. Opt. Soc. Amer.*, **21**, 753, 1931.

cussion. Let I_{pg}, I_y, and I_b represent the observed intensities with the photographic plate, with the cell and yellow filter, and with the cell and blue filter, respectively. Let I^0_{pg}, I^0_y, and I^0_b represent the same intensities prior to reduction by selective scattering in interstellar space. Then we have

$$2.5 \log_{10} \frac{I_{pg}}{I^0_{pg}} = -t\lambda_{pg}^{-4}, \tag{5}$$

$$2.5 \log_{10} \frac{I_y}{I'_y} = -t\lambda_y^{-4}, \tag{6}$$

$$2.5 \log_{10} \frac{I_b}{I^0_y} = -t\lambda_b^{-4}, \tag{7}$$

where t is proportional to the optical path in that part of the interstellar material which scatters according to the Rayleigh law. Subtracting (7) from (6), we have

$$2.5 \log_{10} \frac{I_y}{I_b} - 2.5 \log_{10} \frac{I^0_y}{I^0_b} = -t(\lambda_y^{-4} - \lambda_b^{-4}). \tag{8}$$

The terms on the left-hand side of the equation are seen to be the observed color index and the normal color index, respectively; and their difference therefore represents the color excess. Equation (5) gives simply the photographic absorption in magnitudes due to selective scattering. We find, therefore, from (5) and (8):

$$\frac{\text{Photographic absorption}}{\text{Color excess}} = \frac{\lambda_{pg}^{-4}}{\lambda_b^{-4} - \lambda_y^{-4}} = \frac{4250^{-4}}{4340^{-4} - 4670^{-4}} = 4.29. \tag{9}$$

This result applies when the color excess is expressed on the scale of C_2. When converted to the scale of E, the photographic absorption would be $4.29/1.6 = 2.7\ E$, in fair agreement with the result by the other method.

We must conclude, then, that the value $10\ E$ for the total photographic absorption, derived from counts of nebulae, is three or four times the absorption we might infer from the reddening alone. Some such result as this is to be expected, otherwise faint stars in the ob-

scured areas in the Milky Way would be much redder than they are found to be. In a discussion of the total amount of interstellar matter which causes space reddening it is necessary, in order to avoid an impossibly large mass, to suppose that the scattering material is composed largely of solid particles rather than gas molecules. It would indeed be surprising if some of the particles were not too large to scatter according to the Rayleigh law, and therefore merely obscure without reddening. Further evidence for the existence of non-selective absorption is found in the case of extra-galactic nebulae in regions where the nebular counts indicate heavy absorption but where the colors of the nebulae are not very much affected.

The uncorrected distance R of a globular cluster with distance modulus $m-M$ is given by

$$5 \log R = m - M + 5 ;$$

and the corrected distance R_2 when the absorption is $10\,E$, is given by

$$5 \log R_2 = m - 10\,E - M + 5 .$$

We have, then, for f the correction factor,

$$\log f = \log \frac{R_2}{R} = -2.0\,E . \qquad (10)$$

The distances of the 26 clusters near the galactic center have been revised by means of equation (10); the resulting co-ordinates are in the last four columns of Table VII, and the clusters are shown in Figure 3*b*.

Since the average absorption has been taken as about the same, we should expect the groups in Figures 3*a* and 3*b* to have comparable overall dimensions, which is the case. However, there is not much that is convincing in either system; the clusters are drawn out along the X-axis instead of being condensed about a center. The distances are probably still subject to large errors. Apparently, the proper corrections cannot be made either from the cosecant law or from the colors, or else the original uncorrected distances are uncertain.

It may be noted that the distances for this group near the center are among the weakest in the entire system of globular clusters. The bases of Shapley's estimated distances of the 26 clusters were as follows:

From variable stars and bright stars	2
From bright stars	5
From total magnitudes and diameters	15
From total magnitudes	4
	26

When the diameters are disregarded, there are 19 clusters with distances based on total magnitudes alone; no individual stars were measured in any of them, and they are distributed over ten of Shapley's twelve classes of relative concentration. Moreover, about half of these clusters are fainter than tenth magnitude, which means that the distance modulus must be extrapolated from the calibration-curve. The effect of space absorption is to make these important objects faint and difficult to study.

It is unlikely that the apparent diameter of any obscured globular cluster will contribute much toward the determination of its distance. The contraction of the apparent diameter by space absorption presumably depends upon how much the cluster is condensed toward the center. The effect of absorption can be simulated by long and short exposures for photographs of the same cluster. In the latest work by Shapley and Sayer[14] on the angular diameters of globular clusters, the correction factors for the revision of diameters, previously used for estimates of distances, range from 1.3 to 10, an indication of the difficulties involved in measuring consistently so indefinite a thing as the diameter of a globular cluster. It seems best, therefore, to follow van de Kamp and use only the strictly photometric data for the derivation of distances.

The effect of errors in the measured colors on the corrected distances in Figure 3*b* may be traced as follows: For the 26 clusters the probable error of one color index C_2 from the mean of two observations is $\pm 0^{M}.023$, which corresponds to $\pm 0^{M}.04$ in E, ± 0.08 in log R, and ± 20 per cent in R. Roughly a deviation of $0^{M}.01$ or 1 per cent

[14] *Proc. Nat. Acad.*, **21**, 593, 1935.

in the measured color corresponds to 8 per cent in the derived distance; and it would be strange, indeed, if the integrated colors of clusters which look so strikingly different at the telescope do not differ by several hundredths of a magnitude. Even so, the assumption of equal intrinsic colors for all clusters does not seem to us as far fetched as the assumption that any considerable number of clusters have the same total light and the same linear diameter, no matter how many stars they contain.

If any new globular clusters should be discovered near the galactic center, their magnitudes and colors could no doubt be measured with the present equipment; but the clusters would probably be in rich

TABLE VIII

Photographic Optical Thickness	Distance to Center	Basis
$0^{M}0$	16.4 kpc	Shapley, original moduli
0.32	10.0	From colors of globular clusters
0.50	8.0	From Hubble's counts of nebulae
0.8	5.5	Van de Kamp, from Harvard counts of nebulae

star fields, and it would be best to get data on individual stars, preferably variables, which could be identified as belonging to the clusters. Such stars would be of the seventeenth or eighteenth magnitude and would be too faint for a photocell on the 100-inch reflector. With the 200-inch telescope they might be reached, but the measures would be tedious. Probably the best procedure would be to use the cell to establish faint standards among the field stars of a cluster, and let the detailed work on the variables be done by photography.

The values of the distance to the center of the system of globular clusters derived from different assumed values of the optical thickness of the absorbing layer from pole to pole are summarized in Table VIII. The different results are not strictly comparable, as there were revisions or omissions of data for individual clusters in the later determinations; but the general effect of different optical thicknesses of a uniform layer is shown. All three of the revised systems agree in

placing most of the clusters within a sphere of 15,000–20,000 parsecs in radius. A better revision of the general system might be made on the basis of the individual colors, but we have not the colors of clusters south of declination $-40°$.

Any picture of the system is necessarily incomplete without the clusters in the zone of avoidance; and to us it seems probable that the clusters in the central group, Figure 3*b*, are mostly on the side of the center toward the sun. If, then, clusters extend beyond the center and some of them lie outside the main region of absorption, we ought to find extra-galactic nebulae in the same fields; but this is not the case. The nebulae are blotted out, but the light of the clusters comes through. The center of the system can still be at a distance of the order of 10 kpc, without requiring the extreme overall dimensions for the galaxy that were first inferred from the uncorrected distances of the globular clusters. It remains to be shown that there is any great star density in the regions of the outlying clusters, and comparisons with other galaxies should be based upon the same data in each case. Hubble finds a possible distance of nearly 30 kpc between two globular clusters of the Andromeda nebula, and other such objects might extend that system still further. Our galaxy is a large one; but when its apparent dimensions are corrected for space absorption, and the extension of the Andromeda nebula, both in stars and in clusters, is considered, the two systems seem to be of the same order of size.

The work of the present paper was supported by grants from the Alumni Research Fund of The University of Wisconsin, the National Research Council, and the California Institute of Technology, the last in connection with plans for the 200-inch reflector.

CARNEGIE INSTITUTION OF WASHINGTON
MOUNT WILSON OBSERVATORY,
UNIVERSITY OF WISCONSIN
WASHBURN OBSERVATORY
April 1936

THE LUMINOSITY FUNCTION OF NEBULAE*

EDWIN HUBBLE

I. THE LUMINOSITY FUNCTION OF RESOLVED NEBULAE AS INDICATED BY THEIR BRIGHTEST STARS

ABSTRACT

The brightest star, arbitrarily defined as the mean of the three or four brightest individual, non-variable stars in a nebula, is calibrated as a criterion of distance ($\overline{M}_s = -6.35$, $\sigma_s = 0.41$).

The luminosity function of resolved nebulae is then derived from the frequency distribution of $m_s - m_n$, which measures the luminosity of a nebula in terms of its brightest star as the unit. The luminosity function approximates a normal error-curve with $M_{on} = -14.2 \pm$, $\sigma_n = 0.85$, and $\overline{M}_n = -15.18$.

Incomplete data for brightest stars in members of the Virgo cluster suggest a modulus, $m - M$, of 26.6 or slightly larger. Cluster members are roughly comparable with resolved field nebulae, and, within the cluster, different types of nebulae are comparable among themselves.

FUNDAMENTAL CRITERIA OF DISTANCE

Fundamental distances of nebulae[1] are derived from their stellar contents—from the apparent faintness of familiar objects whose intrinsic luminosities are known. These absolute distances serve to calibrate two other criteria—red shifts and total luminosities—which would otherwise furnish only relative distances. Investigations of stellar contents are necessarily restricted to neighboring nebulae. The problems are simplified by the fortunate chance that the galactic system is one component of a triple nebula (the Magellanic Clouds being the satellites) which is itself a member of a local group, isolated in the general field of nebulae. Thus a number of stellar systems are concentrated in our immediate neighborhood and can be studied in considerable detail. The local group furnishes a sample collection of nebulae for the determination of the general characteristics of stellar contents.

Stars in the Magellanic Clouds are studied with existing instru-

* *Contributions from the Mount Wilson Observatory, Carnegie Institution of Washington*, No. 548.

[1] The term "nebulae" is used throughout this paper for extra-galactic nebulae only. Galactic nebulae are referred to as nebulosities.

ments down to about $M = 0$, and later with the completion of telescopes now under construction the limit will be extended to $M = +2$ or fainter.[2] The present limit for other members of the local group, all of which are within a million light-years of the earth, is about $M = -1.5$, and the completion of the 200-inch reflector should push this limit down toward zero. As for nebulae in the general field, possibly half a dozen are within 2.5 million light-years, and the present limit for investigating stellar contents at that distance is about $M = -4$. The assembling of a significant sample collection from the general field would evidently have been a difficult task with existing equipment.

The local group is the peculiar realm of the Cepheid criterion of distance. Cepheids can be readily observed out to the limits of the group, and distances would be well determined if it were not for uncertainties in the effects of galactic obscuration. Since the local group is elongated and the galactic system with its two satellites is situated near one end, the other members are seen in one general direction. The center of the apparent distribution is near M 31, at galactic latitude about $-20°$. Only one member—NGC 6822, which is the nearest—lies more than 40° from this center. The nebulae tend to cluster in low (southern) latitudes, where local obscuration is considerable. Even the satellites are subject to appreciable obscuration, the Large Cloud being at $\beta = -33°$ and the Small Cloud at $\beta = -45°$. Therefore, uncertainties are introduced into the very data which must be used in calibrating other criteria of distance.

For investigations of stellar contents the precise amount of the obscuration is not important provided the obscuration is uniform over the area covered by each nebula. Since this condition is presumably fulfilled, the Cepheids in each system furnish a zero point for the scale of absolute magnitudes, regardless of obscuration. In this way it has been possible to determine the luminosity function of globular clusters and of novae at maxima in M 31 and of the supergiant stars in several nebulae. Fragmentary data have been assembled for various other constituents of stellar contents.

Cepheids are by no means the brightest objects in nebulae. They

[2] The magnitudes in this paper are all on the international photographic system unless otherwise stated.

are surpassed by certain types of irregular variables, supergiants, novae, globular and open clusters, as well as by star clouds and patches of emission nebulosity. With increasing distances these objects should fade out, class by class (about in the order named), until the last constituents of stellar contents are lost and no general criterion remains except the total luminosities of the nebulae themselves. The observations do, in fact, present just this sequence of phenomena.

The general distance criterion which may be applied throughout the observable region of space is furnished by total luminosities, or, more precisely, the luminosity function of nebulae. The sample collection of nebulae in the local group is too small for the purpose of definitive calibration;[3] some other criterion must be selected, intermediate between Cepheids and total luminosities, which may be applied to nebulae on the inner fringe of the general field. The criterion actually adopted is the brightest star, which is arbitrarily defined as "the mean of the three or four brightest objects which are judged to be individual, non-variable stars situated in a nebula."

BRIGHTEST STARS AS A CRITERION OF DISTANCE[4]

The selection is the result of a process of elimination among the brighter elements of the stellar contents in members of the local group. Brightest stars are surpassed by star clouds, patches of emission nebulosity, and occasionally by globular clusters and, possibly, open clusters. Among these objects the globular clusters alone are

[3] The local group includes elliptical nebulae, intermediate and late, normal spirals, and irregular nebulae, but no early normal spirals or barred spirals at any stage. The intrinsically largest and brightest known nebulae are included and also the faintest (although not the smallest). The range in absolute magnitude is about 6.5 mag. as compared to a known range of about 5 mag. among other nebulae. The mean magnitude is $M = -14$, if the galactic system is included with a hypothetical luminosity equal to that of the Andromeda spiral, or -13.6 if the galactic system is omitted. The latter value is fainter than the average in the general field (of the order of -14.2), partly because of the relatively large number of irregulars. This feature is a unique characteristic of the group and distinguishes it from the many otherwise similar groups that are found over the sky.

[4] The present investigation of the criterion of brightest stars is a revision and extension of previous discussions by the writer in *Mt. W. Contr.*, No. 324; *Ap. J.*, **64**, 321, 1926; and, in collaboration with Humason, in *Mt. W. Comm.*, No. 105; *Proc. Nat. Acad.*, **15**, 168, 1929; *Mt. W. Contr.*, No. 427; *Ap. J.*, **74**, 43, 1931.

serious contenders for the rôle of distance criterion; the others exhibit dispersions so large that satisfactory calibrations cannot be made with the data now available.

Globular clusters can be readily distinguished from individual stars (or stellar images) down to about $m = 19.0$ or, under exceptional conditions, to perhaps 19.5. An examination of the nebulae in which brightest stars are not fainter than these limits indicates that the intrinsic luminosities of the brightest clusters vary widely from nebula to nebula and seldom surpass those of the brightest stars. The clusters in the galactic system are outstanding exceptions. Two of them (NGC 6356 and 6864) apparently surpass the brightest star by 1.5 mag. or more; they would be conspicuous objects in the nearer field nebulae and would be easily identified in members of the Virgo cluster. In M 31, M 101, and, possibly, the Small Cloud, the brightest clusters are slightly brighter than the brightest stars, but in the Large Cloud, M 33, NGC 6822, M 81, and most of the remaining nebulae the order is reversed, and in some cases the difference is considerable. Among these nebulae whose distances are known the brightest stars clearly offer the more uniform criterion. Occasional misidentifications in the more remote nebulae may be expected, but the effect on mean results of statistical investigations will probably be unimportant.

Two criticisms might be urged against the validity of the criterion. The first is the possibility of confusing groups, or compact clusters, with individual stars. The danger seems quite real because the contents of large volumes of space in the very distant nebulae would register on the photographic plate as sensibly stellar images. Nevertheless, it is reasonable to suppose that the brighter supergiants, which are rare and are scattered at wide intervals, are so outstanding that other objects in the vicinity, or in the line of sight, would contribute very small increments to their apparent magnitudes. A study of the galactic system and the neighboring nebulae lends some color to the assumption. A stronger and purely empirical argument is found in the observations. Regardless of their true nature, the objects selected as brightest stars, as will appear later, form a homogeneous group in which the absolute magnitudes do not vary systematically with apparent magnitudes (or distances). The

brightest stars in faint, distant nebulae are comparable with those in members of the local group. The latter stars, as judged by their luminosities relative to Cepheids, are probably individuals, comparable with the brightest star in the galactic system; therefore, the objects in the distant nebulae may also be regarded as individual stars.

The second criticism is the fact that, with existing telescopes, stars are not found in all types of nebulae. Resolution is restricted to irregular nebulae of the type of the Magellanic Clouds and to the later section of the sequence of classification—namely, to the intermediate and late-type spirals, whether normal or barred. The brightest stars, moreover, in the intermediate spirals are systematically fainter than those in late spirals, the difference being of the order of 0.7 mag. Consequently, the nebulae actually resolved are mostly the late spirals, Sc and SBc. The intermediate spirals are not only less frequent per unit volume of space, but those that can be resolved are distributed through a smaller total volume than the resolved, late spirals. The irregulars, although scattered over the same volume as the late spirals, are relatively rare objects. The brightest stars, therefore, furnish information mainly concerning a single stage in the sequence of nebular forms, and the question of whether or not the systems at this stage are fair samples of nebulae in general must be investigated by other methods. Actually, an affirmative answer is derived from the mixture of types in clusters and in the list of nebulae whose velocities are known.

Foreground stars may be eliminated by star counts in the case of nebulae covering large areas, or by simple inspection in the case of the smaller nebulae. The latter method involves rather arbitrary judgments and for this reason is subject to the personal equation of the investigator. Single, outstanding objects are generally assigned to the foreground, and the selection of the brightest star is based on the three or four objects, with about the same luminosity, below which the numbers steadily increase. This method of estimation tends to reduce the effects of exceptional objects which might be contained in a nebula. Moreover, the method furnishes a reasonable compromise between the use of the single brightest star, which would be extremely difficult to identify, and the use of, say, the

twenty-fifth star, or the mean of a considerable number, which would seriously restrict the range of the criterion.

CALIBRATION OF THE CRITERION OF BRIGHTEST STARS

Preliminary examination of the available data indicates that the range among brightest stars is conspicuously smaller than the range among nebular luminosities. The differences, therefore, in the apparent magnitudes of nebulae and their brightest stars, $m_s - m_n$, measure the absolute luminosities of nebulae in terms of the brightest stars as the unit. No corrections are required for effects of local obscuration. The first step in such investigations is the determination of the luminosity function of brightest stars from the data in nebulae whose distances are known from other criteria.

Before the particular problem is discussed, some general remarks will be made which concern the nebulae as well as their brightest stars. The large-scale distribution of nebulae and, consequently, of brightest stars is approximately uniform. The luminosity function of nebulae—the frequency distribution of absolute magnitudes of nebulae in a given volume of space—is known to approximate a normal error-curve, and the present investigation confirms this previous conclusion. The precise form of the luminosity function of brightest stars cannot be determined but, if it is nearly symmetrical about some point, it also may be represented by a normal error-curve. This assumption is adopted; it is unverified, but it is not inconsistent with the few data available, and moderate deviations, in view of the small dispersion actually found, will not seriously affect the final results that are based on the assumption.

Let M and σ, with subscripts n and s, be the absolute magnitudes and the dispersions of nebulae and of brightest stars, respectively. Let M_0 be the mean absolute magnitude for a given volume of space, and $\overline{M}$ the mean for a given apparent magnitude. Then, by a well-known relation developed by Malmquist,[5] among others,

$$\overline{M} = M_0 - 1.382\,\sigma^2 .$$

[5] Malmquist gave the relation in *Arkiv för Matematik, Astronomi och Fysik* (Stockholm, 1921), **16**, No. 23, and later made a provisional determination of M_{0n}, σ, and $\overline{M}_n$ from incomplete data in the Virgo cluster (*Lund. Medd.* 1st ser., No. 118, 1928).

The object of the present investigation is to determine first M_{os}, $\overline{M}_s$, and σ_s and thereafter M_{on}, $\overline{M}_n$, and σ_n.

The data for the luminosity function of brightest stars are given in Table I. All the nebulae are included for which distances have been estimated from other constituents of their contents. The values of M_s for the Magellanic Clouds are taken from Harvard publications and are uncertain because the particular problem has not been investigated. The Large Cloud is known to be exceptionally rich in supergiants, but the extraordinary magnitudes formerly suggested

TABLE I

ABSOLUTE MAGNITUDES OF NEBULAE AND THEIR BRIGHTEST STARS

Nebula	Type	M_n	M_s	Δ Type
LMC	Ir	−15.9	−7.1	.....
SMC	Ir	14.5	5.8	.....
IC 1613	Ir	11.2	5.8	.....
NGC 6822	Ir	11.0	5.6	.....
M 33	Sc	14.9	6.3	.....
M 101	Sc	14.5	6.0	.....
NGC 2403	Sc	13.9	6.0	.....
M 31	Sb	17.5	6.0	−0.7
M 81	Sb	15.9	5.5	−0.7
Galactic system	(Sc)	(−17.5)	(−7.0)	.....
Mean	.....	−14.7	−6.11	.....

have been considerably revised. Shapley's latest report[6] mentions the presence of stars as bright as $M=-7$, and the value $M=-7.1$, corresponding to apparent magnitude $m=10$, is adopted. Still brighter stars may possibly be present. The effect of a conservative estimate is much the same as that of adopting a brighter limit and then assigning a low weight to the Cloud in view of the outstanding residual in this one member of the small sample collection.

Star counts in the Small Cloud suggest an upper limit which is considerably fainter than that in the Large Cloud, but no definite value is mentioned.[7] For this reason a former estimate,[8] corrected

[6] *H.B.*, No. 886, 1932.

[7] *H.C.*, No. 260, 1924.

[8] *Mt. W. Contr.*, No. 427; *Ap. J.*, **74**, 43, 1931.

for the latest revision in the distance, is adopted in the present investigation.

The data for IC 1613 are derived from unpublished investigations by Baade; those for M 31, M 33, and NGC 6822, from star counts by the writer. The values for M 81, M 101, and NGC 2403, which lie on the inner fringe of the general field, are not very reliable. No Cepheids have been identified with certainty, and distances have been estimated from apparent luminosities of novae and irregular variables, relative to similar stars in members of the local group.

The data for the galactic system are hypothetical. The nebula is assumed to be a late-type spiral, Sc, because of the rapid rotation, the high degree of resolution, and the prevalence of blue supergiants and patches of emission nebulosity. Its great mass and large dimensions indicate that it is a giant nebula, and for this reason its intrinsic luminosity, actually unknown, is assumed to be equal to that of the other giant spiral, M 31. The estimate of M_s is suggested by Trumpler's reports on the stellar contents of open clusters.

The data in Table I are few and uncertain, but significant additions are not expected for some years. They furnish the simple mean

$$M_{os}=-6.11\,, \qquad \sigma_s=0.52\,.$$

Therefore

$$\bar{M}_s=-6.48\,.$$

With these results as a curb against the dangers of overanalysis, Table I may now be discussed in greater detail. Two sources of systematic variation are apparently involved, and the effects are in opposite directions. One is the previously mentioned dependence of M_s on nebular type, the evidence for which will be presented later. The M_s for the two Sb nebulae, M 31 and M 81, are accordingly corrected by -0.7 mag.

The second systematic effect is a dependence of M_s on M_n, the latter measuring the stellar contents. Each nebula represents a sample collection of stars, and the very brightest of all stars may reasonably be expected to favor the largest samples. A correlation of this kind is suggested by a plot of M_s against M_n. As M_n ranges from -11 to -17.5 (stellar contents increase about four hundred

fold), M_s brightens about 1.4 mag. The Large Cloud is discordant, but it remains so according to any interpretation of the data. A similar correlation is suggested by the fragmentary data for spirals in the Virgo cluster, although the analogy is qualitative rather than quantitative. Nevertheless, the evidence is sufficiently impressive to warrant the reduction of M_s to a constant value of M_n. The latter is adopted as $M_n = -14.2$, which, as will appear later, is of the order of the mean luminosity of nebulae in general.

The data, corrected for type and for stellar contents, lead to the revised mean, for $M_n = -14.2$,

$$M_{0s} = -6.12\,, \qquad \sigma_s = 0.29\,,$$

and

$$\overline{M}_s = -6.24\,,$$

where σ_s is now the dispersion about the correlation-curve (mean of the regression-curves),

$$M_s = 0.222 M_n - 2.97\,.$$

The two sets of results presumably bracket the most probable values because some corrections to the simple mean are clearly indicated, but the corrections actually derived from such limited data may be expected to include accidental deviations as well as systematic effects. The end results differ by only a quarter of a magnitude at most, and, in the absence of further information, it seems permissible to use the averages of the two sets for the provisional calibration. Therefore we adopt

$$M_{0s} = -6.12\,, \qquad \sigma_s = 0.41\,,$$

from which

$$\overline{M}_s = -6.35\,.$$

RELATIVE LUMINOSITIES OF NEBULAE AND THEIR BRIGHTEST STARS

The Mount Wilson photographs include a representative collection of nebulae distributed over a wide range in apparent luminosity. The brighter nebulae are the more completely observed, but

several hundred objects fainter than $m=14$ are also available for study. The nebulae in which stars can be identified with some confidence are listed in Tables II and III, the latter containing only members of the Virgo cluster. The tables give the nebular types, the apparent magnitudes of the nebulae, m_n, and of the brightest stars, m_s, and the differences, m_s-m_n, which measure the absolute luminosities of the nebulae in terms of the luminosities of the brightest stars as units. The data are listed in the order of increasing values of m_s, and no objects are included with $m_s>20.5$.

Some 32 of the nebular magnitudes, m_n, represent careful measures with photoelectric cells (by Stebbins and Whitford) or on schraffierkassette plates;[9] 100 are the values listed in the Harvard Survey, corrected by -0.1 mag. in order to conform to the scale established by the photoelectric cell measures; the remaining 13 are estimated magnitudes of nebulae which are not included in the Harvard Survey.

The magnitudes of brightest stars, m_s, represent actual measures in about 15 cases where $m_s \leqq 19.5$. The remaining values are the means of three independent estimations to the nearest half-magnitude, made at widely different times. These data are provisional and must eventually be replaced by precise measures. A preliminary discussion, based on the estimates, is justified by the length of time that will be required to complete the program of measuring such faint stars with the necessary accuracy. Nevertheless, it is believed that the data now available are fairly homogeneous and that scale errors do not amount to more than a few tenths of a magnitude at most.

The simple mean of the 145 differences is 7.86, and the dispersion, $\sigma=0.93$, includes that of brightest stars as well as that of nebulae. Since the nebulae are selected on the basis of the apparent magnitude of the brightest stars, the zero point of the absolute magnitudes is furnished by $\overline{M}_s$. The simple, uncorrected means for both stars and nebulae give

$$M_{on}=\overline{M}_s-\overline{(m_s-m_n)}=-14.34\,,$$

$$\sigma_n=\sqrt{\sigma^2_{n,s}-\sigma^2_s}=0.77\,,$$

$$\overline{M}_n=-15.17\,.$$

[9] The magnitudes of the Magellanic Clouds are measures by G. van Herk, *B.A.N.*, **6**, 61 (No. 209), 1930.

TABLE II

RESOLVED NEBULAE IN THE LOCAL GROUP AND THE GENERAL FIELD

NEBULA	TYPE	m_s	m_n	$m_s - m_n$	
				Obs.	Corr.†
LMC	Ir	10.0	1.2*	8.8	9.5
SMC	Ir	11.5	2.8*	8.7	9.4
NGC 598	Sc	15.6	7.1*	8.5	.....
6822	Ir	15.8	10.4*	5.4	6.1
224	Sb	16.0	4.5*	11.5	10.8
IC 1613	Ir	16.4	11.0*	5.4	6.1
NGC 4736	Sb	17.4	9.1*	8.3	7.6
5457	Sc	17.5	9.0*	8.5	.....
5194	Sc	17.6	9.4*	8.2	.....
4449	Ir	17.8	10.2	7.6	8.3
1156	Ir	18.0	12.8	5.2	5.9
2403	Sc	18.0	10.1	7.9	.....
253	Sc	18.3	8.2*	10.1	.....
4214	Ir	18.3	10.6	7.7	8.4
300	Sc	18.3	11.2	7.1	.....
578	Sc	18.5	11.6	6.9	.....
3031	Sb	18.5	8.1*	10.4	9.7
4826	Sb	18.5	9.6*	8.9	8.2
5236	Sc	18.5	8.5*	10.0	.....
IC 342	Sc	18.5	12.5*	6.0	.....
NGC 3631	Sc	18.6	11.7	6.9	.....
1068	Sbc	18.7	10.1*	8.6	.....
3627	Sb	18.7	9.8	8.9	8.2
4656	Ir	18.7	11.2	7.5	8.2
4490	Sc	18.8	10.4	8.4	.....
628	Sc	18.9	11.1	7.8	.....
45	Sc	19.0	12.1	6.9	.....
925	Sc	19.0	12.5	6.5	.....
2366	Ir	19.0	12.5	6.5	7.2
2903	Sc	19.0	10.2	8.8	.....
3184	Sc	19.0	11.7	7.3	.....
4088	Sc	19.0	11.1	7.9	.....
4236	Sc	19.0	11.2	7.8	.....
4618	Ir	19.0	11.4	7.6	8.3
4631	Sc	19.0	9.5	9.5	.....
6946	Sc	19.0	11.0	8.0	.....
247	Sc	19.2	10.6	8.6	.....
5055	Sb	19.2	10.4	8.8	8.1
5248	Sc	19.2	11.1*	8.1	.....
4051	Sbc	19.3	11.6	7.7	.....

* Measured magnitude. † Corrected for type (Ir, +0.7 mag.; Sb, SBb, −0.7 mag.).

TABLE II—*Continued*

Nebula	Type	m_s	m_n	$m_s - m_n$	
				Obs.	Corr.†
NGC 134	Sc	19.5	11.3	8.2	.....
871	Sc	19.5	13.0‡	6.5	.....
2967	Sc	19.5	12.3	7.2	.....
3338	Sc	19.5	12.2	7.3	.....
3596	Sc	19.5	12.1	7.4	.....
4030	Sb	19.5	11.1	8.4	7.7
4258	Sb	19.5	10.1	9.4	8.7
4395	Sc	19.5	11.3	8.2	.....
4559	Sc	19.5	10.6	8.9	.....
4605	Sc	19.5	10.8	8.7	.....
4713	Sc	19.5	12.2	7.3	.....
5364	Sc	19.5	11.5*	8.0	.....
5474	Sc	19.5	11.6	7.9	.....
5713	Sc	19.5	11.7	7.8	.....
5964	SBc	19.5	12.9‡	6.6	.....
7331	Sb	19.5	11.1	8.4	7.7
3810	Sc	19.6	11.7	7.9	.....
428	Sc	19.7	12.2*	7.5	.....
1042	Sc	19.7	12.4	7.3	.....
3206	Sc	19.7	12.8‡	6.9	.....
3893	Sc	19.7	10.9	8.8	.....
3953	Sc	19.7	11.4	8.3	.....
5005	Sc	19.7	11.2	8.5	.....
7393	Scp	19.7	12.8‡	6.9	.....
2537	Scp	19.8	12.1	7.7	.....
4725	Sab	19.8	10.7	9.1	8.4
5585	Sc	19.8	11.9	7.9	.....
5970	Sc	19.8	12.3	7.5	.....
2742	Sc	19.9	12.4	7.5	.....
3780	Sc	19.9	12.5	7.4	.....
95	Sc	20.0	13.4*	6.6	.....
200	SBc	20.0	13.3‡	6.7	.....
289	Sc	20.0	12.0	8.0	.....
514	Sc	20.0	12.3	7.7	.....
753	Sc	20.0	12.9	7.1	.....
864	Sc	20.0	12.2	7.8	.....
877	Sb	20.0	12.3	7.7	7.0
1073	SBb	20.0	11.9	8.1	7.4
1084	Sc	20.0	11.3*	8.7	.....
1359	Scp	20.0	12.7	7.3	.....

‡ Estimated magnitude, nebula not included in the Harvard Survey.

TABLE II—*Continued*

Nebula	Type	m_s	m_n	$m_s - m_n$	
				Obs.	Corr.†
NGC 2300	Sc	20.0	12.1	7.9	.....
2389	Sc	20.0	12.9‡	7.1	.....
2748	Sc	20.0	12.3	7.7	.....
2964	Sc	20.0	11.8	8.2	.....
3187	SBc	20.0	13.0‡	7.0	.....
3189	SBc	20.0	13.2	6.8	.....
3395	Sc	20.0	12.3	7.7	.....
3432	Sc	20.0	12.1	7.9	.....
3521	Sbc	20.0	10.2	9.8	.....
3887	Sc	20.0	11.5	8.5	.....
3949	Sc	20.0	11.5	8.5	.....
4102	SBb	20.0	12.0	8.0	7.3
4151	Sb	20.0	11.1	8.9	8.2
4602	Sc	20.0	12.3	7.7	.....
5371	Sc	20.0	11.6	8.4	.....
5633	Sb	20.0	12.7	7.3	6.6
6217	Sc	20.0	12.5	7.5	.....
7348	Sc	20.0	13.1‡	6.9	.....
2976	Sc	20.2	11.1	9.1	.....
3430	Sc	20.2	12.3	7.9	.....
3486	Sc	20.2	11.3	8.9	.....
132	Sc	20.2	13.1‡	7.2	.....
3738	Ir	20.3	12.1	8.2	8.9
5850	SBb	20.3	12.8	7.5	6.8
6070	Sc	20.3	12.6	7.7	.....
3756	Sc	20.4	12.4	8.0	.....
5297	Sc	20.4	12.9	7.5	.....
7716	Sc	20.4	13.2*	7.2	.....
198	Sc	20.5	13.5‡	7.0	.....
210	Sc	20.5	12.4	8.1	.....
278	Sc	20.5	11.7	8.8	.....
941	Sc	20.5	13.2	7.3	.....
1376	Sc	20.5	12.8	7.7	.....
2339	Sc	20.5	12.6	7.9	.....
2633	SBc	20.5	12.5	8.0	.....
3055	SBc	20.5	12.4	8.1	.....
4625	Sc	20.5	12.9‡	7.6	.....
4712	Sc	20.5	12.8	7.7	.....
4793	Sc	20.5	12.4	8.1	.....
4808	Sc	20.5	12.4	8.1	.....
4900	SBc	20.5	11.7	8.8	.....
5962	Sc	20.5	12.4	8.1	.....
6207	Sc	20.5	12.2	8.3	.....
6412	Sc	20.5	12.7	7.8	.....
7309	Sc	20.5	13.0	7.5	.....

With these values determined, the nebular data can be examined in greater detail.

THE CORRECTION FOR NEBULAR TYPE

Tables II and III contain 117 late spirals, 17 intermediate spirals, and 11 irregular nebulae. The intermediate spiral M 31 exhibits an outstanding difference, $m_s - m_n$, and unduly influences the mean for

TABLE III

RESOLVED NEBULAE IN THE VIRGO CLUSTER

Nebula	Type	m_s	m_n	$m_s - m_n$
NGC 4321	Sc	19.0	10.6*	8.4
4254	Sc	19.2	10.6*	8.6
4535	Sc	19.5	11.1*	8.4
4299	Sc	19.7	13.0	6.7
4654	Sc	19.7	11.6	8.1
4178	Sc	20.0	12.3	7.7
4294	Sc	20.0	12.9	7.1
4302	Sc	20.0	13.1	6.9
4567	Sc	20.0	12.2	7.8
4568	Sc	20.0	12.1	7.9
4571	Sc	20.0	12.7	7.3
4651	Sc	20.0	11.7	8.3
4808	Sc	20.0	12.4	7.6
IC 3258	Sc	20.0	14.0	6.0
NGC 4192	Sb	20.2	11.2*	9.0 8.3†
4273	Sc	20.5	12.1	8.4
4501	Sc	20.5	13.8	6.7
4633	Sc	20.5	10.6*	9.9
IC 3476	Sc	20.5	13.4	7.1
3583	Sc	20.5	14.2	6.3
Mean	.....	.....	.....	7.68

* Photoelectric cell measures. † Corrected for type.

the limited number of nebulae of the same type. The mean differences for the various types, omitting M 31, are given in Table IV.

Systematic variations are clearly present, and provisional corrections of +0.7 and −0.7 mag. may be applied to the Ir and Sb nebulae, respectively, in order to reduce them to the system of the late spirals. The interpretations are quite different in the two cases. The intermediate spirals appear to be normal (comparable with the

late spirals), but their brightest stars are systematically faint. On the other hand, the irregular nebulae are systematically faint although their brightest stars are normal. The latter conclusion is based on the four irregulars in the local group and five others in the general field whose distances can be derived from their red shifts. The numbers are small, but they include a majority of the objects in Table IV and show no systematic difference from the remaining irregulars in the table. The constituent elements of Ir and Sc nebulae appear to

TABLE IV

COMPARISON OF TYPES

Type	No.	$\overline{m_s - m_n}$	Δ Type
Sb, SBb.....	16	8.57±0.20	−0.7
Sc, SBc.....	117	7.84±0.05	0.0
Ir.....	11	7.15±0.25	+0.7

be closely comparable; both types are characterized by a high degree of resolution, blue supergiants, and patches of emission nebulosity.

SYSTEMATIC VARIATION OF BRIGHTEST STARS ALONG THE SEQUENCE OF CLASSIFICATION

The comparability of intermediate and late spirals is established in a rough way by comparisons of the two types in clusters and more precisely by their residuals from the velocity-distance relation. Therefore the systematic difference in $m_s - m_n$ must be referred to the brightest stars alone. This interpretation is confirmed by data from the Virgo cluster where many late spirals are resolved but only an occasional intermediate spiral.

The conclusion may be generalized into the very significant hypothesis that the luminosities of brightest stars increase steadily through the later section (or possibly the whole) of the sequence of classification and pass above the observable threshold somewhere between Sa and Sb. The earliest type in Table II is that represented by NGC 4725, listed as Sb but more precisely described as Sab. The difference, $m_s - m_n = 9.1$, is still larger than the mean for Sb nebulae in general. A survey of the brighter, nearer nebulae of earlier types,

none of which is resolved,[10] suggests that the differences, $m_s - m_n$, are greater than 9.5, and are probably greater than 10.

No early spirals are found in the local group, and the only normal, elliptical nebula is M 32, the type example of E2. Stars as bright as $M = -2$ are definitely not present in M 32, and the limit is probably not brighter than $M = -1$. The stellar composition of M 32 is hypothetical but, as Smith[11] has shown, it presents fewer inconsistencies than other theories of structure. The data are still fragmentary, but they strongly suggest a steady increase in stellar luminosity along the sequence, which may have evolutional significance. Further evidence suggests that the brightest stars become bluer (color indices decrease) as they become brighter—that visual luminosity increases less rapidly than photographic luminosity.

HOMOGENEITY OF THE DATA CONCERNING RELATIVE LUMINOSITIES

The systematic variation of $m_s - m_n$ is not very troublesome in statistical investigations, because normal collections of resolved nebulae are dominated by the late spirals. The variations thus tend to increase dispersions without seriously influencing the means. Nevertheless, the dispersion is important for relating M_0 and $\bar{M}$, and, for this reason, the appropriate corrections have been included in the last columns of Tables II and III.

The correction for stellar contents, reducing the brightest stars to the standard, $M_n = -14.2$, may also be applied. This correction increases the dispersion in $m_s - m_n$, so that the final results are much the same as those from the original data.

The homogeneity of the data may be tested by the correlation between the differences, $m_s - m_n$, and the magnitudes of the brightest stars, m_s. Since the scale of nebular magnitudes, m_n, is well established, the procedure amounts to testing the scale of stellar magnitudes and also the comparability of the objects selected as brightest stars. The results are shown in Table V. Corrections for type have

[10] M 87, an elliptical nebula in the Virgo cluster, may be the one exception. Many very faint objects cluster around this nebula, but their nature and hence the resolution of the nebula are still doubtful.

[11] *Mt. W. Contr.*, No. 524; *Ap. J.*, **82**, 192, 1935.

been included, but not those for stellar contents. The latter are not important for the immediate purpose, because the mean values of $m_s - m_n$ for the various groups are closely comparable.

The first six nebulae in Table V are members of the local group. The mean $m_s - m_n$ is 8.4 ± 0.4, but when M 31 is omitted as an outstanding exception, the mean is 7.92. The field nebulae then follow

TABLE V

CORRELATION BETWEEN m_s AND $m_s - m_n$

m_s	No.	$\overline{m_s - m_n}$	
		Uncorrected	Corrected
Local group	6	8.05	8.40
	(5)*	(7.36)	(7.92)
17.1–17.5	2	8.40	8.05
17.6–18.0	4	7.23	7.57
18.1–18.5	8	8.39	8.30
18.6–19.0	16	7.81	7.89
	17†	7.84	7.92
19.1–19.5	20	7.97	7.83
	22†	8.02	7.89
19.6–20.0	42	7.78	7.68
	53†	7.70	7.62
20.1–20.5	27	7.93	7.93
	33†	7.92	7.90
Total	125	7.89	7.86
	145†	7.86	7.84

* M 31 omitted.

† Includes nebulae in the Virgo cluster.

in groups representing successive intervals of 0.5 mag. in m_s. The relative numbers suggest that the data are reasonably complete to $m_s = 19$, and are representative to perhaps $m_s = 20$. The last four groups are tabulated in two forms, the first containing only field nebulae, the second including members of the Virgo cluster as well. Toward the end of the table, where lack of completeness is evident, it is reasonable to assume that faint, resolved nebulae (small differences) have been missed more frequently than bright nebulae

(large differences). The large mean difference for the last group might be attributed to this effect of selection, but it is included without correction. It may be considered as compensating a slight, systematic decrease in the differences with increasing m_s, which might be interpreted as a scale error, or a tendency occasionally to select groups of stars rather than individuals as the brightest stars. In general, the deviations are satisfactorily small, and it seems probable that comparable objects have been selected throughout. Since the objects are known to be individual stars in the neighboring nebulae where Cepheids are found, the same identification may be adopted in the distant nebulae.

THE LUMINOSITY FUNCTION FOR RESOLVED NEBULAE

The frequency distribution of $m_s - m_n$ is shown in Figure 1, where the ordinates are overlapping sums for three successive intervals of 0.1 mag. One plot represents the observed data, and the other, the data corrected both for type and for stellar contents. Normal error-curves with the dispersions calculated from the data indicate the fidelity with which this type of distribution represents the luminosity function.

The form of the curve is established regardless of any information concerning the mean absolute magnitude of the brightest stars. The only condition is the reasonable assumption, supported by all the available data, that the dispersion among brightest stars is appreciably smaller than the dispersion among nebulae. The exceptional case, M 31, has been omitted in the calculations because this one object appreciably influences the dispersions (although not the means). This procedure will be adopted in the discussions which follow.

As in the calibration of the criterion of brightest stars, the determination of the constants in the luminosity function of resolved nebulae will be made, first, from the uncorrected data; second, from the data corrected both for type and for stellar contents; and, finally, from the means of the two sets of values. The results, with M 31 omitted, are given in Table VI. The variations, it will be noticed, occur mainly in the dispersions. Since the combined dispersions, $\sigma_{s,n}$, are of the same general order, a large σ_s leads to a small σ_n, and a small σ_s to a large σ_n. Independent investigations of clusters and

of residuals in the velocity-distance relation suggest that the adopted $\sigma_n = 0.85$ is probably of the right order. Finally, it should be mentioned that the dispersions for both stars and nebulae include accidental errors in estimates, or measures, of apparent magnitudes, as well as the inherent scatter in absolute magnitudes. The accidental

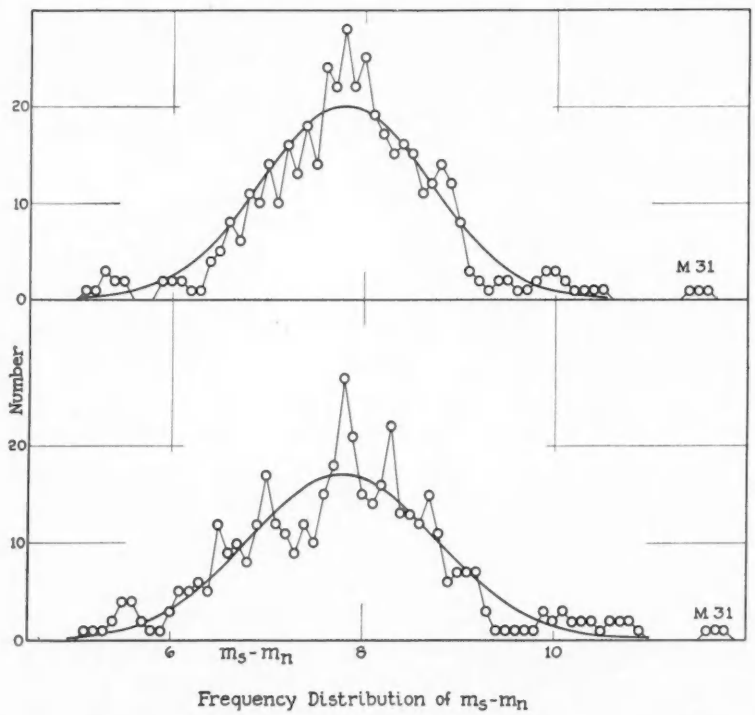

FIG. 1.—Upper curve: frequency-distribution of observed differences between apparent magnitudes of nebulae and of their brightest stars; lower curve: frequency-distribution of observed differences, corrected for types and for stellar contents of the nebulae. Points are overlapping sums of frequencies for three successive intervals of 0.1 mag. The smooth curves are normal error-curves with dispersions of 0.89 mag. (upper) and 0.99 mag. (lower).

errors in the nebular magnitudes are small and probably represent a dispersion not greater than 0.2 mag. The true dispersion in M_n would thus be about $\sigma_n = 0.83$. Similar considerations suggest that the true σ_s is probably about 0.35.

BRIGHTEST STARS IN MEMBERS OF THE VIRGO CLUSTER

The Virgo cluster, which is the nearest of the great clusters, furnishes a rich sample collection of nebulae of all types except the irregulars. Since relative, apparent luminosities within the cluster are equivalent to relative, intrinsic luminosities, the collection offers a means of intercomparing the luminosity functions for the various individual types. The data are still incomplete, but sufficient are available to indicate that the types are all roughly comparable and that any small systematic differences that might exist could be established only by refined investigations. The luminosity function, therefore, for resolved nebulae, derived from the study of their

TABLE VI

CONSTANTS IN THE LUMINOSITY FUNCTIONS OF RESOLVED NEBULAE AND THEIR BRIGHTEST STARS

Constant	Uncorrected	Corrected	Adopted
M_{os}	-6.11, $\sigma_s=0.52$	-6.12, $\sigma_s=0.29$	-6.12, $\sigma_s=0.41$
$\overline{M}_s$	-6.48	-6.24	-6.35
m_s-m_n	7.85, $\sigma_{s,n}=0.89$	7.83, $\sigma_{s,n}=0.99$	7.84, $\sigma_{s,n}=0.94$
M_{on}	-14.33, $\sigma_n=0.72$	14.07, $\sigma_n=0.94$	-14.19, $\sigma_n=0.85$
$\overline{M}_n$	-15.05	15.30	-15.18

brightest stars, may be provisionally applied to nebulae in general, provided cluster nebulae are comparable with field nebulae of similar types. The question as to whether or not the condition is fulfilled can be answered only when the distance of the cluster is known. The distance can be derived from two criteria—red shifts and brightest stars. The results from red shifts will be examined later, but those from brightest stars may be mentioned at the present stage of the discussion.

The data in Table III are fragmentary. The observing program requires the assembling with the 100-inch reflector of sharp photographs of all intermediate and late spirals which are brighter than the fifteenth apparent magnitude in the area covered by the cluster. The field spirals are not numerous, except in the last magnitude interval ($m=14$–15, where about three-fourths of the total number

may be expected), and their influence can be estimated by statistical methods. The cluster must be observed in winter and early spring, when seeing conditions are unfavorable, and the program advances slowly. For this reason the present discussion must be provisional.

The results in hand suggest that practically all the brighter, late-type spirals are resolvable, and many of the fainter. Of the intermediate spirals only one has actually been resolved, and very few others are expected to exhibit this characteristic.[12] The two brightest of the stars in Table III, $m_s = 19.0$ and 19.2, represent the extreme limits in the entire cluster. No other nebulae show stars brighter than $m = 19.5$, and very few, brighter than $m = 20$. The absolute magnitudes of these limiting cases are hypothetical, because the dispersion in M_s is derived from a very small collection of nebulae. Provisionally it seems reasonable to assume that the larger collection in the cluster will show a greater range and that the excess may be represented by the pair of outstanding objects. Apparent magnitude $m = 19.5$, then, corresponds to the upper limit in Table I —namely, $M = -7$—and the modulus of the distance of the cluster is of the general order of 26.5.

More detailed analysis, based on the frequency distribution of m_s and taking account of negative results (threshold magnitudes on photographs of unresolved nebulae), suggests that the most frequent magnitude is not brighter than 20.5. This estimate, together with the corresponding absolute magnitude, $M_{0s} = -6.12$, suggests a modulus of the order of -26.6 or fainter. Corrections for stellar contents lead to data which are evidently on the brighter branch of a frequency-curve and which do not define the maximum. The mean difference in Table III, $\overline{m_s - m_n} = 7.68$, is smaller than that in Table II by about 0.2 mag., and the discrepancy may reflect either a scale-error in m_s or a selection in favor of nebulae with unusually bright stars.

The only conclusion that can be drawn is that the modulus of the cluster is larger than 26.5 and that the order of the true value can

[12] No earlier types exhibit any signs of resolution except the unique case of M 87—an apparently globular nebula about which numerous small objects tend to cluster. The nature of these objects is uncertain. Some are clearly faint field nebulae, but the majority may be either stars or clusters.

probably be determined when the data that can be obtained with existing instruments are completely assembled. Later it will be shown from the red shifts that the modulus is not greater than 27 and that the most probable value is about 26.8. The brightest stars alone indicate that the general order of absolute magnitudes of cluster nebulae is probably comparable with that of field nebulae and, moreover, that the decreasing luminosity of brightest stars along the sequence of classification is an empirical law.

[*To be continued*]

CARNEGIE INSTITUTION OF WASHINGTON
MOUNT WILSON OBSERVATORY
May 1936

A STUDY OF THE SPECTRUM OF 25 ORIONIS

HELEN W. DODSON

ABSTRACT

A study of 147 spectrograms of 25 Orionis, covering the interval 1915–1933, has shown simultaneous variations of the velocities of the central absorptions and the emission lines of hydrogen. These changes are nearly synchronous with changes of the ratio V/R of the components of the emission lines. The period shows a consistent decrease from 1817 days to 1025 days, and the velocity amplitude of the central absorptions was subject to a conspicuous decrease followed by an increase, with extreme values of 40 and 120 km/sec.

The central absorption velocities of $H\beta$, $H\gamma$, and $H\delta$ are in phase; but the amplitude increases in the order named. This is true also of the emission velocities. The changes in the emission velocities anticipate those in the central absorptions by about 100 days. The emission ratio V/R shows a marked difference of phase from line to line, $H\delta$ anticipating $H\gamma$ by about 200 days, and $H\gamma$ anticipating $H\beta$.

The emission lines vary conspicuously in width and show two maxima of width in each velocity cycle. These maxima occur at times of maximum and minimum velocity.

The helium lines and the broad hydrogen absorption which underlies the emission show systematic variations of velocity and changes of contour which are definitely related to the velocities of the hydrogen central absorption, but are conspicuously out of phase with the latter.

With the exception of the phenomena of the helium and broad hydrogen absorption, the variations observed find a satisfactory interpretation in terms of the rotating-pulsating nebulous atmosphere suggested by McLaughlin.

Bright $H\beta$ was discovered in the spectrum of 25 Orionis by Mrs. Fleming.[1] Each hydrogen line consists of a broad region of absorption upon which is superimposed a wide emission line, which in turn is divided almost centrally by narrow absorption. R. H. Curtiss[2] found that the two emission components thus formed undergo cyclic variations in relative intensity in a period first announced as 1875 days. Later work by Curtiss[3] showed considerable irregularity in the period. A close correlation between the variations in velocity of the hydrogen emission and central absorption and the changes of intensity ratio of the two emission components was pointed out by McLaughlin in 1931.[4]

The data for the present study were obtained from 141 spectrograms taken at the University of Michigan Observatory and from

[1] *A.N.*, **171**, 139, 1906.

[2] *Pop. Astr.*, **33**, 537, 1925.

[3] *Michigan Obs. Pub.*, **4**, 169, 1932.

[4] *Ibid.*, **4**, 38, 1931.

six spectrograms kindly lent by the Lick Observatory. These plates are all of one-prism dispersion, approximately 40 A/mm at $H\gamma$, with the exception of seven two-prism plates taken at Ann Arbor. Almost all of the plates are of Seed 23 or Eastman 33 emulsion.

The structural features of the hydrogen lines were measured in great detail. The following settings were made, whenever possible:

a) Violet edge of violet absorption border
b) Center of violet absorption border
c) Violet edge of violet emission component
d) Center of violet emission component
e) Center of central absorption
f) Center of red emission component
g) Red edge of red emission component
h) Center of red absorption border
i) Red edge of red absorption border

The mean of settings (*c*) and (*g*) was used to obtain the so-called "emission velocity." Setting (*e*) gave directly the velocity of the central absorption. The mean of settings (*d*) and (*f*) was used in studying the relation between the emission and the absorption velocities, but is not tabulated in this paper.

The helium lines λλ 4009, 4026, 4388, and 4472 were measured on as many plates as possible. At best they are diffuse and difficult to measure; and of the four, λ 4472 seems by far the most reliable. In addition to the measures with the micrometer measuring engine, the lines λ 4026 and λ 4472 were measured for velocity on microphotometer tracings on which the record of the titanium comparison spectrum had been obtained.[5] For very diffuse lines such as these, this method is believed to be fully as reliable as the direct measurement of the spectrogram.

VELOCITIES DERIVED FROM THE HYDROGEN CENTRAL ABSORPTION

The individual measurements on a single plate were in some cases so different that it was considered unwise to take mean hydrogen velocities. Normal places formed from these velocities are given for $H\beta$, $H\gamma$, and $H\delta$ separately in Table I and are plotted as black dots in Figure 1. The curves determined by them are drawn as full lines.

[5] Dodson, *Pub. A.A.S.*, **8**, 7, 1934.

The variations in velocity of $H\gamma$ and $H\delta$ found by McLaughlin[6] during the interval JD 24116–26414 are confirmed. Similar variations occurred over the entire interval studied, and for $H\beta$ as well as for $H\gamma$ and $H\delta$.

TABLE I

NORMAL PLACES: VELOCITIES AND EMISSION RATIOS FOR HYDROGEN IN 25 ORIONIS

JULIAN DAY	CENTRAL ABSORPTION VELOCITY IN KM/SEC			EMISSION VELOCITY IN KM/SEC			EMISSION INTENSITY RATIO: LOG V/R				NO. OF PLATES
							Eye Est. McL.		Microph. Est. Dodson		
	$H\beta$	$H\gamma$	$H\delta$	$H\beta$	$H\gamma$	$H\delta$	$H\beta$	$H\gamma$	$H\gamma$	$H\delta$	
2400000+											
20827	+ 6	+17	+19	+ 8	+16	+ 44	−.04	−.11	−.06	−.16	4
21562	.....	+14	+16	+21	+49	.....	−.15	−.11	−.05	.00	1
22301	+55	+84	+78	+51	+67	+ 84	+.42	+.28	+.28	+.07	5
22383		+52	+56	+28	+51	+ 63	+.27	+.15	+.11	+.02	4
22661	.....	+24	+18	+31	+10	.....	.00	−.08	−.05	−.28	2
22720	+24	+15		+21		+ 23	−.16	−.17	−.13		8
23094	− 9	−45	−44	−11	−44	− 45	−.42	−.36	−.32	−.08	4
23361	.....	+16	+36	.....	+40	.....	.00	+.08	.00	.00	1
23497	.....			+42	+32	+ 53	+.23	+.23	+.12	+.28	2
23778	+55	+59	+49	+44	+63	.....	+.40	+.36	+.23	+.30	5
23847	+61	+68	+87	+57		+114	+.35	+.32	+.18	+.34	12
24153	+54	+54	+43	+47	+47	+29	+.25	+.17	+.20	+.13	4
24225	+34	+58	+46	+30	+57		+.17	+.13	+.16	−.07	4
24458	+21	+19	+21	+ 8	+16	− 6	−.19	−.17	−.16	−.20	7
24527		+ 2	+ 9	+16	− 5	.....	−.24	−.25	−.27	−.32	5
24832	−10	− 6	+ 1	+ 4	−19	− 21	−.28	−.24	−.20	−.12	7
24867	+ 5	− 3	−29	+10	− 3	− 27	−.30	−.15	−.02	+.03	5
25265	+31	+13	.....	+29	+35	.....	+.08	+.14	+.14	.....	7
25561	+30	+27	+32	+18	+39	+ 40	+.11	+.08	+.13	.....	7
25909	− 4	−10	−19	− 1	−22	− 13	−.32	−.28	−.22	−.22	5
26005	−37	−23	−21	− 2	−30	− 30	−.28	−.15	−.18	.....	6
26276	+38	+35	+29	+34	+37	+ 20	+.25	+.19	+.20	+.11	6
26373	+58	+47	+52	+33	+45	+ 26	+.38	+.40	+.19	+.48	5
26657	+39	+48	+54	+30	+49	+ 30	+.26	+.21	+.09	+.10	7
26752	+38	+45	+57	+30	+36	+ 21	+.19	+.17	+.10	−.16	5
27011	+26	+31	+21	+24	+29	+ 17	+.01	−.01	.00	−.09	9
27109	+32	+22	+24	+36	+28	+ 33	+.01	−.01	.00	−.03	9

The velocity curves vary in a similar manner in period, amplitude, and form. There has been a consistent decrease in period during the interval of observation. Starting with the maximum of JD 22100,

[6] *Op. cit.*, p. 39.

we have the following approximate values for the length of a cycle:

	Length of Cycle in Days			
	Hβ	*Hγ*	*Hδ*	Mean
Maximum to maximum	1825	1875	1750	1817
Minimum to minimum	1650	1625	1750	1675
Maximum to maximum	1500	1550	1600	1550
Minimum to minimum	1250	1300	1125	1225
Maximum to maximum	950	1000	1125	1025

This evidence alone is sufficient to discount finally any attempt to explain the variations in terms of binary motion.

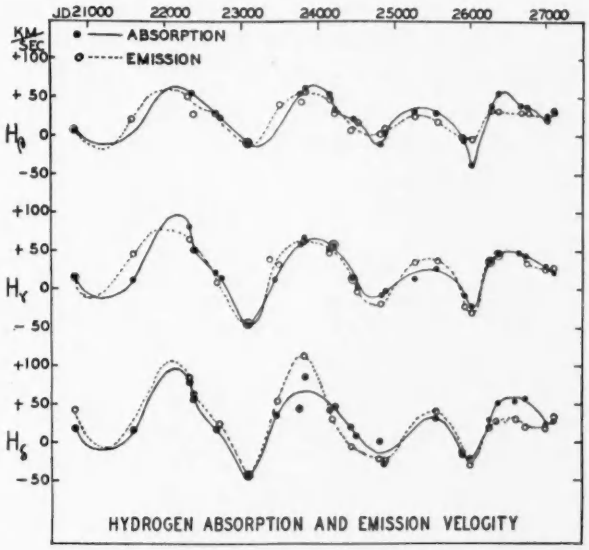

Fig. 1.—Velocity-curves of 25 Orionis

The amplitudes of the three central absorption velocity-curves differ systematically; the range is greater for the lines of shorter wave-length. This difference is small and is probably of questionable significance between *Hγ* and *Hδ*, but it is very marked between *Hβ* and *Hγ*. There has been a conspicuous change of amplitude from

cycle to cycle, as is shown by the following approximate values of the range of velocity:

		Range in Km/Sec		
Cycle	JD	$H\beta$	$H\gamma$	$H\delta$
(I)	21300–23100	75 (−12 to +63)	120 (−20 to +100)	121 (−15 to +106)
(II)	23100–24800	76 (−11 to +65)	111 (−45 to + 66)	115 (−45 to + 70)
(III)	24800–26000	50 (−16 to +34)	40 (−14 to + 26)	45 (−11 to + 34)
(IV)	26000	98 (−40 to +58)	74 (−23 to + 51)	83 (−25 to + 58)

There seems to be no prescribed shape for the velocity-curves; each cycle has been unique, and the last one shows a maximum of a distinctly new form. It can perhaps be stated that the minima are generally sharper than the maxima. There is little or no evidence of a lag in phase between the three curves of hydrogen central absorption, and the conclusion seems justifiable that they pass simultaneously through maximum and minimum values.

Central absorption and emission velocities had previously been measured by McLaughlin on 57 of the 147 spectrograms. A comparison of his measures and those of the writer showed a high degree of accordance. During each season there was a wide scattering of the velocities given by individual plates. A comparison of the differences, plate *minus* normal place, for Dodson and McLaughlin showed a close agreement. This demonstrated that the variations during any season were actually inherent in the plates, although this does not fully establish their physical reality as attributes of the star.

Efforts to find a period for these more rapid changes met with little success. For the most part the data were too far apart in time to give conclusive results. For $H\gamma$, data for single seasons could be fairly well represented by periods of from 25 to 39 days. For five different seasons the periods found are as follows:

1923–24	39 days	1930–31	30 days
1926–27	25	1931–32	39
1929–30	39		

More data would be needed before definite conclusions could be reached concerning the existence of a short period.

VELOCITIES DERIVED FROM THE HYDROGEN EMISSION LINES

Normal places of the emission velocities of $H\beta$, $H\gamma$, and $H\delta$ are tabulated in the fifth, sixth, and seventh columns of Table I, and are plotted in Figure 1 as open circles. The curves based on them are drawn as broken lines.

The emission velocity-curves are very similar to those for the central absorption lines. The minima are sharper than the maxima, and there is no evidence of lag in phase between the three curves. As in the case of the absorption, the range of velocity is greater for the lines of shorter wave-length, as is shown in the following table:

	Max.	Min.	Range in Km/Sec
$H\beta$	+ 55	−10	65
$H\gamma$	75	45	120
$H\delta$	+110	−45	155

Comparing the absorption and the emission velocity-curves, it is evident that there is a phase difference between the two sets. For each line the emission velocity anticipates the absorption velocity by as much as 100 days. There is also a difference of amplitude of emission and absorption. For $H\beta$ and $H\gamma$ the range is greater for the absorption than for the emission. This, combined with the difference in phase, results in a slight asymmetry in the position of the central absorption line. During the increase of velocity the absorption lies slightly to the violet side of the center of the emission; at maximum emission velocity it is truly central; and during decreasing velocity it is on the redward side of the emission center. Considering normal places, the greatest observed deviation of the absorption from the center of the emission amounts to about 4 per cent of the width of the emission line.

THE WIDTHS OF THE EMISSION LINES

The widths of the emissions at $H\beta$, $H\gamma$, and $H\delta$ undergo variations of more than an angstrom unit. Normal places formed from the measures of width are given in the second, third, and fourth columns of Table II, and are plotted in Figure 2, where the velocity

curve of the $H\gamma$ central absorption is displayed at the top for purposes of comparison. In the main, the widths of all three emission

TABLE II

NORMAL PLACES: WIDTHS OF EMISSION LINES AND VELOCITIES OF EMISSION EDGES FOR HYDROGEN

JULIAN DAY	EMISSION WIDTHS IN ANGSTROMS			VELOCITIES OF EMISSION EDGES IN KM/SEC					
				$H\beta$		$H\gamma$		$H\delta$	
	$H\beta$	$H\gamma$	$H\delta$	Red Edge	Violet Edge	Red Edge	Violet Edge	Red Edge	Violet Edge
2400000+									
20827	5.9	5.2	4.8	+192	−176	+192	−163	+195	−140
21562	7.0	5.4	.....	232	198	234	136	.....	.....
22301	6.4	5.0	5.6	250	145	240	107	290	116
22383	5.8	5.1	4.3	209	149	228	124	222	96
22661	5.6	5.4	.....	208	136	190	182	.....	.....
22720	6.4	5.3	4.7	213	182	195	173	165	150
23094	7.0	5.9	5.4	205	227	165	245	138	242
23361	.....	5.5	.....	.....	.....	230	151	.....	.....
23497	5.6	5.4	4.3	219	128	221	149	211	105
23778	5.6	4.7	.....	215	130	198	112	.....	127
23847	6.5	5.5	5.6	260	139	256	115	318	99
24153	6.0	4.8	4.4	231	139	212	119	192	130
24225	5.9	5.1	5.1	216	146	235	120	231	147
24458	6.2	4.7	5.1	199	184	179	148	177	192
24527	5.7	5.8	5.3	192	161	183	201	183	214
24832	5.8	5.1	4.7	180	177	164	196	159	184
24867	5.7	4.9	4.9	187	166	167	173	153	206
25265	5.2	4.8	(2.2)	191	132	193	140	40	121
25561	5.4	5.5	5.2	185	148	231	136	231	137
25909	6.5	5.1	4.6	192	206	154	198	156	182
26005	6.9	5.8	5.3	205	218	177	228	166	251
26276	6.6	5.4	4.8	243	165	222	149	201	144
26373	6.4	5.3	.....	230	163	228	139	.....	123
26657	7.0	5.6	6.0	243	185	270	144	256	172
26752	6.3	5.5	5.3	223	163	226	153	214	172
27011	5.9	5.2	4.9	207	158	211	152	199	166
27109	6.8	5.9	5.1	+244	−175	+230	−179	+218	−146

lines vary together, and exhibit maxima of width at both maxima and minima of velocity, and minima of width at the times near

median velocity. The only marked exception to this rule occurs at about JD 25400, when the maximum of velocity is unusually low. The plates which furnish the discordant data are the two-prism spectrograms, most of which are underexposed.

A closer insight into the nature of the variations is gained from a study of velocities of the separate emission edges. These are given

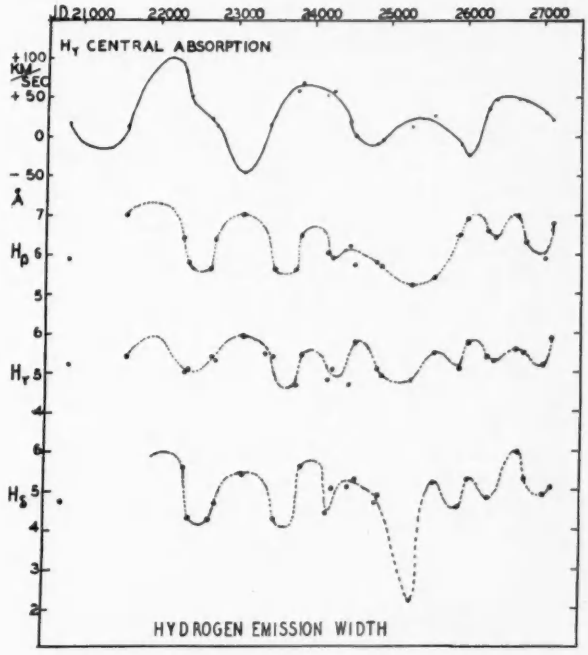

FIG. 2.—Hydrogen emission widths in 25 Orionis

in the last six columns of Table II and are plotted in Figure 3. For each hydrogen line, the velocity curve for the red edge is plotted above that for the violet edge, so that changes in the distance between the two curves indicate (but are not proportional to) changes of the width of the line. In general, the violet edges show sharp minima at the times of velocity minima, but rather blunt maxima at the times of velocity maxima. The red edges, however, show the reverse effect: sharp maxima at velocity maxima and blunt minima at velocity minima, although the differences are less pronounced. It is thus suggested that the variations of emission width

are caused by a flaring-out of the weak violet edge of the emission at velocity minima and a flaring-out of the weak red component at velocity maxima. This rather striking phenomenon has an important bearing on the interpretation of the variations in terms of a physical model, which will be discussed in a later section.

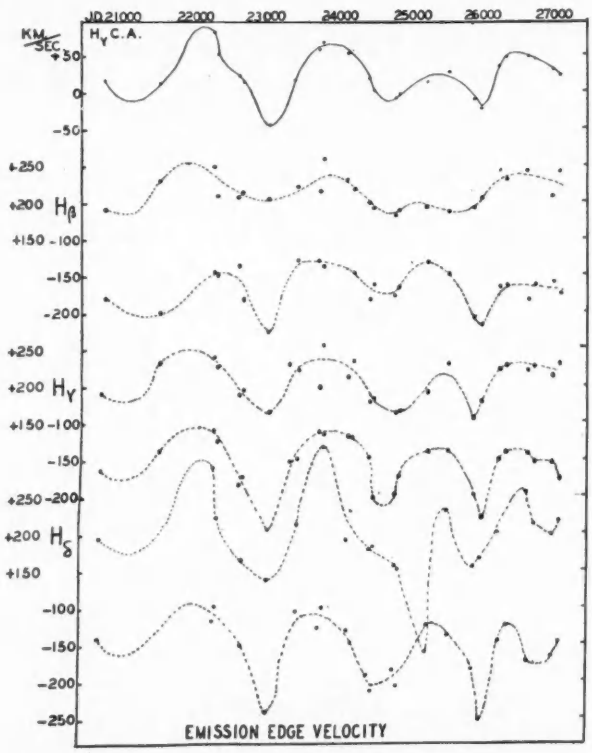

FIG. 3.—Velocities of hydrogen emission edges in 25 Orionis

Line widths, when caused by Doppler shift, should be proportional to the wave-lengths, if the widths are given in wave-length units. Mean values based on all the normal places, except those of JD 25265, are as follows:

$H\beta$	6.2 A	382 km/sec
$H\gamma$	5.3	367
$H\delta$	4.8	351

The agreement seems satisfactory, and the systematic change with wave-length is in the right direction and of the right order of magni-

tude to be accounted for by the effect of the slit-width in increasing the apparent width of the emission.

THE RATIO OF INTENSITY OF THE VIOLET TO THE RED EMISSION COMPONENTS

Values of the ratio of intensity of the two emission components of $H\gamma$ and $H\delta$ were estimated from the microphotometer tracings.

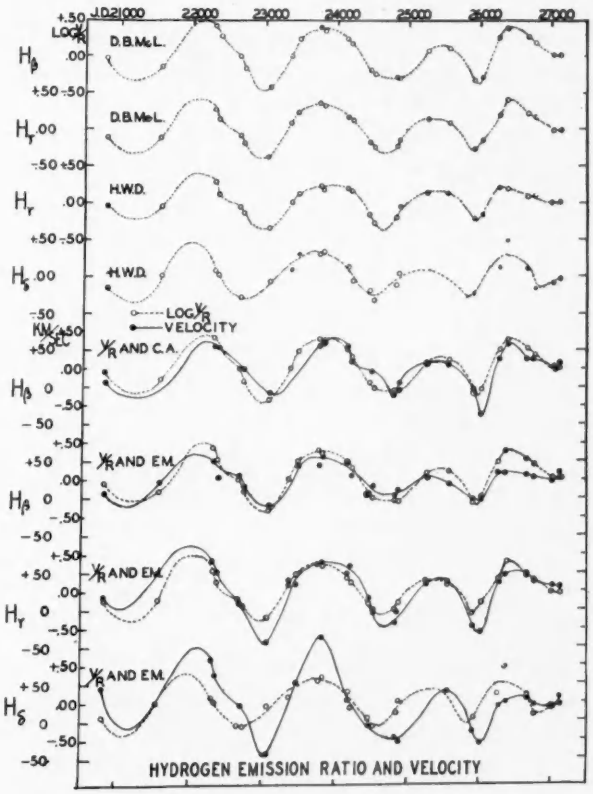

FIG. 4.—25 Orionis. In the lower half of the diagram the figures nearest the margin are log V/R; the others are velocities.

Normal places of these data are given in the tenth and eleventh columns of Table I, in the form of logarithms of V/R. Similar data by McLaughlin, determined by eye estimates from the spectrograms, are given for $H\beta$ and $H\gamma$ in the eighth and ninth columns. The resulting curves are plotted in Figure 4. The close agreement

of the two curves for $H\gamma$ obtained by different observers and by quite different methods furnishes a convincing check on the accuracy of the data.

McLaughlin has pointed out that the curves of V/R show a close similarity to the velocity curves. A comparison of his curves for $H\beta$ and $H\gamma$ shows a slight difference in phase: changes of $H\gamma$ slightly precede the corresponding changes of $H\beta$. A comparison of the writer's curves for $H\gamma$ and $H\delta$ shows a conspicuous difference of phase in the same direction; $H\delta$ anticipates $H\gamma$ by 200–300 days. This difference is so conspicuous that it is unquestionably real, and unpublished observations by McLaughlin show this effect strikingly in π Aquarii. On some plates of that star the inequalities of the components at $H\beta$ and $H\gamma$ are opposite in direction, and the appearance of $H\gamma$ predicts the change which is about to occur at $H\beta$.

Rather interesting relationships result from a comparison of the curves of emission ratio and of velocity. The maxima and minima of the former occur earlier than corresponding phases of the central absorption velocities, and the difference in phase is greatest for $H\delta$. (For $H\beta$, see curve 5, Fig. 4.) The relation of the curves of emission ratio to those of emission velocity is shown in the last three curves of Figure 4. At $H\beta$ the two curves are practically in phase; at $H\gamma$ the emission velocity curve lags about 100 days with respect to the curve of emission ratio; and at $H\delta$ the lag is about 250 days in the same sense.

VELOCITIES DERIVED FROM THE HELIUM LINES

Measurements of the helium lines in this spectrum are very uncertain. The lines are broad and diffuse; and the difficulty of measurement is further complicated by apparent structure, doubling, or marked asymmetry. The lines λ 4026 and λ 4472 were measured independently with the micrometer measuring engine and on microphotometer tracings. Normal places formed separately for λ 4026 and λ 4472 for the two methods are given in Table III. The individual velocities are plotted in Figure 5 as small dots and the normals as circles.

In spite of the large scattering of the individual values, the normal places for λ 4472 measured by the two methods are in satisfactory

accord. The same, unfortunately, cannot be said concerning λ 4026. In view of the more diffuse character of the latter line and the weaker exposure of that region, it seems best to regard the data obtained from it as inconclusive. The curves for λ 4472 show a cyclic varia-

TABLE III

NORMAL PLACES: HELIUM AND HYDROGEN BORDER ABSORPTION VELOCITIES; TYPE OF CONTOUR FOR HELIUM

JULIAN DAY	HELIUM VELOCITIES IN KM/SEC				HYDROGEN BORDER ABSORPTION VELOCITY IN KM/SEC		TYPE OF CONTOUR FOR HELIUM	
	λ 4472		λ 4026					
	Measur. Eng.	Micro-photom.	Measur. Eng.	Micro-photom.	Measur. Eng.	Micro-photom.	λ 4472	λ 4026
2400000+								
20827	−10	−27	+10	+ 6	+27	+ 62	−3.2	−0.8
21562	.....	.....	+58	+20	.....	144	.....	+2.0
22326	− 8	−33	− 5	−16	+67	127	+0.6	+1.0
22708	−21	−19	+ 6	−19	+19	126	−2.1	−0.6
23094	+30	+19	−16	−12	−16	161	0.0	−0.3
23439	+58	+21	+26	− 8	.....	108	+2.5	+2.0
23827	+ 6	− 9	− 4	+ 9	+81	157	+3.1	+2.1
24189	−19	−36	+ 8	+30	+51	49	−1.2	−1.3
24487	−32	−29	+ 7	+ 5	+89	51	−3.1	−0.7
24847	+ 8	− 8	+12	+ 6	+ 8	99	+0.7	−0.5
25265	.....	−14	.....	.....	.....	.....	.....	.....
25561	− 1	−42	−14	−13	+49	39	−3.7	−0.5
25961	+24	+10	+18	− 2	−63	77	−1.6	−0.3
26320	+ 4	−16	+41	+ 3	+15	116	+3.6	+0.8
26657	+22	−35	+37	−13	+38	109	+1.6	+0.3
26752	−32	−33						
27011	−26	−23	− 4	−17	+31	+102	0.0	−1.0
27109	+ 8	−17					−2.8	

tion of velocity with an amplitude of about 70 km/sec. The relation between these velocities and those of the hydrogen central absorption is evident from Figure 6, where the latter are reproduced at the top of the chart and the curve for λ 4472 is the second from the top. The two variations have similar periods, but are conspicuously out of phase. Maxima and minima of the helium velocity occur at least one-third of a period before those of the hydrogen velocity. The lag

of the hydrogen velocity amounts to as much as 600 days in cycles I and II, and 400 days in cycles III and IV.

One unfamiliar with the behavior of Be spectra might find it easy to dismiss this difference of phase as an indication that the observations are without meaning. On the contrary, other Be spectra show that it must have some very great significance, for in only one Be

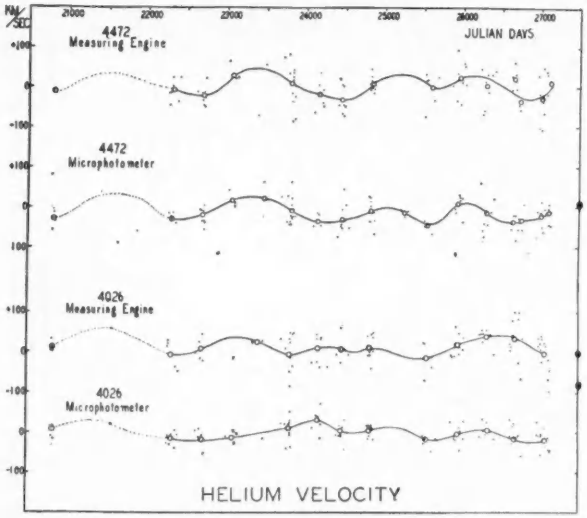

FIG. 5.—25 Orionis

star so far investigated has the helium been found to vary in phase with the hydrogen.[7]

[7] BD +11° 4673: helium anticipates hydrogen by roughly one-fifth of a period (Merrill, *Ap. J.*, **69**, 351, 1929).

ζ Tauri: helium is almost opposite in phase to hydrogen (Losch, *Michigan Obs. Pub.*, **4**, 20, 1931).

β Monocerotis: helium velocities are contradictory; mean for all lines is nearly constant (at maximum?), while hydrogen is still increasing (Hawes, *Vassar Pub.*, No. 4, p. 35 [Pl. II], 1934).

11 Camelopardalis: helium is approximately opposite in phase to hydrogen (*ibid.*, p. 45).

β Piscium: helium and hydrogen are opposite in phase (*ibid.*, p. 48).

χ Opiuchi: helium anticipates hydrogen by about one-quarter of a cycle (Cleminshaw, unpublished thesis, University of Michigan, 1934).

HD 33232: "helium velocities apparently have no relationship to the curve for hydrogen" (Merrill, *Ap. J.*, **79**, 347, 1934).

φ Persei: helium is in phase with hydrogen (Dustheimer and Schiefer, unpublished theses, University of Michigan, 1927 and 1929).

VARIATIONS OF CONTOUR IN THE HELIUM LINES

Because of this apparently significant, though confused, character of the helium variations, it was considered worth while to study in greater detail the behavior of the helium lines. Microphotometer tracings show that the helium lines are asymmetrical and that the asymmetry changes. These changes were studied by

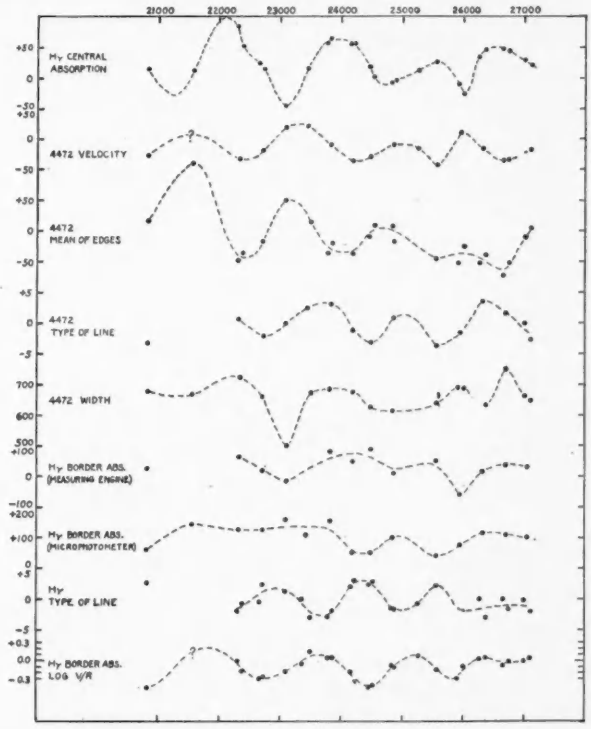

FIG. 6.—25 Orionis

classifying the lines according to degree and direction of asymmetry. The type of line was called positive when the side of greater wave-length showed the steeper gradient, negative when the contour was steeper on the side of shorter wave-length, and zero when the contour was symmetrical. Degree of asymmetry was indicated by the numbers 1–5. These estimates of type of line for λ 4472 show cyclic variations with a period similar to that of the helium and hydrogen velocity curves but out of phase with both of them. The values are given in Table III and are plotted in Figure 6.

The helium velocities from both the microphotometer and measuring engine data were determined from settings on what was considered to be the center of density of the line. This measure was undoubtedly influenced by the radical changes in the contour of the line. If the change in line contour had been the sole cause of the apparent variation in the helium velocity, then the type-of-line curve and the velocity curve should have been in phase. These curves are not in phase; instead, the greatest asymmetry occurs at times of median velocity. The edges of λ 4472 were measured separately, and the mid-point of the line was determined by taking the average of the two measures. Normal places formed from these measures are plotted in the third curve of Figure 6. The mid-point of the line has undergone cyclic shifts in position and is of exactly opposite phase to that of the $H\gamma$ central absorption velocity. The helium velocity curve (center of density measure) is now seen to be the resultant of two separate effects: a shift of the line as a whole, and a variation in the asymmetry of the line.

Normal places of the widths of λ 4472, based on the measures of apparent edges, are given in Table IV and are plotted in curve 5 of Figure 6. This curve shows that the helium lines tend to be narrower when shifted toward the red than when displaced in the opposite direction.

Individual spectrograms differ widely from the seasonal means, and time-averages may have distorted certain relationships between contour, mid-position, and width of line. Accordingly, the data were regrouped by values of these characteristics. In general, when the line λ 4472 was deep on the violet side, it was narrow and the mean of the edges was displaced redward. When symmetrical, it had average width and position. When the absorption was more intense on the redward side, it was wide and the mid-position was displaced toward the violet.

THE UNDERLYING HYDROGEN ABSORPTION

It was thought that the broad underlying absorption lines of hydrogen probably originated in the same region of the stellar atmosphere as the helium absorption, and that similar behavior should therefore be expected. Accordingly, these lines were investigated by

measuring their apparent edges on the spectrograms and microphotometer tracings. The normal places obtained from these measurements are given in the sixth and seventh columns of Table III. Both

TABLE IV

NORMAL PLACES: EMISSION RATIO AND ABSORPTION BORDER RATIO FOR $H\gamma$; VELOCITY OF MEAN OF EDGES AND WIDTHS OF HELIUM λ 4472

JULIAN DAY	$H\gamma$ EMISSION RATIO: LOG V/R	$H\gamma$ ABS. BORDER: LOG V/R	TYPE OF CONTOUR $H\gamma$ ABS. BORDER	HELIUM λ 4472	
				Velocity of Mean of Edges in Km/Sec	Width in Km/Sec
2400000+					
20827	−.06	−.45	+2.7	+ 17	680
21562	−.05	.....	.....	+110	671
22301	+.28	.00	−2.0	− 48	726
22383	+.11	−.18	−0.7	− 36	
22661	−.05	−.30	−0.5	− 18	660
22720	−.13	−.27	+2.3		
23094	−.32	−.18	+1.3	+ 50	500
23361	.00	−.05	0.0	.....	.....
23497	+.12	+.15	−3.0	+ 14	674
23778	+.23	+.04	−2.8	− 36	686
23847	+.18	+.06	−1.8	− 20	
24153	+.20	−.19	+2.0	− 37	677
24225	+.16	−.36	+3.0		
24458	−.16	−.43	+2.4	− 10	628
24527	−.27	−.41	+2.8	+ 8	
24832	−.20	−.08	−1.5	+ 8	616
24867	−.02	−.11	−1.6	− 18	
25265	+.14	+.08	−0.7	.....	.....
25561	+.13	−.15	+2.2	− 46	642
25909	−.22	−.29	−1.8	− 52	691
26005	−.18	−.10	−2.0	− 25	686
26276	+.20	+.03	0.0	− 52	631
26373	+.19	+.05	−3.0	− 39	636
26657	+.09	−.07	0.0	− 72	748
26752	+.10	−.02	−1.6	− 52	
27011	.00	−.01	−0.2	− 9	664
27109	.00	+.04	−2.0	+ 4	651

sets of normals are plotted in Figure 6 as the sixth and seventh curves. Mere random discordance would have been less disturbing than the obviously systematic difference that is shown by the two curves. The curve determined from the measures of the spectrograms is in phase with that for the central absorption; the curve based on the

microphotometer tracings is apparently in phase with the velocity curve for λ 4472.

In face of the necessity of choosing between the two curves or dismissing both as meaningless, it appears logical to accept that based on the microphotometer tracings. The line contour on the tracing is a definite and measurable feature; the apparent "edge" of the absorption as seen by the eye on the spectrogram is a thing impossible to define. The large positive velocity of the measures from the tracings is doubtless produced by the influence on the contour of four faint lines of *O* II to the redward of $H\gamma$, but this should not affect the validity of the observed variations of position.

McLaughlin[8] made the qualitative observation that the absorption border on the side of the strong emission component is greatly strengthened, while the other border often nearly disappears. He suggested that this may be due to a motion of the emission as a whole across a stationary underlying absorption, with consequent uncovering of the strong central core. The writer made estimates from microphotometer tracings of the ratio V/R for the absorption borders of $H\gamma$. Normals of these are tabulated in the third column of Table IV and are presented graphically at the bottom of Figure 6. The curve appears well determined and shows that, in general, a strong emission component is flanked by a strong absorption border (since this curve is nearly in phase with that of the hydrogen central absorption velocity and consequently with the curve of emission ratio). McLaughlin's observation is thus confirmed qualitatively, but more accurate study shows that the ratio V/R of the absorption borders reaches its maximum and minimum values about one-sixth of a cycle before the corresponding phases of the emission velocity. There is thus some cause other than a mere uncovering of the deeper portion of the absorption contour with the shift of the emission.

Just as in the case of the helium lines, the microphotometer tracings show that the exposed portions of this underlying hydrogen absorption are unsymmetrical and that the asymmetry changes. In order to make estimates of the type of line, it was necessary to extend the exposed portions of the contours until they intersected. The

[8] *Op. cit.*, p. 48.

normal places of the estimates thus made are given in Table IV, column 4, and are shown graphically in Figure 6, curve 8.

This type-of-line curve for $H\gamma$ sheds some light on the changes in intensity of the two absorption borders. In the main, the change of contour alone would account qualitatively for the change of the ratio V/R of the absorption borders. As the absorption is becoming deep on the violet side (negative type of line), the ratio V/R is seen to approach a maximum. The coincidence is not exact, however, and the ratio V/R for the absorption borders continues to increase for about 100 days after the type-of-line minimum. By an intercomparison of the curves of Figure 6, this difference is found to be satisfactorily accounted for by the further uncovering of a deeper part of the line contour as the emission line shifts toward the red. Similar phenomena occur at the time of maximum asymmetry in the opposite sense.

THE IRON EMISSION

An examination of the tracings shows the presence of broad and faint emission at λ 4584. There are some indications that it became weaker after about JD 27000. It is interesting to note that there was some evidence of a fading of the hydrogen emission at the same time. Prior to JD 25500 the $H\gamma$ emission was consistently stronger than the continuous spectrum of the region, but after JD 27000 it usually appeared distinctly weaker than the continuous spectrum.

DISCUSSION

It is hardly to be expected that all details of the very complex behavior of the spectrum of 25 Orionis will be immediately explained by a simple physical model, but the problem is by no means hopeless. The cyclic variations of velocity and emission intensity constitute the nucleus of the problem. The variations of φ Persei are repeated with such regularity that it was natural to attempt an explanation in terms of orbital motion and attendant phenomena. Such an explanation, however, cannot be valid for Be spectra in general, since several of them are utterly irregular in their behavior. The changes of period of 25 Orionis and π Aquarii[9] definitely rule out the binary hypothesis.

[9] McLaughlin, *Ap. J.*, **77**, 224, 1933.

The suggestion that the changes are due to a type of pulsation is due to R. H. Curtiss.[10] A further advance was made by Struve,[11] who pointed out that the diffuse character of the absorption lines indicated rapid rotation and suggested that the emission lines arise from a ring of gas ejected by the rapidly rotating star. This hypothesis, while accounting for the duplicity of the emission, did not satisfactorily explain the relations of velocity and emission ratio.

Recently, Gerasimovič[12] has suggested that Be spectrum variations can be accounted for by a stellar atmosphere in which, for hydrogen, the outward acceleration due to radiation pressure is greater than gravitation. As a result, there is a dissipation of material. This outflow continues until the optical thickness of the expanding chromosphere is sufficient to produce an inward flux of radiation in the dangerous frequencies which will stop the outflow. When this material has been sufficiently dispersed as an expanding shell of gas, the outflow of material will begin again. This mechanism gives a very satisfactory and plausible explanation of the variations in the relative intensities of the red and the violet hydrogen emission components, but is not so successful in explaining the variations in hydrogen absorption and emission velocities.

McLaughlin,[13] working from the similarities of Be spectra to those of novae, suggested an extensive stellar atmosphere, pulsating as well as rotating. Two atmospheric levels are distinguished: an inner emitting atmosphere where the atoms are frequently photoelectrically ionized by the stellar radiation and recombine, giving the emission lines; and an outer atmosphere shielded from the ionizing radiation by the absorption of atoms below it, and therefore acting mainly to produce the absorption superimposed on the emission. The rotation of the atmosphere accounts for the breadth of the emission. In a stage of atmospheric expansion the receding gases on the far side of the star give the strong red component of the emission, which is not subject to absorption by the approaching gases on the near side of the star because of the Doppler shift due to their relative veloci-

[10] *Michigan Obs. Pub.*, **4**, 174, 1932.

[11] *Ap. J.*, **73**, 100, 1930.

[12] *M.N.*, **94**, 737, 1934; *Observatory*, **58**, 115, 1935.

[13] *Proc. Nat. Acad.*, **19**, 44, 1933.

ties. The violet component, produced by approaching gases, is weakened by absorption by the approaching gases of the absorbing layers. At this phase the central absorption, originating between the observer and the star, is produced by approaching gases and is shifted in the negative direction. Opposite effects occur when the expanded atmosphere collapses. However, it is not to be supposed that the velocities observed indicate the extent of the expansion. The observed velocities refer to individual atoms streaming outward or inward, while the region of origin of the emission is considered to undergo only a relatively small change of size.

From the account just given, it should be clear that the general features of the spectral variations of 25 Orionis are satisfactorily accounted for by McLaughlin's hypothesis. It is therefore important to examine the finer details of the behavior of the spectrum.

The hydrogen central absorption velocity curves indicate an increase in range of velocity with decrease in wave-length. Since we may assume that $H\beta$ originates at a higher effective level than $H\gamma$, and $H\gamma$ higher than $H\delta$, this means, in terms of the proposed model, that the maximum velocities attained by the atoms are greater in the inner absorbing atmosphere than in the outer. Such a state of affairs appears reasonable; as the atoms recede from the star, we may expect them to be retarded by gravitational attraction, and the maximum velocity observed for atoms in the outer regions should be less than that in the inner layers. Similarly, during collapse the gravitational acceleration should lead to the greatest velocities in the inner absorbing layers, just before the atoms begin to be checked by radiation pressure as they enter the region where screening is no longer complete. This aspect of the observed velocities is therefore distinctly favorable to the proposed hypothesis.

If the central star were small compared with the gaseous envelope, so that no appreciable occultation of atmosphere by the star occurred, then there should be no variation of emission velocity. As expansion and contraction occurred, there should be symmetrical increases and decreases of width of the emission without change of position. If the model is correct, the fact that the emission lines oscillate indicates that significant occultation occurs. During expansion some of the most rapidly receding gases are occulted, with re-

sultant shift of the emission toward the violet (in the same direction as the central absorption) because of the cutting-off of its red edge. We should expect that a larger percentage of the gases at lower levels would be occulted, i.e., that the effect would be greatest for $H\delta$ and least for $H\beta$. The observations show a greater range of emission velocity for $H\delta$ than for $H\gamma$, and least of all for $H\beta$. These data, therefore, are also favorable to the model.

The variation of emission widths furnishes additional convincing evidence. Whether occultation and its accompanying variation of emission velocity occurs or not, there should be marked changes in the widths of the emission lines if the inward and outward motions of the atoms exceed the rotational velocities. According to the model, greatest emission width should occur at the times of fastest expansion and fastest collapse, i.e., twice during a cycle. The observed emission widths exhibit precisely this behavior. The study of the separate emission edges shows that the increase of width at velocity minimum (fastest expansion) is due to the addition of large velocities of approach on the side of the weak violet component of the emission. Light from the atoms having the greatest velocities of recession fails to reach us on account of occultation by the star. It should be noted that these observations of variation of the emission width are not unique. Schiefer and Dustheimer[14] observed changes of emission widths in φ Persei. The relation between emission width and velocity was precisely that observed in 25 Orionis.

The observed central absorption velocity curves show no difference in phase between $H\beta$, $H\gamma$, and $H\delta$, even though these lines presumably originate at different effective levels. The cause of their velocity changes must therefore act practically simultaneously throughout the extensive absorbing outer atmosphere. This points toward radiation pressure and gravitation as the forces controlling the motions of the gases. A similar interpretation is to be placed on the lack of difference in phase between the emission velocity curves.

The slight phase difference of the central absorption and emission velocities and the great difference in the minima of the emission ratio and the hydrogen velocities cannot be so readily explained without some rather arbitrary assumptions as to the extent of the

[14] Unpublished theses, University of Michigan, 1927 and 1929.

various layers, the values of the outward acceleration at different levels in the atmosphere, and the law of rotational velocities as a function of distance from the star. The observed differences in phase of V/R and the velocity curves suggest a compressional wave beginning at the photosphere and traveling outward through the extensive nebulous atmosphere about the star, but this attractive hypothesis appears incompatible with the low densities required and with radiation pressure as the postulated cause of the outward acceleration.

If we consider the screening effect of the atoms, the acceleration acting on the atoms of the inner absorbing layers (the $H\delta$ level) should be much greater than that acting on the atoms higher up (the $H\beta$ level). Therefore, we might expect that the $H\delta$ shell would attain its maximum rate of expansion more quickly than the higher layers, and that it would be more quickly checked during the collapsing phases. This difference is in the direction actually observed for the emission ratio V/R ($H\delta$ anticipates $H\gamma$, and $H\gamma$ anticipates $H\beta$), but it is difficult to believe that it would account for so large a lag in phase as that observed. If we accepted this interpretation, then we should find it difficult to account for a lack of phase difference between the velocity curves for the several lines, either in emission or absorption. We must therefore admit this as a difficulty in connection with the hypothesis proposed by McLaughlin.

The interpretation of velocity variations shown by the helium and the underlying hydrogen absorption is obscure. These variations do not fit directly into the mechanism suggested by McLaughlin. However, the model proposed by Gerasimovič requires that all absorption lines in the spectrum show cyclic variations in velocity and in a manner such that, when the red emission component is weaker than the violet (when the hydrogen lines are shifted toward the red), the spectrum lines other than those of hydrogen should be displaced toward the violet. Regardless of which measure—the mean of the edges or the center of density—be accepted as the helium velocity, it can be said that the helium lines in 25 Orionis show cyclic displacements which are distinctly out of phase with the hydrogen velocities. To what extent the variable asymmetry of the helium lines can be accounted for by variable weak emission is un-

certain. Further work will have to be done before any definite conclusions can be reached from the study of these lines.

It is with pleasure that I acknowledge my indebtedness to Dr. Dean B. McLaughlin for his untiring help and encouragement throughout this investigation. I wish to thank Dr. Heber D. Curtis, director of the University of Michigan Observatory, for the data and equipment made available to me, and the director of the Lick Observatory for the loan of spectrograms of 25 Orionis.

This investigation was undertaken while the writer held the Dean Van Meter Fellowship granted by Goucher College.

WHITIN OBSERVATORY
WELLESLEY, MASSACHUSETTS
November 1935

SCATTERING OF LIGHT IN DIFFUSE NEBULAE

OTTO STRUVE AND HELEN STORY

ABSTRACT

The degree of obscuration of faint background stars has been estimated for 90 nebulae, of which 68 were listed by Hubble in his study of the origin of nebular luminosity. Nebulae having continuous spectra are associated with an appreciably greater degree of obscuration than nebulae having emission spectra. The difference is of the order of 0.6 mag. The nebulae in the Pleiades are much less efficient in reflecting starlight than are the nebulae near ρ Ophiuchi and near ν Scorpii. An application of Seeliger's theory to the nebulae having continuous spectra leads to a determination of the albedo p of the particles, provided the opacity is complete. This condition is probably nearly fulfilled in the region of ρ Ophiuchi, for which $p=0.7$. For the Pleiades $p=0.03$, but this value includes departures arising from a lack of opaqueness. The high value for the nebulae near ρ Ophiuchi is probably not real and may be caused by absorption.

Recent investigations of the properties of interstellar matter deal largely with absorption phenomena. It is now generally believed that in addition to free atoms which give rise to "stationary" absorption lines, interstellar space contains an appreciable amount of finely divided matter which causes selective, as well as non-selective, absorption. It is reasonable to suppose that the non-selective absorption is produced by particles which are considerably larger than the wave-length of light and which, therefore, act as screens, without causing complicated diffraction effects of the type required to produce Rayleigh scattering. The selective absorption is probably caused by particles which are somewhat too large to produce true Rayleigh scattering but which are small enough to give an appreciable amount of space reddening, which, in general, follows the more complicated laws derived by Mie.

The absorption coefficients of the two types of absorption are apparently not constant in all parts of interstellar space, and even the ratio of the selective to the non-selective absorption varies from one region to the other. Barnard's dark nebulae seem to be characterized by large values of the non-selective absorption coefficient, and in at least some of them the selective absorption coefficient is not nearly as large as would be expected if their ratio were constant. On the other hand, regions of pronounced space reddening are known

to occur in parts of the Milky Way where there are no particularly dense dark nebulae.

Information of a different kind concerning the properties of interstellar matter may be obtained by considering not only the diminution of the transmitted beam of light but also the scattered radiation produced by the particles. Here we must again consider separately the effects produced by the larger particles and those produced by the selectively scattering smaller particles.

In a recent paper[1] an attempt was made to investigate the scattering of light produced by the larger particles. The theory of Seeliger,[2] which is particularly adapted to this problem, leads to very simple expressions for the surface brightness of an opaque cosmic cloud illuminated by a known quantity of light. Accordingly, in the paper mentioned above, an attempt has been made to apply these expressions to some of Barnard's dark nebulae and to derive their surface brightnesses, which are due to the general illumination of the starry sky. The result seemed to indicate that this surface brightness should be about 0.15 mag. greater than that of the background of the sky. Actual observations made by a photographic method first suggested by Fabry led to a much smaller value. This could mean one of two things: either the albedos of the nebular particles are much smaller than one-third, the value used in the computations, or the surface brightness of the sky background contains an amount of scattered starlight, produced by interstellar particles, which tends to reduce the contrast between the dark nebula and the background.

But before it is really safe to depend upon conclusions which are derived from an application of Seeliger's theory, it is necessary to test the reflection hypothesis for cosmic clouds, and this can best be done by a study of diffuse galactic nebulae having continuous spectra.

The reflection hypothesis was advanced by V. M. Slipher[3] to explain the fact that several galactic nebulae possessed spectra which were true copies of the spectra of nearby stars. A study of the nebula

[1] Struve and Elvey, *Ap. J.*, **83**, 162, 1936.

[2] See Schönberg, *Handbuch d. Astrophysik*, **2**, Part 1, 163, 1928.

[3] *Bull. Lowell Obs.*, No. 55, 1912, etc. See also Struve, Elvey, and Keenan, *Ap. J.*, **77**, 274, 1933.

in the Pleiades, by Hertzsprung,[4] gave additional support to the hypothesis. In his fundamental investigations of galactic nebulae, Hubble[5] concluded that "within the errors of observation, the data can be represented on the hypothesis that diffuse nebulae derive their luminosity from involved or neighboring stars, and that they re-emit at each point exactly the amount of light radiation which they receive from the stars." Finally, Zanstra,[6] from a rediscussion of Hubble's data, decided that "the reflection theory leads, therefore, to a reasonable value of the albedo."

EFFICIENCY OF SCATTERING AND OBSCURATION

It is a matter of considerable surprise that in Hubble's discussion the same relation,[7] $m_* + 4.90 \log a_1 = 11.02$, holds for nebulae having emission spectra[8] and for nebulae having continuous spectra.[9] That this agreement was merely a coincidence is obvious: an ideal light filter absorbing the strongest nebular emissions would have destroyed the similarity. There is, however, a more serious discrepancy: if all galactic nebulae are essentially similar in composition, and if the mechanism suggested by Zanstra for the nebular emission lines is merely superimposed upon ordinary reflection phenomena, we should have expected that the emission nebulae would all lie above Hubble's curve. The fact that they do not must be explained: if the reflection hypothesis is correct, the densities of the *e* nebulae must be, on the average, considerably lower than those of the *c* nebulae. In other words, to be visible a nebula of the *c* type must have a greater efficiency, either in albedo or in density, than a nebula of the *e* type.

To investigate this question we may use estimates of the degree of obscuration of each nebula. Hubble[10] has already remarked that

[4] *A.N.*, **195**, 449, 1913.

[5] *Ap. J.*, **56**, 416, 1922. [6] *Ibid.*, **65**, 67, 1927.

[7] m_* is the photographic magnitude of the exciting star, and a_1 is the maximum distance from the star in minutes of arc at which the nebula could be seen on one-hour exposures obtained with the Mount Wilson 60-inch reflector, on a Seed 30 plate.

[8] These will be designated hereafter by the letter *e*.

[9] These will be designated hereafter by the letter *c*.

[10] *Ap. J.*, **56**, 190, 1922.

his *c* nebulae usually exhibited more general obscuration than his *e* nebulae. However, he has given no numerical treatment of this subject. Because of its bearing upon the reflection hypothesis we have made a more detailed study of this problem.

The degree of obscuration was estimated for each nebula from the photographs available at the Yerkes Observatory. The new Milky Way atlas by Ross and Calvert and the earlier one by Barnard were especially useful. Zero indicates no appreciable obscuration, while 10 indicates the maximum of obscuration of background stars. For example, obscuration 0 was recorded for the nebulae near γ Cassiopeiae and near λ Orionis, while obscuration 10 was recorded for the region around ρ Ophiuchi and 22 Scorpii. Since in the densest regions the obscuration is several magnitudes, each step of our arbitrary scale corresponds to, roughly, 0.3 mag. of absorption. It is not possible, at the present time, to obtain a better calibration of the estimates. Their uncertainty must, furthermore, be considerable, although, in general, there was never any doubt whether the absorption was negligible, intermediate, or large.

The estimates contain 65 of the 82 objects measured by Hubble. For the remaining 17 nebulae no suitable photographs were available. In addition to the 65 nebulae from Hubble's list we obtained estimates of obscuration for 25 additional nebulae located on the photographs made by Barnard and by Ross. For 90 nebulae we measured the maximum angular distance *a*, following the procedure of Hubble. These values were corrected by us to an exposure of one hour, again following the method of Hubble. However, these values cannot be compared in precision with those of Hubble, because they were obtained from the prints of Barnard's atlas and of a few unpublished negatives. Their purpose was to provide a means for the inclusion of the 25 additional nebulae in the discussion. Tables I and II contain the observational data.

The results of the estimates are shown in Figures 1 and 2. The former gives the 68 nebulae investigated by Hubble. The ordinates are Hubble's values of $\log a_1$, and the abscissae are the values of m_*. The lower half of the figure contains the *c* nebulae and the upper half the *e* nebulae. Figure 2 gives the 91 nebulae with our values of $\log a_1$, and with the values of m^* given in the two Tables I and II. The

TABLE I

NEBULAE LISTED BY HUBBLE

No.	Hubble's No.	Object	Sp. Neb.	m_*	log a_1		Obscuration	Source†
					Hubble	Story		
1	1	BD+64°13	c	10.4	+0.065	−0.153	2	R 20
2	2	NGC 281	E	7.3	+0.874	+1.062	2	R 20
3	3	IC 59, 63	E	2.2	+1.458	+1.403	0	R 20
4	4	BD+60°596	c	9.7	+0.326	+0.102	4	B 2
5	5	NGC 1333	C	10.9	+0.364	+0.472	10	B 3
6	6	BD+31°597	c	8.6	+0.301	+0.178	7	B 3
7	7	BD+29°565	c	9.6	+0.483	+0.473	8	B 3
8	8	Merope	C	4.0	+1.247	+1.172	6	B 4
9	9	Pleiades	c	1.2	+1.926	+1.415	6	B 4
10	10	IC 348	C	9.0	+0.124	+0.651	9	B 3
11	12	NGC 1499	E	3.7	+1.634	+1.582	2	R 29
12	13	NGC 1514	E	9.7	+0.167	−0.140	3	B 5
13	14	IC 359	C	13.5	−0.699	−0.028	0	B 5
14	17	IC 405	E	5.8	+0.973	+0.789	4	B *
15	18	IC 2118	C	0.2	+2.195	+2.295	2	B *
16	20	NGC 1976	E	4.8	+1.396	+1.393	7	B *
17	21	NGC 1977	C+E	4.6	+1.150	+0.992	8	B *
18	22	IC 431	c	7.6	+0.326	+0.204	7	B *
19	23	IC 432	c	6.9	+0.451	+0.495	7	B *
20	24	NGC 2023	C	7.9	+0.744	+0.495	8	B *
21	25	NGC 2024	E	1.4	+1.430	+1.318	9	B *
22	26	IC 435	C	8.2	+0.514	+0.374	8	B *
23	27	NGC 2068	C	10.8	+0.502	+0.505	8	B *
24	28	NGC 2071	C	10.8	+0.150	+0.204	8	B *
25	29	Orion	c	1.4	+1.820	+1.639	8	B *
26	31	NGC 2170	c	11.0	+0.088	+0.197	3	B *
27	32	BD−6°1417	c	10.2	+0.403	+0.274	2	B *
28	33	BD−6°1418	c	9.9	+0.088	+0.197	2	B *
29	34	NGC 2182	c	9.0	+0.150	+0.104	3	B *
30	35	NGC 2183	C	14.0	−0.452	−0.201	3	B *
31	36	NGC 2185	C	12.9	−0.037	+0.098	3	B *
32	37	BD−6°1444	c	10.8	−0.452	−0.201	3	B *
33	38	NGC 2175	E	7.3	+0.845	+1.038	0	B 9
34	39	NGC 2237	E	5.3	+1.246	+1.337	0	B *
35	40	IC 446	C	11.8	+0.104	−0.139	6	B *
36	42	NGC 2245	C	11.2	+0.177	+1.092	5	B *
37	45	IC 2177	E	7.3	+0.803	+0.881	2	B *
38	46	BD−12°1771	C	8.1	+0.343	+0.477	1	B *
39	47	BD−23°5277	c	9.2	+0.310	+0.366	3	B 10
40	48	BD−23°5296	c	9.0	+0.310	+0.429	3	B 10
41	49	π Scorpii	C	2.8	+1.641	+1.724	0	B 11
42	50	IC 4592	C	3.9	+1.665	+1.629	5	B 12
43	51	IC 4601 a	C	7.1	+0.765	+0.603	10	B 12
44	52	IC 4601 b	C	7.1	+0.765	+0.540	10	B 12
45	53	σ Scorpii	c	3.2	+1.819	+1.577	5	B 13
46	54	IC 4604	C	5.1	+1.451	+1.467	10	B 13

† Source: R = *Atlas of the Milky Way* by F. E. Ross and M. R. Calvert; B = *Atlas of Selected Regions of the Milky Way* by E. E. Barnard; B* = unpublished photographs by E. E. Barnard.

TABLE I—*Continued*

No.	Hubble's No.	Object	Sp. Neb.	m_*	log a_1		Obscuration	Source†
					Hubble	Story		
47.....	55	IC 4605	C	4.7	+1.372	+1.224	10	B 13
48.....	56	NGC 6514	E	7.0	0.912	1.021	3	B 29
49.....	57	NGC 6523	E	5.4	0.931	1.300	3	B 30
50.....	58	IC 4678	c	10.4	0.362	0.125	5	B 30
51.....	59	IC 1274	c	8.7	0.431	0.322	7	B 29
52.....	61	NGC 6589	c	9.8	0.191	0.466	7	B 32
53.....	62	NGC 6590	c	10.5	0.234	0.396	7	B 32
54.....	63	IC 1284	c	7.7	0.611	0.697	7	B 32
55.....	64	NGC 6611	E	7.3	0.690	0.942	0	B 34
56.....	65	IC 1287	c	6.1	1.011	0.942	7	B 34
57.....	68	NGC 6888	E	6.7	0.665	0.672	0	B 43
58.....	72	NGC 6914 a	C	8.9	0.239	0.190	4	B 44
59.....	74	γ Cygni	(*c*)	3.0	1.763	1.690	5	B 44
60.....	76	NGC 7000	C+E	1.8	2.044	2.121	5	B 45
61.....	77	NGC 7023	C	7.4	0.627	0.519	9	R 22
62.....	78	BD+57°2309	c	6.5	0.803	0.740	2	B 47
63.....	79	BD+67°1332	c	8.2	0.514	0.218	1	R 22
64.....	81	IC 5146	c	10.4	0.548	0.723	6	R 19
65.....	82	NGC 7635	E	8.5	+0.690	+0.580	1	R 20

relation between log a_1 and m_* is practically the same for all four diagrams, agreeing with Hubble's expression

$$m_* + 4.90 \log a_1 = 11.02 . \qquad (1)$$

Thus we find from the lower half of Figure 2,

$$m_* + 5.2 \log a_1 = 10.9 . \qquad (2)$$

It is evidently permissible to use the average expression

$$m_* + 5 \log a_1 = 11 . \qquad (3)$$

An inspection of the diagram shows that, on the average, there are more black spots in the two lower halves than in the upper. This indicates that the obscuration is greater for the *c* nebulae. This is brought out in numerical form in Table III.

The average difference between *c* and *e* nebulae amounts to about two steps on our arbitrary scale. This would indicate that the ab-

sorption of the *c* nebulae is roughly 0.6 mag. more than that of the *e* nebulae. Thus, the efficiency of scattering of the former is markedly greater than that of the latter, which agrees well with the requirements of the reflection theory.

TABLE II

NEBULAE NOT INCLUDED IN HUBBLE'S LIST

No.	Object	Sp. Neb	m_*	log a_1	Obscuration	Source†
1	BD+23°507	c	3.7	+0.840	6	B 4
2	BD+23°516	c	3.9	1.038	6	B 4
3	BD+24°553	c	5.8	0.473	6	B 4
4	BD+23°524	c	8.6	0.697	6	B 4
5	BD+23°541	c	2.8	0.897	6	B 4
6	BD+28°645	c	var. 9.0→11.2	0.378	6	B 5
7	BD+8°933	c	5.5	0.892	10	B 6
8	BD+12°801	c	7.3	0.682	10	B 6
9	BD+9°879	e	3.25	1.177	0	B 6
10	BD+23°1301	c	7.0	0.471	3	B 8
11	BD+10°1220	e	4.44	1.715	4	L 28
12	BD+20°1293	c	9.5	0.590	0	B 9
13	CD−23°5285	c	8.2	0.366	6	B 10
14	BD−22°1897	c	4.9	0.665	0	B 10
15	CD−24°12352	c	4.5	0.908	1	B 11
16	CD−24°12354	c	5.8	1.084	2	B 11
17	BD−19°4357	c	7.6	0.467	9	B 12
18	CD−24°12684	c	8.3	1.101	10	B 13
19	CD−26°11359	c	2.57	1.949	7	B 13
20	CD−23°14005	c	7.1	0.658	6	B 29
21	BD−16°4811	c	10.0	0.205	1	B 31
22	BD−16°4812	c	9.8	0.286	1	B 31
23	BD+17°3986	e	10.7	0.593	3	B 42
24	BD+34°3830	c	9.1	0.398	5	B 43
25	BD+56°2495	c	7.0	+0.678	0	B 47

† Source: B = *Atlas of Selected Regions of the Milky Way* by E. E. Barnard; L = photographs of the Milky Way and comets, by E. E. Barnard (*Pub. Lick Obs.*, 11, 1913).

Within each of the two lower halves of Figures 1 and 2 the scatter of the points in the diagrams results from (1) observational errors, (2) uncertainty in the value of the inclination to the line of sight of the line joining the star and the nebulous patch measured, and (3) differences in efficiency resulting from differences in the densities of the nebulae and in the albedos of their particles. Accordingly, we should expect the nebulae having greater obscurations to lie systematically higher than those having smaller obscurations. The effect,

if present at all, is masked by other factors: a slight tendency in the required direction may be present in Figure 2, but it cannot be detected in Figure 1.

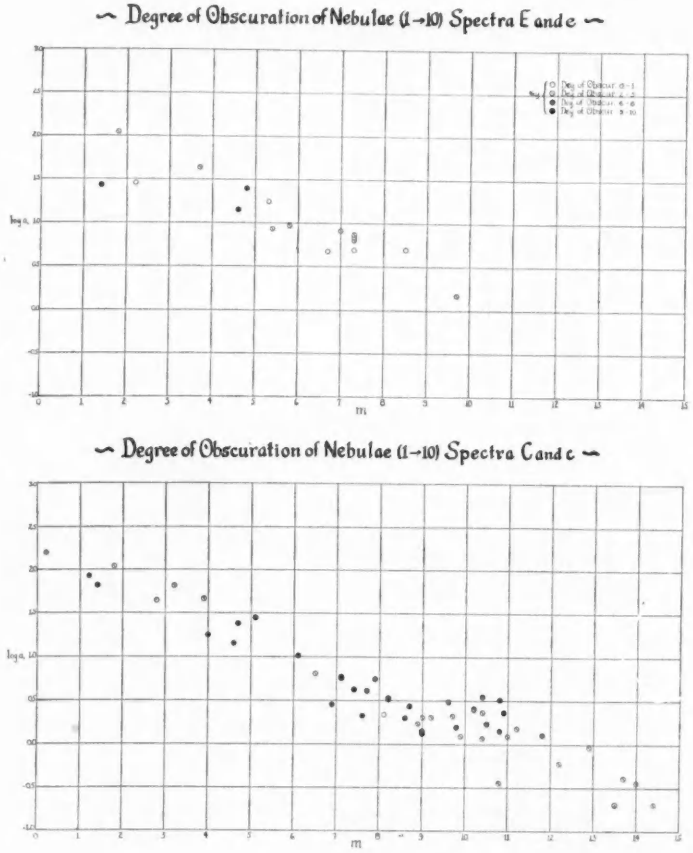

FIG. 1.—Hubble's relation in galactic nebulae and degree of obscuration

It is more instructive to arrange the data according to groups of nebulae which are close together in the sky and therefore probably form physically connected systems. This has been done in Figure 3. The best groups of *c* nebulae are those in the Pleiades, near ν Scorpii and near ρ Ophiuchi. Of these, the first shows definitely a departure indicating less than the average amount of efficiency, while the third

shows exceptionally great efficiency. This agrees well with the fact that the obscuration is relatively small for the Pleiades and ex-

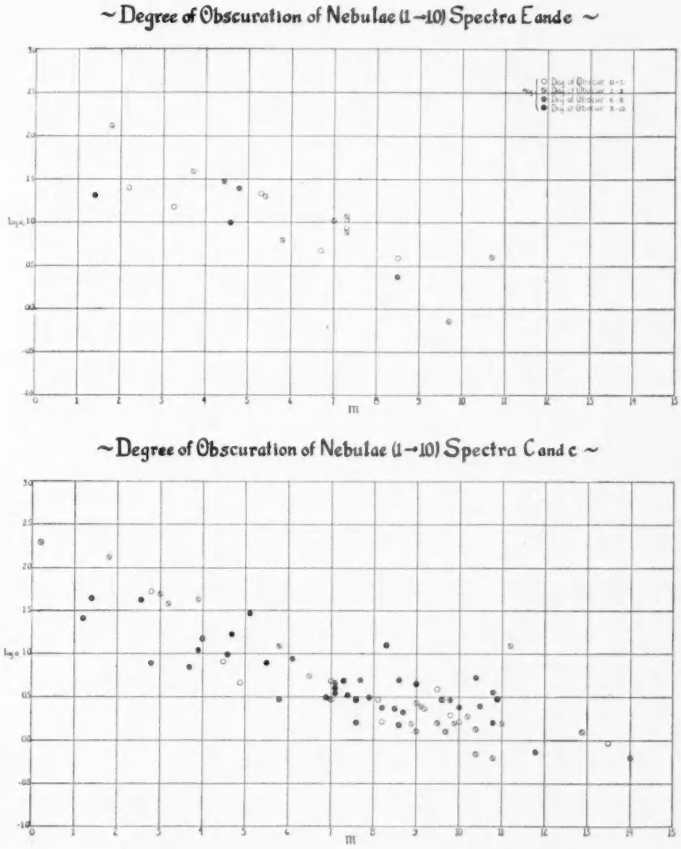

FIG. 2.—Hubble's relation in galactic nebulae and degree of obscuration

ceptionally large for the region near ρ Ophiuchi. For these two extreme groups Hubble's relation takes the form:

$$\text{Pleiades:} \quad m_* + 5 \log a_1 = 8.5 ; \tag{4}$$

$$\rho \text{ Ophiuchi:} \quad m_* + 5 \log a_1 = 12.0 . \tag{5}$$

The other groups give intermediate values. Some of them consist completely or in part of *e* nebulae and are therefore not relevant.

Thus the nebulae in the Orion, Sagittarius, γ Cassiopeiae and 15 Monocerotis groups contain emission spectra.

TABLE III

DEGREE OF OBSCURATION IN *c* AND *e* NEBULAE

Degree of Obscuration	No. of *e* Neb.	Percentage of *e* Neb.	No. of *c* Neb.	Percentage of *c* Neb.
	From Figure 1†			
0, 1	6	35	5	9
2, 3, 4, 5	8	47	22	42
6, 7, 8	2	12	19	36
9, 10	1	6	7	13
Total	17	100	53	100
	From Figure 2†			
0, 1	7	33	10	14
2, 3, 4, 5	10	48	24	33
6, 7, 8	3	14	28	38
9, 10	1	5	11	15
Total	21	100	73	100

† Several nebulae, the spectra of which are uncertain, were counted twice.
Three objects not given in Table I were used in Fig. 1 from Hubble's data of log a_1.

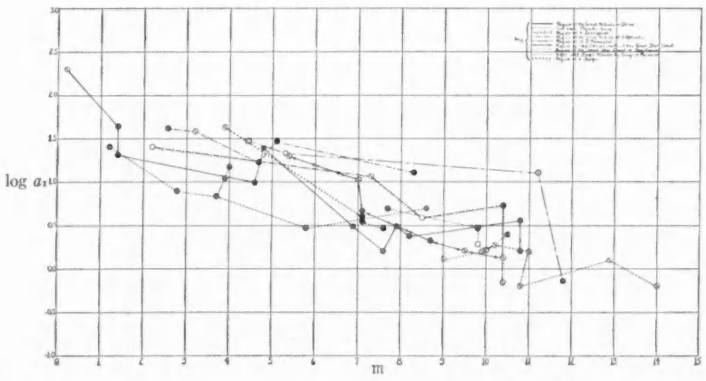

FIG. 3.—Hubble's relation in groups of galactic nebulae and degree of obscuration

THEORY OF NEBULAR SCATTERING

Since the mechanism of nebular radiation was not known when Hubble's papers appeared in 1922, the best assumption that could be made was that the nebula re-emitted the light received from the stars uniformly in all directions. This assumption is probably fulfilled in the case of *e* nebulae, but it does not apply to *c* nebulae. Zanstra assumed for the *c* nebulae that they re-emitted the starlight uniformly into a solid angle 2π. Hence, all surface brightnesses on Zanstra's theory were twice as luminous as on Hubble's theory. If there is no absorption of starlight between the star and the nebular patch measured and if the nebula reflects uniformly in all directions, the surface brightness at *maximum* angular distance from the star is $m_* + 5 \log a_1 + 11.64$, expressed in terms of the apparent magnitude per square second of arc. On Zanstra's assumption, the surface brightness is $m_* + 5 \log a_1 + 10.89$. The surface brightness selected in Hubble's work was 23.25 mag. per second of arc.

Since an effort had been made in Hubble's measures, and also in those made by us, to measure for a_1 the *maximum* distance of the faintest visible patches of nebulous matter, the true value of the numerical constant in the surface brightness should not be computed for the mean value of $r \sin \alpha$, where α is the phase angle. The difference between the constant for ($r \sin \alpha$) max. and ($r \sin \alpha$) mean is $5 \log \pi/4 = 0.52$ mag. in the numerical constant, according to Zanstra. Since, however, "in each case the maximum a was consciously sought,"[11] the true corrections should be considerably smaller, and probably would not exceed 0.1 or 0.2 mag. Without more specific information concerning the number of nebulous patches having the limiting surface brightness it is not possible to derive this correction accurately.

We shall now apply to the problem the theory of Seeliger, which promises to give useful results because of its remarkable success in the interpretation of the photometric observations of the rings of Saturn. In order to bring out the differences of the results based on the theory of Seeliger from those of Hubble and of Zanstra, we shall follow their assumptions as closely as is possible. The most impor-

[11] Hubble, *ibid.*, p. 412.

tant of these is that there is no appreciable reduction due to absorption in the amount of starlight reaching the nebula. Accordingly, we shall picture the nebula as consisting of detached masses, scattered at random in space, so that if we select a constant surface brightness and consciously seek the most distant spot, we shall presumably select one for which the starlight has suffered no absorption by intervening patches and for which the value of $r \sin a$ is near its maximum value. We shall next assume that the nebulous patch is opaque, which corresponds to Hubble's assumption that the efficiency is perfect. This is approximately verified by our former results on the amount of obscuration associated with the c nebulae. We shall not, however, assume that the albedo is 1.

For convenience in applying Seeliger's theory we shall assume that the nebulous patch is spherical. Then we may apply Seeliger's expression for the surface brightness of the nebula:

$$I = \frac{pI_0S^2}{r^2}\,\varphi(a)\,\frac{\cos i}{\cos i + \cos \epsilon}\,. \tag{6}$$

Here I_0 is the surface brightness of the star, expressed as the equivalent number of stars of magnitude 0 per square second of arc; S is the radius of the star in linear units; r is the distance between star and nebula in the same units; i is the angle of incidence; ϵ is the angle between the line of sight and the normal to the particular spot on the nebula under observation; $\varphi\,(a)$ is the phase function; and p is the albedo of the nebular particles.[12] I is also expressed as the equivalent number of stars of magnitude 0 per square second of arc.

As Seeliger has pointed out,[13] equation (6) represents the brightness of a smooth solid body whose surface obeys the law of diffuse reflection of Lommel-Seeliger and whose albedo varies as $\varphi\,(a)$. The brightest spot on a sphere obeying the Lommel-Seeliger law is on the light equator, near the positive limb,[14] where $\cos i/(\cos i + \cos \epsilon) = 1$ and where the surface brightness is twice that observed in the center

[12] For the definition of p see Schönberg, *op. cit.*, p. 162.

[13] *Sitzungsberichte d. Akad. d. Wiss., München*, Heft III, p. 272, 1901.

[14] G. Müller, *Die Photometrie der Gestirne*, p. 72, 1897.

of the sphere at $\alpha = 0$ This value remains constant for all values of α (except when $\alpha = 0$). We shall assume, therefore, that we have always observed the brightest spot on each spherical nebulous patch, and that its surface brightness is

$$I = \frac{pI_0 S^2}{r^2} \varphi(\alpha) . \tag{7}$$

We notice that $\pi S^2/r^2 = \omega$ is the solid angle under which the star is seen from the nebula. Substituting

$$\omega = \frac{4\pi\omega_s}{41,253 \times 60^4},$$

where ω_s is the solid angle in square seconds of arc, under which the star is seen from the nebula, we have

$$I = p \frac{4}{41,253 \times 60^4} I\omega_0 \frac{D^2}{r^2} \varphi(\alpha) . \tag{8}$$

Here ω_0 is the solid angle in square seconds of arc under which the star is seen from the earth, and D is the distance of the star from the earth. $I\omega_0$ is the total brightness of the star as seen from the earth. Passing now to stellar magnitudes, we find

$$m_{\text{neb}} = m_* + 5 \log a_1 + 10.1 - 2.5 \log p\varphi(\alpha) \sin^2 \alpha .$$

Assuming again that $m_{\text{neb}} = 23.2$, we obtain

$$m_* + 5 \log a_1 = 13.1 + 2.5 \log p\varphi(\alpha) \sin^2 \alpha . \tag{9}$$

Combining (9) and (3),

$$\log p\varphi(\alpha) \sin^2 \alpha = -0.8 .$$

If we assume that we observe at $\alpha = 90^\circ$, and that $\varphi(\alpha) = \cos^2 \alpha/2$,

$$\varphi(\alpha) = 0.5; \qquad \sin^2 \alpha = 1; \qquad \text{and } p = 0.3 .$$

This value is, however, too small because it also includes the effects of any departures from perfect opacity, as well as from $\alpha = 90°$. Allowing 0.1 mag. for the effect of foreshortening,

$$p = 0.5 ,$$

which now includes only the albedo and the departures from complete opacity. This value seems entirely reasonable.

The two extreme values represented by (4) and (5) give:

Pleiades: $p = 0.03$ (uncorrected for $\sin^2 \alpha$) ;

ρ Ophiuchi: $p = 0.7$ (uncorrected for $\sin^2 \alpha$) .

The difference between the two values must be attributed, of course, to departures from complete opacity in the nebula of the Pleiades. Our result for the Pleiades is quite similar to that obtained by Hertzsprung.[4] The value of 0.7 for the region near ρ Ophiuchi seems too large: a value of 0.1 to 0.3 would be more reasonable. The departure is not serious, and may be caused by errors of observation or by the influence of the highly absorbing masses upon the values of m_*. It should be possible to test the latter because the stars are all bright and their distances are fairly accurately known. A photometric study of the distribution of the light of the nebula should also be useful in deciding whether the stars are in front of the nebula or are situated in it.

It will be seen that the constant in equation (9) differs from that of Hubble by 2.5 log 4 and from that of Zanstra by 2.5 log 2. In other words, Seeliger's theory makes the surface brightness of the nebula four times greater than the simplified theory by Hubble. For different values of α, however, the surface brightnesses, according to Seeliger's theory, depend upon the form of $\varphi(\alpha)$. Thus, on the assumptions of Hubble and of Zanstra, all nebulae for which $I_{\text{neb}} =$ const. are at the same distance from the star. On Seeliger's theory the distance r is given by

$$r = \sqrt{\frac{c}{I_{\text{neb}}}} \sqrt{\varphi(\alpha)} .$$

For Euler's expression of $\varphi(\alpha)$,

$$r=\sqrt{\frac{c}{I_{\text{neb}}}} \qquad \text{if } \alpha=0\,,$$

$$r=\sqrt{\frac{1}{2}}\sqrt{\frac{c}{I_{\text{neb}}}} \quad \text{if } \alpha=90^\circ\,,$$

$$r=0 \qquad \text{if } \alpha=180^\circ\,.$$

The locus of constant I_{neb} is, therefore, a roughly heart-shaped surface of rotation. Since the nebulae are distributed, by assumption, at random in space, the distribution function of the $r \sin \alpha$ and the mean $r \sin \alpha$ can be computed, but it would only be of use if we could actually observe this distribution.[15]

Incidentally, Seeliger's theory shows that the maximum value of a_1 is not measured for $\alpha=90^\circ$, as would be true under the simplifying assumptions of Hubble and of Zanstra. To determine $(r \sin \alpha)$ maximum, we must know the form of $\varphi(\alpha)$. Let us first assume Euler's law

$$\varphi(\alpha)=\cos^2\frac{\alpha}{2}\,.$$

Then the maximum value of $r \sin \alpha$ is obtained from

$$\frac{d(r\sin\alpha)}{d\alpha}=0\,,$$

which gives

$$tg\,\alpha\; tg\,\frac{\alpha}{2}=2\,.$$

This is satisfied for approximately $\alpha=70^\circ$, so that in equation (9) $\sin^2\alpha=0.89$, which does not appreciably alter our results, because at the same time $\varphi(\alpha)=0.67$, and their product is 0.60, instead of 0.50 as for $\alpha=90^\circ$.

[15] Professor Walter Bartky has recently succeeded in deriving an expression for this distribution, under the assumption that the phase function is that of Euler. His data indicate that the mean value of $r \sin \alpha$ is very close to the maximum, and that the dispersion resulting from different values of the phase angle may be neglected.

The use of Lambert's law

$$\varphi(\alpha)=\frac{\sin\alpha+(\pi-\alpha)\cos\alpha}{\pi}$$

leads to a maximum value of $r\sin\alpha$ at about $\alpha=62°$, in which case $\sin^2\alpha=0.78$ and $\varphi(62°)=0.45$. In this case the effect upon the result would also be small because the product of the two factors is 0.35 instead of $1/\pi$ as for $\alpha=90°$. Unfortunately, we have no knowledge of how closely the measures do approach the maximum in the distribution of the values of $r\sin\alpha$. It is of interest, however, to notice that, in general, the measured points must lie behind the star.[16]

The application of Seeliger's theory appears to be entirely successful. However, the limitations of the method imposed by the assumption that the nebula consists of separate masses distributed at random in space and that there is no absorption of starlight by intervening nebulosity make it unprofitable to refine the work. It seems more promising to investigate individual nebulae whose appearance suggests a definite model. For example, the nebulae in the region of ρ Ophiuchi are obviously produced by scattering from a more or less continuous mass of opaque matter, by stars either located in front of the nebula or slightly involved in the nebulous matter. A photometric study of this region, supplemented by a determination of the polarization and by a study of the color indices of the nebulae illuminated by stars of different spectral types, is now under way.

YERKES OBSERVATORY
May 1, 1936

[16] It should be emphasized that the value of $\varphi(\alpha)$ for $\alpha=90°$ is equal to 0.5 only on the basis of Euler's function. For the law of Seeliger we have $\varphi(90°)=0.38$ and for that of Lambert $\varphi(90°)=0.32$. The choice of the correct expression depends upon the properties of the reflecting surfaces.

REFLECTION NEBULAE

OTTO STRUVE, C. T. ELVEY, AND F. E. ROACH

ABSTRACT

In order to test the reflection theory of galactic nebulae having continuous spectra, observations were made, with a Schmidt camera, of the nebulosities in the dark cloud in Scorpius and Ophiuchus. A large red nebula was found, extending about one degree to the north from Antares and only a few minutes of arc to the south. The color index of this nebula is about +1.9 mag., which agrees satisfactorily with the color index of Antares. The average color index of the nebulae surrounding the B stars σ Sco, 22 Sco, $-24^{\circ}12684$, ν Sco, and ρ Oph is −0.4 mag., which is also in good accord with the color indices of these stars. The color index of the night sky was found to be about +0.5 mag. The color index of a nebula near γ Cyg is −0.2 mag., which is much bluer than this F8 star. Perhaps this is a case of Rayleigh scattering. There can be no appreciable Rayleigh scattering in the nebulae in the Scorpius-Ophiuchus region.

A small amount of radial polarization was found in the nebula surrounding ρ Oph.

1. The reflection theory of galactic nebulae having continuous spectra rests upon the following data: (*a*) Slipher's observations of the spectra of several nebulae, which he found to be identical with the spectra of neighboring stars; (*b*) Hubble's and Zanstra's statistical discussions of the former's measures of the maximum distances between exciting stars and nebulae; (*c*) Struve, Elvey, and Keenan's spectrophotometric results for the nebulae in the Pleiades which revealed that these nebulae are very slightly, if at all, bluer than the stars, while Rayleigh scattering demands a difference of about 1 mag. in the color equivalents; (*d*) Struve and Story's correlation between the opacity of the nebula and its efficiency in scattering the light of the illuminating stars.

This evidence proves fairly conclusively that the mechanism of nebular luminosity is to be found in some form of scattering. However, except for the spectrophotometric observations of the nebulae in the Pleiades, we have no indication of any sort of the character of the scattering medium. The problem is obviously related to that of the nature of interstellar material in general. If it can be shown that the nebular particles are large enough to produce primarily nonselective effects, the way will have been prepared for an application of Seeliger's theory. In that case a search for phenomena depending upon the phase function will be appropriate. On the other hand, if

the nebular particles are predominantly small enough to produce selective scattering, future methods will have to follow those lines of investigation which have been applied by Schalén, Schönberg, Jung, Mrs. Rudnick, and others to the problem of interstellar reddening.

In order to decide which of these two lines of attack will have to be adopted, we shall attempt to answer the following questions: (*a*) Are there any nebulae which are obviously connected with stars of advanced spectral type, and are these nebulae definitely redder than those which are connected with stars of early spectral type (but not of spectral type earlier than B1, since then the nebular spectrum would not be continuous)? (*b*) Are the color indices of the nebulae identical with those of the illuminating stars? (*c*) Is there any evidence of radial polarization in these nebulae?

Questions *a* and *b* are not identical. It is much easier to measure the difference in the color indices of two nebulae than to measure the difference between the color indices of a nebula and its exciting star. An answer to question *a* would not definitely rule out selective effects; for example, Rayleigh scattering would make all nebulae bluer than their exciting stars but would leave the difference in color index between the nebulae and the stars about the same.

The problem of polarization in nebulae has heretofore been investigated only by Meyer.[1] However, of the objects in his list, only one—namely, Hubble's variable nebula—can be regarded as a true reflection nebula. The others are spirals, irregular emission nebulae, and planetaries. In Hubble's nebula Meyer suspected a small amount of polarization, but the evidence was inconclusive. The microphotometer curves (which apparently were not reduced into intensities) show a slight effect in the expected direction, but the illustration shows no visible difference between the two photographs. Unfortunately, this particular nebula extends to only one side of the exciting star, and even there over a narrow range in angle. Accordingly, two photographs taken with the polarizer in two orientations, one perpendicular to the other, will show but little difference even if the light is partly polarized.

2. Hubble's list of nebulae contains several which are fairly definitely connected with stars of late spectral type. Some of these are

[1] *Lick Obs. Bull.*, **10**, 68, 1920.

now being investigated at the Yerkes Observatory by Mr. O. C. Collins. For the purpose of the present investigation we have selected the nebulosities near ρ Oph (B5), 22 Sco (B3), σ Sco (B1), etc., which have been photographed by Barnard and also by Ross. These nebulae are obviously connected with the large dark cloud which has recently been investigated by R. Müller,[2] from star counts. Barnard's photograph shows a faint nebulosity around Antares, which extends mostly toward the north and envelops the globular cluster NGC 6144. In his earlier Lick photographs[3] Barnard attributed the glow around Antares and τ Sco to halation. However, in his *Milky Way Atlas* he writes: "The nebulosity extends southward (from 22 Sco) in wave-like forms over Antares and even beyond τ Scorpii. . . . . σ Scorpii is involved in a very dense mass which connects with the fainter part of the great nebula."[4] An inspection of Ross's recent photograph[5] of the same region leaves no doubt as to the reality of the faint nebula north of Antares and strongly suggests that it is connected with the dark cloud of the Scorpius-Ophiuchus region.

If the reflection theory is correct, the nebula, illuminated by the cMo star Antares, must be strikingly red in color.

The photographs shown in Plates V–IX were made at the McDonald Observatory with a Schmidt camera of 94-mm aperture and 180-mm focal length. The optical parts, consisting of a silvered spherical pyrex mirror and a correcting plate of UV Jena glass, were made by Mr. C. H. Nicholson of Chicago, while the mechanical parts shown in Figure 1 were designed by Dr. G. W. Moffitt. The scale of the original plates is about 20′ per millimeter. The size of the field is 9×18 mm. The instrument is intended to serve as a short-focus camera for the new Cassegrain spectrograph, and, consequently, no provision has been made for curving the plates. The focus is a compromise between center and edge. It is exceedingly sharp, and on the original plates taken without a filter the size of the fainter star images is quite similar to that of the grain of the plate.

[2] *Zs. f. Ap.*, **3**, 369, 1931.

[3] *Pub. Lick Obs.*, **11**, Pl. 36, 1913.

[4] *A Photographic Atlas of Selected Regions of the Milky Way*, Pl. 13, 1927.

[5] *Atlas of the Milky Way*, Pl. 5, 1934.

Each field was taken on an Eastman Process plate without a filter and on an Eastman IG plate with a gelatin "minus blue" filter. The exposures ranged from one hour to ninety minutes. The density of the sky background was made approximately equal on the Process and the IG plates.

The existence of a strong red nebula near Antares is clearly shown on the photovisual exposures (Pls. V and VI). The nebula envelops

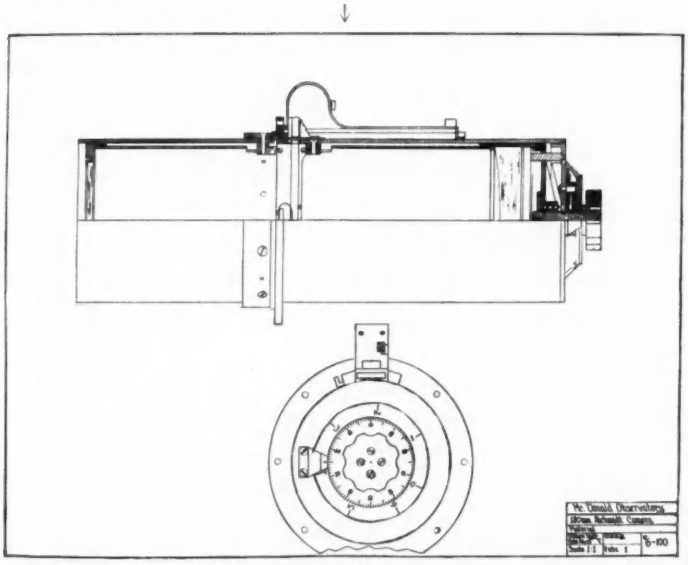

FIG. 1.—Schmidt camera of the McDonald Observatory, designed by Dr. G. W. Moffitt. The aperture is 94 mm and the focal length is 180 mm. The arrow points to the loading device.

Antares and extends in a diamond-shaped form for more than a degree toward the north, where it almost reaches 22 Sco. It definitely extends into the regions of obscuration of the dark cloud. The nebulae near 22 Sco, and especially near σ Sco, are much weaker on the photovisual plate, indicating that they are appreciably bluer than the sky background. The nebula near the star $-24^{\circ}12684$ is possibly a little less blue than the other two nebulae.[6]

[6] The measures in Table I seem to indicate that the nebula near $-24^{\circ}12684$ is the bluest of all. This result is somewhat uncertain, however, and the qualitative impression from a visual inspection of the plate is probably more reliable.

Plates VII and VIII show that the nebula near ν Sco is exceedingly blue, as is also the nebula around ρ Oph. The nebula near the A and B9 stars $-19°4361$ and $-19°4359$ is not quite so blue, while the faint trace of nebulosity around the K star $-19°4357$ is slightly stronger on the photovisual plate and is therefore probably a trace redder than the sky.

Of very great interest are the dark cores in the starless regions extending toward the east from $-24°12684$. These cores are considerably darker than other starless regions in their vicinity. The opacity of the material is therefore approximately the same, and the difference in surface brightness is related to the phenomenon mentioned in our discussion[7] of B15. Plate VIII shows that the dark cores and the surrounding brighter regions are equally well visible on the photovisual and on the photographic exposures. The cosmic illumination giving this effect of contrast is, consequently, of approximately the same color as the night sky.

3. Very little is at present known concerning the color of the night sky. Lord Rayleigh[8] found it to be similar to that of the sun. Similarly, Dufay[9] concluded from his observations that "the color of the night sky resembles that of the sun much more than that of the blue daylight sky."

Observations made by us on three nights with the Schmidt camera (on Mount Locke) give for the region near the North Pole an average color index of +0.5 mag., corresponding approximately to spectral type F5. Rayleigh's formula shows that the color index of the blue sky is in the neighborhood of −0.2 mag., which would correspond to spectral type B.

From one night's observations obtained at the Yerkes Observatory by Mr. A. H. Mikesell with the Fabry photometer, Mr. Collins finds for the night sky a color index of +0.6 mag.

It is probable that this important astrophysical quantity is variable, both with respect to the time and with respect to the region of the sky examined. However, we shall adopt the value +0.5 mag., which is doubtless fairly close to the correct value.

[7] *Ap. J.*, **83**, 162, 1936.

[8] *Proc. R. Soc.*, **99**, 10, 1921.

[9] *Bull. de l'Obs. de Lyon*, **10**, No. 9, 1928.

4. All our nebular plates were supplied with sensitometer exposures, so that characteristic curves were available for the derivation of the differences between the surface brightness of the sky and of the nebulae. Table I gives the results of the measurements, which in each case refer to the most conspicuous portion of each object. A positive sign in the last line means that the object is yellower than the sky; a negative, that it is bluer. On the average, the red nebula near Antares is 0.4 mag. redder than the sky, while the nebulae il-

TABLE I

Nebula	Near α Sco	Near σ Sco	Near 22 Sco	Near $-24^{\circ}12684$	Near υ Sco	Near ρ Oph	Core of Dark Nebula
Neb.−Sky pg.	$+0^{m}.18$	$+0^{m}.40$	$+0^{m}.66$	$+0^{m}.40$	$+0^{m}.30$	$+0^{m}.31$	$-0^{m}.08$
Neb.−Sky pv.	.58	+ .24	+ .30	+ .07	+ .11	+ .16	− .05
Difference	+0.40	−0.16	−0.36	−0.33	−0.19	−0.15	+0.03

luminated by B stars are 0.24 mag. bluer. These values must be corrected for the effect of superposition with the night sky, which is quite appreciable for such faint objects. The result, freed from the skylight, must then be corrected to fit the international scale. Table I gives us the values of Δm_{pv} and Δm_{pg}. From these we compute

$$2.5 \log \frac{i_{\text{neb}}+i_{\text{sky}}}{i_{\text{sky}}} = \Delta m ;$$

$$\frac{i_{\text{neb}}}{i_{\text{sky}}} = \frac{i_{\text{neb}}+i_{\text{sky}}}{i_{\text{sky}}} - 1 ;$$

$$\Delta m_{\text{corr}} = 2.5 \log \frac{i_{\text{neb}}}{i_{\text{sky}}} .$$

The results are given in Table II. For a very rough computation the conversion factor to the scale of the International System was assumed to be 1.0.

The agreement of the spectral types with those of the illuminating stars is quite within the rather low precision of the measurements.

We now understand why Barnard found that "all the nebulosity in this region . . . . is so faint that it cannot be seen with the eye

PLATE V

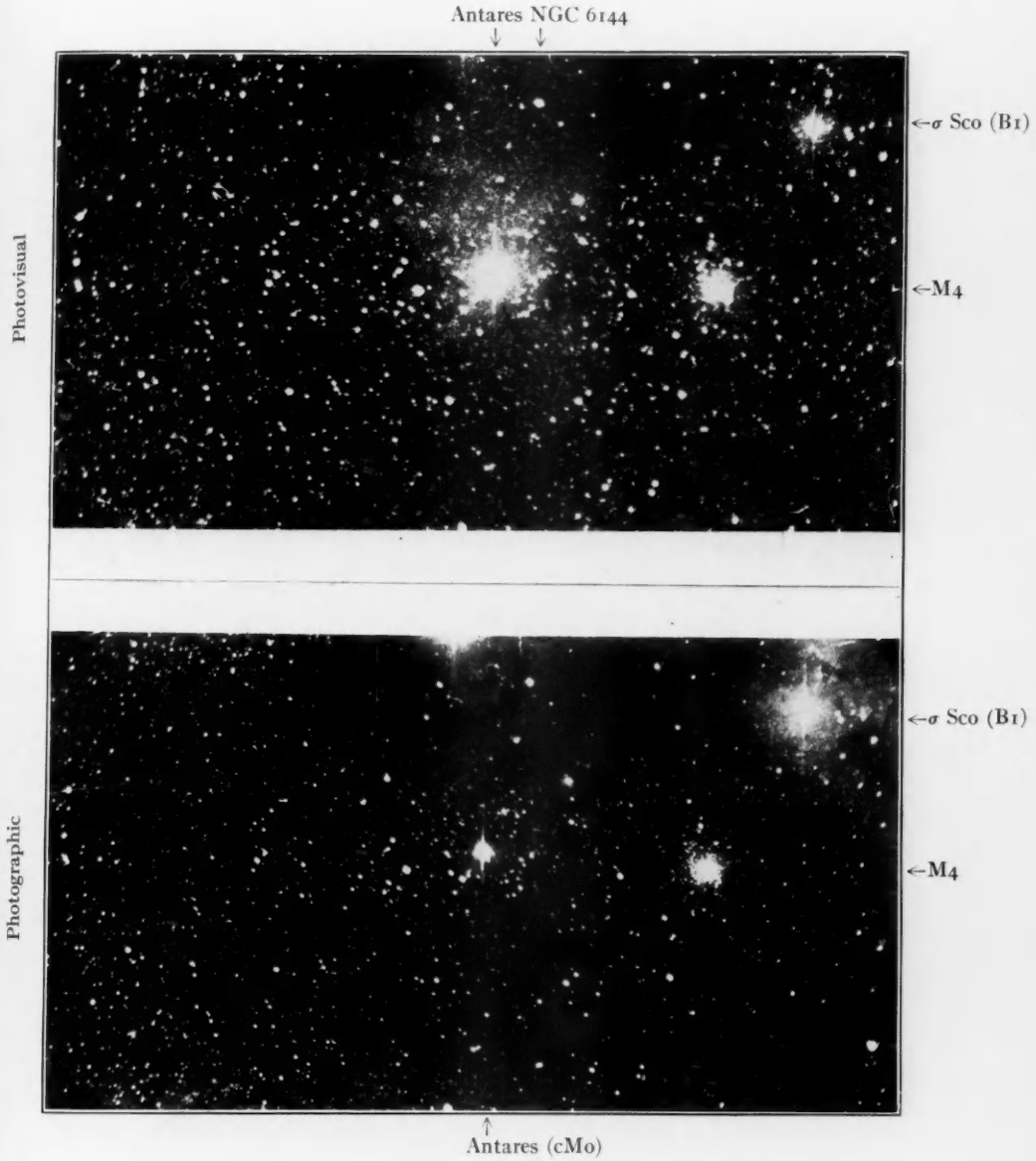

RED NEBULA NEAR ANTARES

The red nebula is clearly shown on the photovisual exposure obtained with an Eastman IG plate and yellow filter. Only a faint trace of this nebula appears on the ordinary photographic exposure obtained with an Eastman Process plate. Enlarged 7.4 times.

PLATE VI

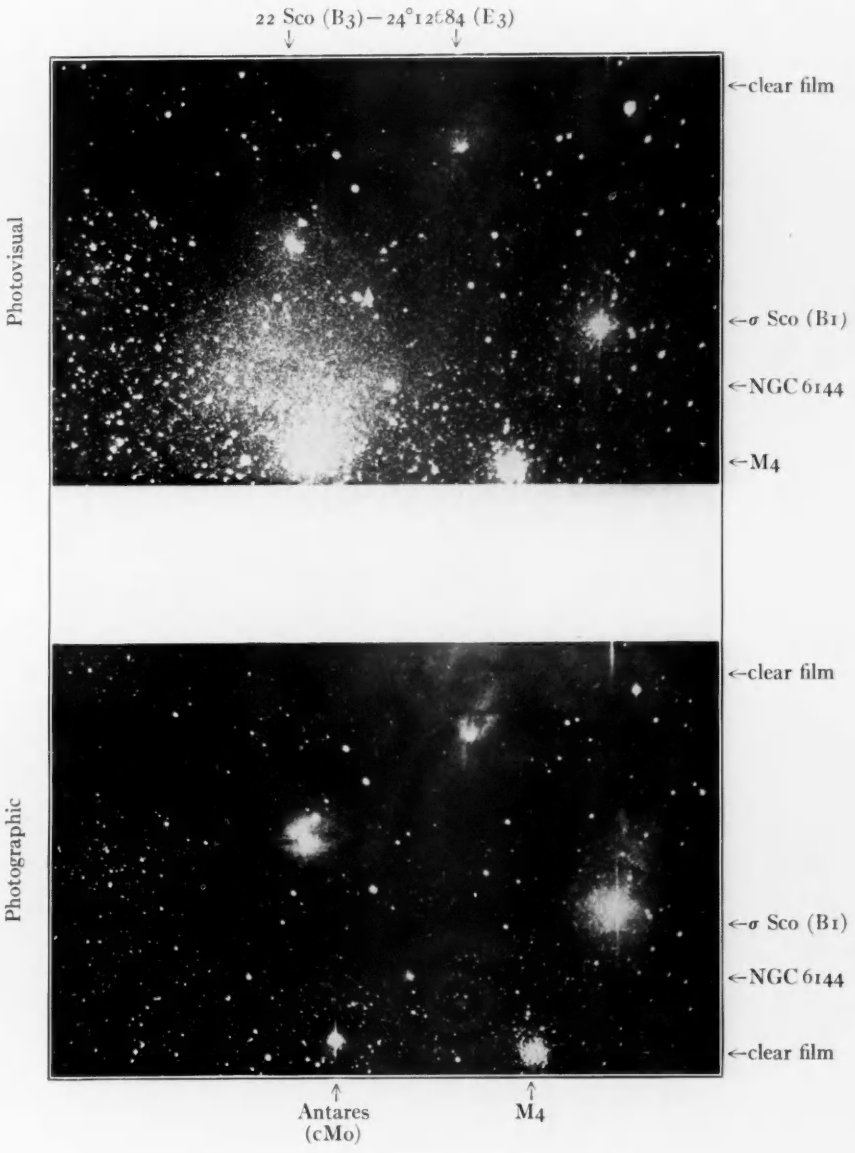

NEBULAE IN THE REGION OF 22 SCORPII

At the bottom is the red nebula near Antares. The blue nebulae around 22 Sco, σ Sco, and −24°12684 are much stronger on the photographic (Eastman Process) than on the photovisual (Eastman IG and yellow filter) exposure. These photographs should be compared with Plate XIII of Barnard's *Atlas*. The black corners show the clear film of the plates. Enlarged 6.5 times.

PLATE VII

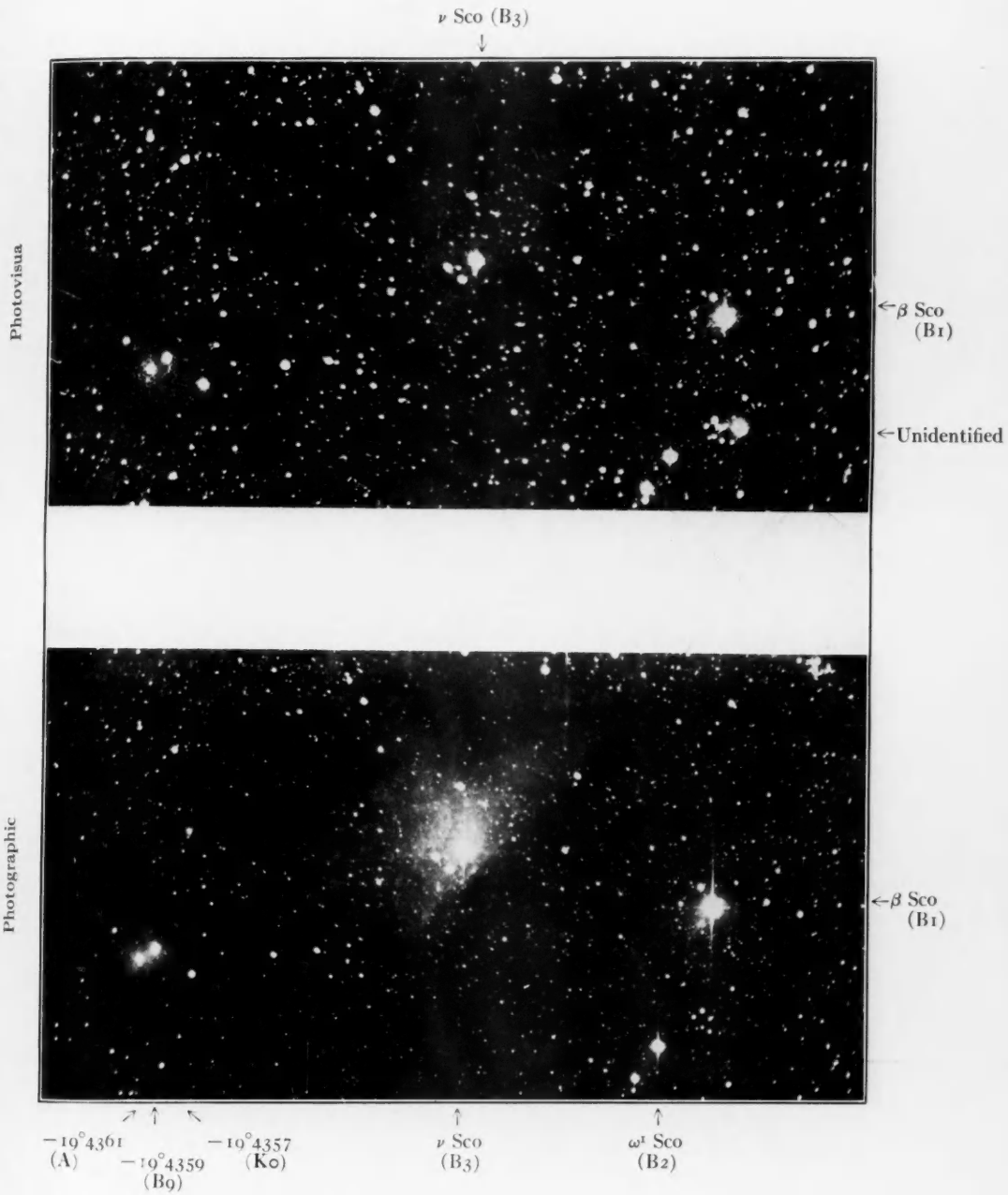

NEBULAE NEAR ν SCORPII
Enlarged 7.3 times

PLATE VIII

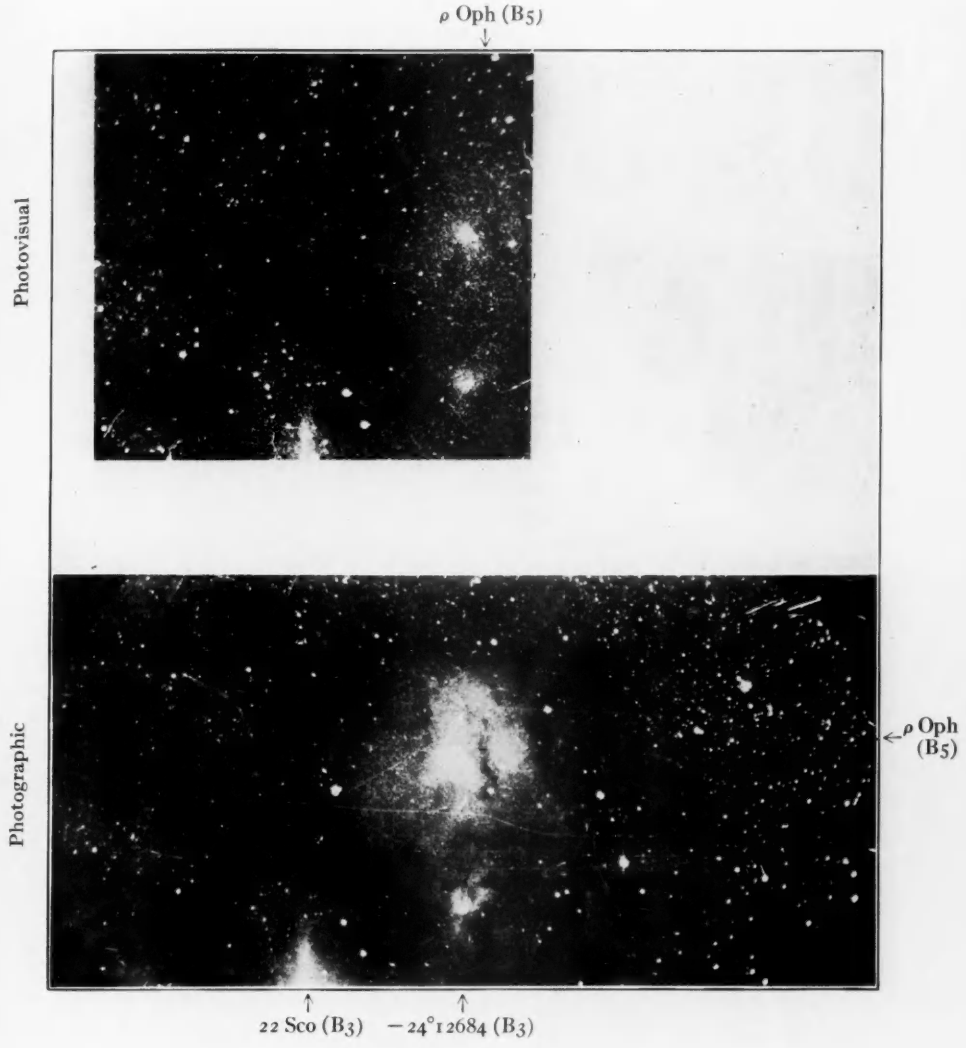

NEBULAE NEAR ρ OPHIUCHI

The dark lanes extending toward the east from −24°12684, and toward the north and northeast from 22 Sco are equally visible on the two exposures. The straight black lane at the top of the photographic exposure is spurious. Enlarged 6.4 times.

even in a powerful telescope." The average difference between the nebulae illuminated by the B stars and the sky is less than 0.2 mag. on the photovisual plates. It is surprising that there have been no previous visual observations of the red nebula near Antares. An examination of the field with a powerful Zeiss binocular showed an unmistakable brightening in the region of the nebula. However, the

TABLE II

	Red Nebula near Antares	Blue Nebulae near B Stars
Δm_{pg} / Δm_{pv} Uncorr.	+0.18 / +0.58	+0.41 / +0.18
Δm_{pg} / Δm_{pv} Corr.	−1.8 / −0.4	−0.9 / −1.8
Difference	+1.4	−0.9
Color index of sky	+0.5	+0.5
Color index of nebula	+1.9	−0.4
Corresponding spectral type	M	B

presence of Antares is somewhat disturbing, and it is best to place it behind some sort of an obstruction. The nebula is then fairly easily visible.

The fact that Antares is now definitely linked with the dark nebula around ρ Oph is of considerable importance. Schlesinger gives the following parallaxes for Antares:

Trigonometric	$\pi = +0''.028$
Spectroscopic	$\pi = .010$
Dynamical	$\pi = +0.0016$

The dynamical parallax is doubtless too small. The distance is probably about 100 parsecs. This agrees well with the distance of the nearer edge of the dark nebula found by R. Müller[2] to be about 100–150 parsecs. It is of interest that the red giant Antares and the

normal B stars ρ Oph, σ Sco, 22 Sco, $-24°12684$ are all at approximately the same distance. It would be dangerous, however, to draw from this any conclusions concerning the absolute magnitudes of these stars, because some of them may be appreciably dimmed by nebulous matter. The peculiar ring-shaped nebulosity around 22 Sco suggests that the star shines through the nebula, and that the absence of bright nebulosity in the immediate vicinity of the star is caused by the phase effect.

The dynamical parallax of ρ Oph, $+0''.015$, is probably approximately correct.

Two globular clusters, NGC 6121 (M4) and NGC 6144, are in the field. The former lies outside the red nebula, at a considerable distance from the edge of the dark nebula. The latter is distinctly enveloped by the red nebula, and it almost certainly shines through some of the thinner portions of the dark nebula. Stebbins and Whitford[10] find color excesses of +0.22 mag. for NGC 6121 and +0.15 mag. for NGC 6144. It is probably fair to conclude that the presence of the red nebula does not materially affect the color index of the cluster. Whether the total light of the cluster is appreciably dimmed is not known.[11]

5. In a manner similar to that described above we have obtained from two pairs of plates the color index of the nebula near BD+39°4206, which is almost certainly related to γ Cyg (Sp. F8p).

The final color index of the nebula is −0.2 while that of a normal giant F8 star is about +0.5 mag. An inspection of the plates shows clearly that the nebula is much bluer than the background of the night sky. In view of the decisive character of the results for the red nebula near Antares, we are inclined to suggest that the constitution of the nebula in Cygnus is different from that of the one in Scorpius. In the former the obscuration is small, while in the latter it is very large. In view of the symmetry of the nebulae around γ Cyg, it is hardly possible to doubt that this star is responsible for the light of these nebulae. Possibly the Cygnus nebulae consist of particles small enough to give Rayleigh scattering (Table III).

6. Four pairs of plates have been obtained during the month of

[10] *Ap. J.*, **84**, 132, 1936. (On this scale Ao–Ko=0.74 mag.)

[11] H. Shapley, *Star Clusters*, p. 22, 1930.

PLATE IX

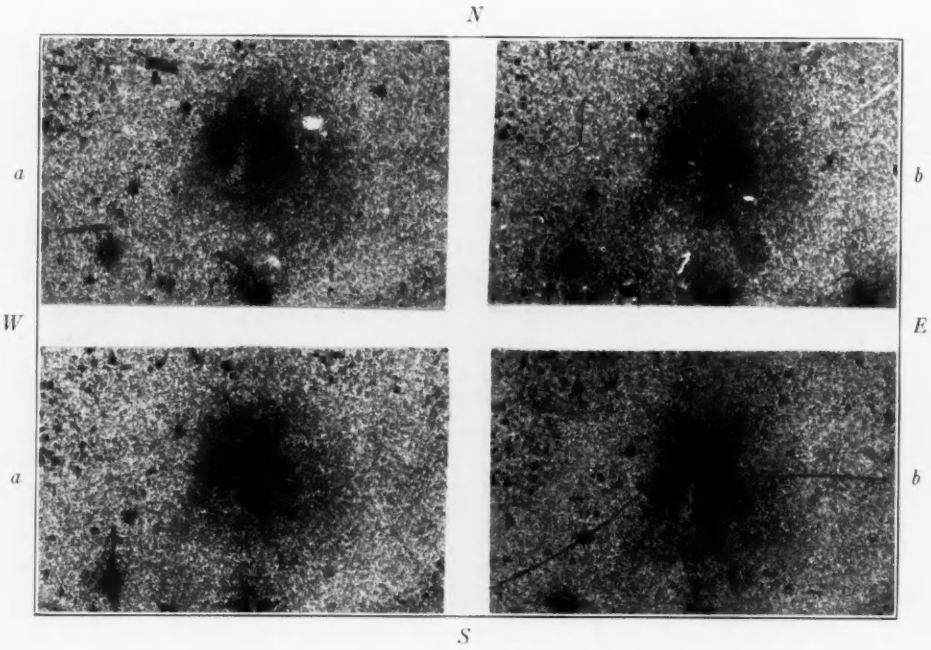

POLARIZATION IN NEBULA NEAR ρ OPHIUCHI

The two exposures marked *a* were taken with the principal axis of the Polaroid in a vertical orientation. The two exposures marked *b* were taken with the principal axis of the Polaroid horizontal. The principal difference is in the tail-shaped extension pointing south from ρ Oph; it is fairly strong in *b*, but is almost absent in *a*. (Cf. Fig. 2.) Enlarged 6 times.

July for the purpose of testing the polarization of the nebula near ρ Oph. Plate IX shows some of the results. An unlaminated piece

TABLE III

	July 20, 1936	July 19, 1936	Mean
Δm_{pg} Uncorr.	+0.40	+0.30	+0.35
Δm_{pv} Uncorr.	+0.15	+0.21	+0.18
Δm_{pg} Corr.	.....	.....	−1.05
Δm_{pv} Corr.	.....	.....	−1.76
Difference	.....	.....	−0.7
Color index of sky	.....	.....	+0.5
Color index of nebula	.....	.....	−0.2

of "Polaroid" film was fastened to the plate in the Schmidt camera. In (*a*) the principal axis was perpendicular to the equator; in (*b*) it was parallel to the equator. If radial polarization is present, those features of the nebula should appear strengthened in (*b*) which have the same right ascension as ρ Oph, while in (*a*) those will be strengthened which have the same declination. This was found to be actually the case. Figure 2 shows the principal differences between (*a*) and (*b*). The amount of polarization is relatively small, but no numerical estimate is possible. It is certainly smaller than the maximum polarization of the solar corona,[12] which is about 37 per cent. The transmission of the "Polaroid" is rather small in the photographic region. The exposure times on Eastman I O plates averaged

FIG. 2.—Polarization in the nebula near ρ Ophiuchi. The straight lines indicate the positions of the principal axis of the Polaroid. The tail-shaped extension, marked by arrows, is much more pronounced in (*b*) than in (*a*). This suggests that the light of the nebula is partially polarized along the radius. (Cf. this drawing with the photographs in Plate IX.)

[12] R. K. Young, *Lick Obs. Bull.*, **6**, 166, 1911.

two hours, while ten minutes would have been sufficient without the "Polaroid." This corresponds to a ratio of 12, or to $\Delta m = 2.7$ mag. Since the I O emulsion is sensitive slightly beyond λ 5000 and the "Polaroid" cuts off quite rapidly in the blue and violet, the effective wave-length of the plates is probably near λ 5000. For this region Ingersoll, Winans, and Krause[13] find a transmission for unpolarized light of about 25 per cent. The same authors find that the degree of polarization at λ 5000 is somewhat greater than 90 per cent.

The existence of a small amount of polarization in the nebula around ρ Oph not only confirms the reflection theory but also strengthens our belief that the particles in this dark cloud are relatively large in size. Were Rayleigh's law exactly obeyed the polarization would have been much more conspicuous.

Miss A. Friedman assisted in the measurements.

YERKES OBSERVATORY
UNIVERSITY OF CHICAGO
AND
McDONALD OBSERVATORY
UNIVERSITY OF TEXAS

[13] *J. Opt. Soc. Amer.*, **26**, 233, 1936.

THE SYSTEM OF POLARIS

B. P. GERASIMOVIČ

ABSTRACT

Determinations of α and δ of Polaris made at Poulkovo, Washington, and Greenwich reveal an irregularity in the proper motion having a period of about 30 years, closely corresponding to the period of γ in the spectroscopic orbit. These give the following orbital elements of Polaris with respect to the center of gravity of the system $a'' = 0''.11$, $i = 63°$, and $\Omega = 147°$. A new spectroscopic orbit of long period in conjunction with the foregoing value of a'' gives $\pi = 0''.025$ and $M_{vis} = -0.9$. The visual absolute magnitude of the secondary derived from the mass-luminosity relation is $+1.3$, and its mass is $2.4\odot$.

Polaris is a well-known Cepheid with an abnormally small variation in light and in velocity. Its visual range is only 0.08 mag., while the range in velocity does not exceed 6 km/sec. According to the period-luminosity relation, to a period of $3^d.968$ there corresponds a visual absolute magnitude of -1.6 and a parallax of $0''.018$, which, being six times larger than the adopted trigonometric parallax, is only slightly larger than the mean spectroscopic parallax ($0''.014$, Mount Wilson).

Since its discovery by W. W. Campbell, the variation in radial velocity during the four-day period has been thoroughly investigated both at Poulkovo and at Mount Hamilton. During the last 28 years Dr. Belopolsky[1] has derived 16 "orbits" for separate yearly cycles of observation, and has proved that the velocity curve undergoes some important progressive changes. At the same time the Lick observers secured seven hundred spectrograms and published some partial results of great interest. Campbell found that γ is variable, which indicated that Polaris is either a triple system or a real binary with a Cepheid-like bright component. On the basis of the first oscillation period of γ announced by Campbell in 1910, L. Courvoisier[2] found from the Poulkovo observations of α and δ a long-period oscillation ($P \sim 10$ years) in the mean place of Polaris. This result led me to undertake a special investigation of the Poulkovo

[1] *Zs. f. Ap.*, **5**, 294, 1932.

[2] *A.N.*, **203**, 85, 1917.

fundamental observations of the last century, which did not reveal periods of either 10 or 8 years in the mean places of Polaris.[3]

Since that time new extended series of spectroscopic observations of Polaris have been made both at Mount Hamilton and at Poulkovo, which proved that the period of γ is considerably longer than had been supposed. From the Lick data Moore found the period to be 29.6 years, and he derived the elements of the long-period orbit of Polaris,[4] this result being fully substantiated by Belopolsky.[5] Moore's period and the observed range in γ of about 8 km/sec, in conjunction with the Cepheid parallax of Polaris, correspond to an angular radius of the orbit of the bright component of about $0''.1$ (for $i=45°$) or more. Oscillations of this size should certainly be noticeable in the best series of numerous observations of Polaris made at Washington, Poulkovo, and Greenwich, and the detection of these oscillations would be interesting from various points of view. It would afford a unique occasion for determining the parallax of a Cepheid in a direct way, avoiding the spectroscopic and the Cepheid parallaxes, which, in the case under consideration, differ systematically from the trigonometric parallax. This would prove that Polaris is a binary, one component of which is a Cepheid—a rather curious mechanical system. On the other hand, Polaris is one of the most important fundamental stars (especially for the azimuth determinations), and the oscillations in its α and δ are by no means harmless to fundamental astronomy.

Oscillations in the mean places of Polaris.—Having in view the smallness of the expected changes in both co-ordinates, and taking into account the high declination of Polaris, it did not seem advisable to use the classical method of investigating variable proper motions, so brilliantly developed by Auwers. In the case of Polaris the only way open was that of using long series of the best observations, deriving from them portions of the curves of $\alpha-\alpha_0$ and $\delta-\delta_0$ and then properly adjusting these in case of the reality of the long-period oscillations. The Poulkovo and Washington data ("positions isolées") are given reduced to the system of a corresponding catalogue,

[3] *A.J.*, **35**, 181, 1924.

[4] *Pub. A.S.P.*, **41**, 254, 1929.

[5] *Op. cit.*

smoothed and corrected for carefully investigated sources of errors. On the contrary, the Greenwich data are published in annual volumes of observations, not combined into catalogue form. Since observations of α of such a circumpolar star are known to be less accurate than observations of δ, it seemed advisable to avoid the use of the α data, which are not combined in catalogue form. To exclude all kind of seasonal influences and errors (including the parallax and the inaccuracy of the aberration), only the annual means have been used in this investigation. To get rid of the errors depending upon the kind of culmination and of some unexcluded latitude variations, the means "above the pole" have been combined with those "below the pole" with equal weights.

The final annual means $\alpha-\alpha_0$, $\delta-\delta_0$ (α_0, δ_0 are the mean data of the catalogue) can be considered as essentially free of seasonal and personal errors, the only remaining errors being progressive changes in personal equation, the inaccuracy of the constant of nutation and of the *variatio annua*. It should be, however, noticed that the last sources of error are easily controlled. In this manner the following fundamental series of observations have been investigated:

Right ascensions: Poulkovo, 1845; Poulkovo, 1865; Poulkovo, 1885; Nikolaieff, 1915; and Washington, 1915.

Declinations: Poulkovo, 1865; Poulkovo, 1885; Washington, 1915; Greenwich annual data (1890–1913).

Figures 1 and 2 give full account of the results obtained. They leave no doubt as to the reality of the 30-year oscillations in δ, those in α being not so clear, although their existence cannot be doubted. The separate series of data are adjusted by adding certain constants to the values of $\alpha-\alpha_0$ and $\delta-\delta_0$. The detailed results derived from the analysis of the catalogues will be published in *Poulkovo Circular No. 19*.

Orbit of the brighter component.—Plotting the x and y co-ordinates taken from the normal curves of Figures 1 and 2, it is possible to draw the apparent orbital ellipse. However, since the data of $\alpha-\alpha_0$ are very uncertain, it would be rather dangerous to give much weight to this apparent orbit and to derive from it the orbital elements in the usual way. The best we can do is to deduce the mean separation of the bright component from the center of gravity, a'',

the inclination i, and the longitude of the ascending node Ω, which do not depend much upon the details of the curve of $\alpha - \alpha_0$ but only upon its range and general run. This gives

$$a'' = 0''.11$$
$$i = 63°$$
$$\Omega = 147°$$

The correctness of Ω can be indirectly checked by the spectroscopic orbit, which (see below) gives 1900.6 as the time of the ascend-

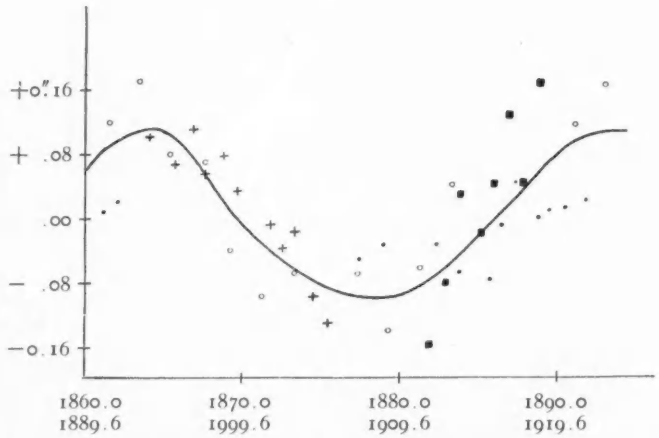

FIG. 1.—Orbital motion in the declination of Polaris. The ordinates are adjusted values of $\delta - \delta_0$, the zero-point being arbitrary. The abscissae are phases in time, reduced with Moore's period of 29.6 years. + = Poulkovo, 1865; • = Poulkovo, 1885; ■ = Washington, 1915; ○ = Greenwich annual results (1891–1913).

ing node, while the corresponding time from the visual orbit is 1903.6 (or 1874.0).

The spectroscopic orbit.—The final long-period spectroscopic orbit as based upon the Lick observations was published by Moore in 1929.[6] In order to provide an independent set of elements I calculated the orbit on the basis of the Poulkovo data as published by Belopolsky, which start from 1900.2. Both sets of elements, as given in Table I, are quite similar. The value of the inclination gives

[6] *Op. cit.*

$a = 3.5$ astronomical units (Lick) and 4.4 astronomical units (Poulkovo).

Parallax and masses.—The combination of the angular separation with the values of a gives for the parallax $\pi = 0''.031$ (Lick orbit) and

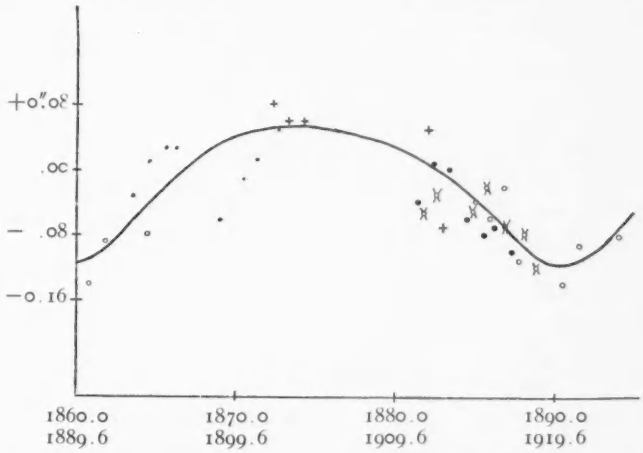

FIG. 2.—Orbital motion in the right ascension of Polaris. The ordinates are adjusted values of $\alpha - \alpha_0$, the zero-point being arbitrary. The abscissae are phases in time, reduced with Moore's period of 29.6 years + = Poulkovo, 1845; • = Poulkovo, 1865; • = Poulkovo, 1885; o = Nikolaieff, 1915; □ = Washington, 1915.

TABLE I

THE LONG-PERIOD SPECTROSCOPIC ORBIT

	Lick	Poulkovo
Period	$29^{y}.6$	$29^{y}.6$ (assumed)
K	4.05 km	4.35 km
e	0.63	0.50
ω	332°.0	315°.8
T_π	1899.5	1899.8
$a \sin i$	3.1 a.u.	3.9 a.u.
$m_2^3 \sin^3 i/(m_1+m_2)^2$	0.035	0.075
γ	− 17.4 km	− 16.5 km

$\pi = 0''.025$ (Poulkovo orbit). Both values are several times larger than the mean trigonometric parallax, which is much smaller than that derived from the period-luminosity relation with Shapley's revised zero-point ($\pi = 0''.018$) and the recent Mount Wilson spectroscopic

parallax ($\pi = 0''.014$). The Poulkovo value of π ($0''.025$) gives for the absolute visual magnitude $M = -0.9$, while the Cepheid parallax leads to $M = -1.6$. The difference of $+0.7$ mag. (which, incidentally, is close to the value of the zero-point correction as derived some years ago by the present writer) can result from (1) the inaccuracy of the observational data, (2) the zero-point correction, and (3) a deviation from the period-luminosity relation due to the individual properties of Polaris.

The value of π as derived from the visual and spectroscopic data is sufficiently close to the Cepheid parallax. It should, however, be clearly stated that all these indirect values of the parallax can by no means be reconciled with the vanishingly small value ($0''.003$) of the mean trigonometric parallax, which leads to an impossible value, $M = -5.5$.

Adopting $a = 4.4$ astronomical units (which is in better agreement with the period-luminosity relation than the value $a = 3.5$ astronomical units) we derive for the ratio of masses (brighter to fainter component) $m_1/m_2 = 2.2$. On the basis of Eddington's mass-luminosity curve, there corresponds to $M = -0.9$ a mass of $m_1 = 5.2$, and therefore the mass and the absolute magnitude of the secondary are $m_2 = 2.4$ and $M_2 = +1.3$, which give a difference in magnitude of about 2.2 mag., the apparent visual magnitude of the secondary being 4.3. If the spectrum of the secondary is later than that of the primary, this difference should be slightly larger (for instance, for type *K*0 by $+0.21$ mag.). Adopting $M = -1.6$, we get the same value of the apparent magnitude of the secondary. The maximum angular separation of the two components being between $0''.3$ and $0''.4$, and the difference in magnitude being about 2.2, it is not impossible that the secondary could be observed visually. At present the secondary is not far from maximum separation, which occurred at about 1933, its position angle (referred to the classical Polaris), being 297° for 1936.2.

POULKOVO, U.S.S.R.
March 1936

RECENT CHANGES IN THE SPECTRUM OF γ CASSIOPEIAE

DEAN B. McLAUGHLIN

ABSTRACT

Beginning in October, 1935, the helium lines of γ Cassiopeiae developed strong sharp absorptions, with distinct emission borders. Simultaneously, the central absorption of the hydrogen lines exhibited a marked strengthening. The radial velocities of the hydrogen and helium absorptions are identical, within the error of measurement.

Variations in the spectrum of this bright Be star have been the subject of four papers by Lockyer[1] and of an extensive investigation by Cleminshaw[2] based on the long series of Ann Arbor spectrograms. Cleminshaw's study extended to March, 1935; the present paper describes changes which have occurred since that date.

Approximately four years ago the writer[3] stated: ". . . . the brighter Be stars deserve continuous close attention for some years to come. Unusual developments may occur at any time in the spectrum of any one of them. . . . ." At the time that was written, the star which appeared least likely to serve as an example was γ Cassiopeiae. Its history up to that time gave no hint whatever that it was about to embark upon a sequence of spectral changes which has been unique.

There was very little change previous to 1930, and it was not until 1932 that the emission components developed conspicuous inequality. At the end of 1933 the violet components were very strong and the red components were hardly visible. No sensible changes of intensities of absorption lines occurred up to that time; the hydrogen central absorption remained sharp and rather weak (intensity 1.0–1.5 on the scale used in this paper); and the helium lines were invariably extremely diffuse absorptions without emission edges.

Early in 1934 the central absorption of the hydrogen lines disappeared and the emission appeared single and narrow.[4] The first

[1] *M.N.*, **93**, 362, 1933; **93**, 619, 1933; **95**, 520, 1935; **96**, 2, 1935.

[2] *Ap. J.*, **83**, 495, 1936.

[3] *Pub. Obs. U. of Mich.*, **4**, 198, 1932.

[4] Cleminshaw, *op. cit.*

trace of returning absorption was seen on October 14, 1934, but the lines were not distinct until December. The hydrogen emission again showed two components, the red component being much the stronger. This condition continued until March 24, 1935 (the date of the last plate studied by Cleminshaw), and probably through the succeeding six months, for only slight changes had occurred when the star was again observed in September.

TABLE I

EMISSION AND ABSORPTION INTENSITIES IN γ CASSIOPEIAE

DATE U.T.	EMISSION RATIO V/R		HELIUM EMISSION		HYDROGEN ABSORPTION			λ 3889 ABS.	HELIUM ABSORPTION		
	$H\gamma$	$H\delta$	λ 4026	λ 4472	$H\gamma$	$H\delta$	$H\epsilon$		λ 3964	λ 4026	λ 4472
1935											
Mar. 24.03	0.36	0.45	.....	.....	1.0	1.5	1.5	1.5	1:	1:	0.5
Sept. 18.32	0.5	0.63	.....	.....	1.0	1.0	1.0	1.5	0	0	0.5
19.29	0.6	0.77	.....	.....	0.5	1:	.....	.....	.....	1—	1—
30.21	0.45	0.6	.....	0.5	1.5	1.5	1	3	0.5	1	1
Oct. 9.19	0.43	0.67	.....	0.5	1.5	1.5	1—	4	0.5	1—	1—
30.23	0.5	0.42	0.5	1:	2—	2—	1	5	1	1.5	1.5
Nov. 22.26	0.43	0.62	.....	0.5	1	1.5	1—	4	1—	1	1
1936											
Jan. 15.05	0.67	0.83	.....	1—	3	3	2	5	1.5	2.5	3
Feb. 8.09	0.9	.....	?	?	4	4	3	5	2	3	3
Mar. 29.05	0.67	0.9	0.7	1.0	4	4	4	6	3	3.5	4
May 27.37	1.0	1.3	1—	1.0	3	3	2	6	1.5	2	2
27.38	0.9	1.3	0.5	1.5	3.5	3	3	7	2.5	2.5	3

The data obtained from the Ann Arbor spectrograms between March 24, 1935, and May 27, 1936, are given in Tables I and II. We shall discuss first the changes in intensity exhibited in Table I.

1. The emission ratio V/R changed gradually from about 0.4 to approximate equality of components.

2. A sharp strong absorption line appeared at λ 3889 (first announced by Lockyer in his fourth paper). It was first seen on September 30, though it was possibly faintly present (blended with $H\zeta$) on September 18. It has remained very strong and sharp up to the present time. Measures of the velocity show it to be unquestionably *He* I 3888.65.

3. The line λ 3889 was merely the first helium line to become conspicuous. It was followed by others, equally sharp but not so strong. Of these, λλ 3964, 4026, and 4472 were the most conspicuous; and at the date of writing they are still strong and very sharp absorption lines. Other lines of helium which have been measured on one or more spectrograms are: λλ 3820, 3926, 4009, 4144, 4388, and 4713.[5] Of these, λ 4026 and λ 4472 are flanked by distinct emission components of approximately the same width as those of the hydrogen lines.

4. The hydrogen central absorption lines were of "normal" intensity (i.e., approximately as they had been from 1911 to 1933) in March and September, 1935. Simultaneously with the emergence of the strong sharp helium lines, the hydrogen central absorption began to increase; and these lines are now remarkably strong and sharp, so that the spectrum reminds one of that of φ Persei.

The velocities in Table II show interesting relations. For the earlier dates the differences of hydrogen and helium velocities are large and possibly significant, as the first three plates show the helium velocities to be systematically negative. On the other hand, the helium lines were then so ill-defined that their velocities are not very trustworthy. After they had become strong and sharp, they gave velocities which are in essential agreement with those of the hydrogen lines.

The velocities in the fourth and fifth columns of Table II are obtained by assuming the line λ 3889 to be due wholly to helium and hydrogen, respectively. For the first date the identification as hydrogen gives better agreement with other velocities; for the second, the interpretation is uncertain; and for all the later dates the measures indicate definitely that the line is due almost wholly to helium. The velocities of the lines of *Fe* II agree with hydrogen and helium as well as could be expected in view of their small number and their faintness.

The hydrogen velocities show a very marked lag with respect to the emission ratios V/R. In normal Be stars the greatest negative velocities occur shortly after the time when the red component of

[5] As the spectrograms were taken on Process emulsion, the lines λ 4922 and λ 5016 were not observable.

the emission is strongest. In the present case the lag was so great that the emission components had practically reached equality (March 29, 1936) before the velocity reached its greatest negative value. This, however, is simply an exaggeration of a relation which is common in Be spectrum variables.

TABLE II

RADIAL VELOCITIES OF LINES IN γ CASSIOPEIAE

DATE U.T.	HYDROGEN KM/SEC.	HELIUM KM/SEC.	λ 3889 KM/SEC.		*Fe* II KM/SEC.	REMARKS
			He	*Hζ*		
1935						
Mar. 24.03	−10 3*	−20 3*	+15	−16	−31 2*	
Sept. 18.32	+ 1 3	−29† 2	−13	44	−17 2	
19.29	− 7 2	−42 2	.....	.....	.....	Poor
30.21	+ 2 3	0† 3	−36	67	−17† 2	
Oct. 9.19	− 1 3	+17† 2	−22	53	− 7† 2	
30.23	− 3 5	−12 3	−16	47	− 7 3	
Nov. 22.26	− 3 6	− 2† 4	− 7	38	+ 3† 3	
1936						
Jan. 15.05	−33 4	−40 6	−35	66	−19 2	
Feb. 8.09	−21 3	−23 4	−10	41	.....	Weak
Mar. 29.05	−41 6	−44 8	−40	71	+ 2 2	
May 27.37	−34 5	−37 4	−41	72	−33 2	*O* II −30
27.38	−39 5	−42 4	−41	−72	−34 2	*Si* II −47

* Number of lines measured.

† Velocities of individual lines very discordant.

It is too early to theorize, but the changes suggest the formation of a more extensive outer shell of absorbing gases by the process of outward streaming of atoms. The fact that the red emission components were the stronger during these changes is in accord with this hypothesis.

THE OBSERVATORY
UNIVERSITY OF MICHIGAN
June 10, 1936

REVIEWS

The Quantum Theory of Radiation. By W. HEITLER. ("The International Series of Monographs on Physics.") Oxford University Press, 1936. Pp. xi+252. $6.00.

This is a systematic account of the principles of quantum electrodynamics in the form developed by Dirac and Fermi. The author wisely makes no attempt to present the subject in a historical fashion and thus avoids distracting the reader with alternatives. Neither is there any attempt to follow up all of the implications of the theory; instead, a limited number of applications are discussed in detail, the remaining possibilities being left unmentioned. The topics are selected with due regard to their importance.

The first of the five chapters of the book deals with classical electrodynamics in a summary fashion. The standard principles are discussed with the intention of exhibiting the weaknesses of the Lorentz-Abraham theory of the interaction of the electron with its own field. This is an important point since it is now clear that many of these weaknesses have been inherited by the quantum theory. It would seem that it could have been treated more effectively even in the space allotted. The most unusual features of the chapter are the discussion of the Rayleigh-Jeans resolution of the field into plane waves, and the solution of the problem of emission by means of it. It is known that any classical problem that can be solved by the standard methods can also be solved by this method, but most writers have neglected to give any examples and have left the impression that the details of the solution would be quite elaborate.

The introduction of the general principles of the quantum theory of radiation is accomplished in an able fashion in the second and third chapters. They are then applied to the various processes of emission, absorption, scattering, photoelectric effect, etc. The discussion is systematic, the processes being classified according to the order of the approximate solution of the general equations which is required for their discussion. This systematic nature of the theory is its strongest claim to consideration in this field, since most of the equations can be derived from other theories as well. The formula for the natural width of spectrum

lines is an exception to this rule, and its derivation is appropriately followed by a consideration of the experimental data.

The fourth chapter deals with the theory of the positron, on the basis of which Dirac predicted the existence and general properties of this particle. While this theory involves assumptions not needed for the previous work, it has no competitor. The creation and annihilation of positrons are discussed theoretically, and the conclusions are compared with the experimental evidence. The inherent difficulties of the theory are not hidden, but one is left with the conviction that here the theory has scored a very great triumph.

In the last chapter the penetrating power of high-energy radiation is discussed, and a marked divergence between theory and fact presents itself. It is possible, however, to give a precise delimitation of the domain within which the theory remains applicable; it is also seen that the origin of these limitations can be traced to the classical predecessor of the present theory. The discussion of the possibility of developing a theory which will not be subject to these limitations is brief, and one feels that the author places too much hope in the possibility of modifying the classical theory without considering the chance that the rapidly developing field of nuclear physics will present empirical material which is relevant. On the whole, the author has done an excellent piece of work, and the book will probably remain a standard reference for the field which it covers.

CARL ECKHART

University of Chicago